

A RESONANCE RAMAN STUDY OF  
MYELOPEROXIDASE, EOSINOPHIL PEROXIDASE, AND  
CYTOCHROME OXIDASE

Scott S. Sibbett  
B.S., University of California, Berkeley, 1979

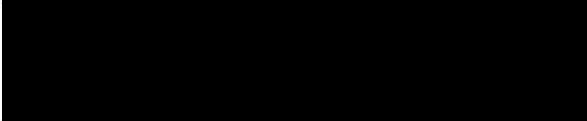
A dissertation submitted to the faculty  
of the Oregon Graduate Center  
in partial fulfillment of the  
requirements for the degree  
Doctor of Philosophy  
in  
Inorganic Chemistry

December, 1986

The dissertation "A Resonance Raman Study of Myeloperoxidase,  
Eosinophil Peroxidase, and Cytochrome Oxidase" by Scott S.


Sibbett has been examined and approved by the following

Examination Committee:



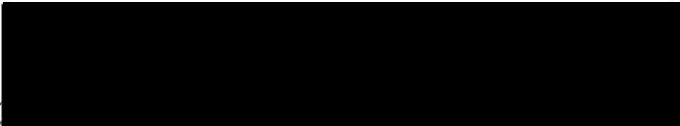
---

James K. Hurst  
Professor  
Thesis Advisor



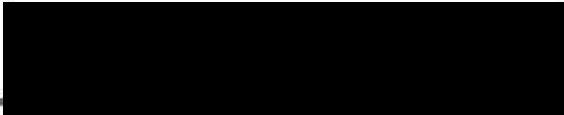
---

Thomas M. Loehr  
Professor  
Thesis Advisor



---

Joann Sanders-Loehr  
Professor  
Examination Committee Chair



---

Howard S. Mason  
Professor Emeritus, Oregon Health  
Sciences University

## ACKNOWLEDGMENTS

The research described here was conducted over a five year period while I was a graduate student in the Department of Chemistry and Biological Sciences at the Oregon Graduate Center. During that time, many people contributed to the work leading to this thesis. James K. Hurst and Thomas M. Loehr equipped me initially with a delight for chemistry, then guided my research from start to finish. I owe to them a debt of gratitude much greater than I have paid. Andrew K. Shiemke and Laura A. Andersson joined in many informative and enjoyable conversations. Joann Sanders-Loehr is thanked for her helpful editorial suggestions. I have been influenced by the thinking of Howard S. Mason and Seymour J. Klebanoff, and have been the fortunate beneficiary of their generous donations of protein samples. To them both, I express deep appreciation.

My ambition to pursue an advanced degree in chemistry was advocated and supported by several friends, particularly John & Jabke Buesseler, Gene & Beverly Rollins, William & Dana Keese, William & Carrie Ghirardelli, William & Becky Sibbett V, David Lundberg, Frank Hauser, Grace Sammet, and Edith Mereen. I have experienced deep satisfaction from my writing, scientific and otherwise; this I credit to the early nurturing of William Sibbett IV, Eleanor Cummings, and the late Louise Gaines. Special thanks go to all my Oregon friends, from OGC, Intel, and elsewhere, for diverting me thoroughly and pleasantly on many welcome occasions.

My aspirations as a scholar derive in large measure from the example and influence of Loy Sammet, to whom I am boundlessly grateful.

## DEDICATION

---

To the one above all others  
who encouraged and nurtured me  
through the duration of this work,  
*Karen Hansen Sibbett.*

---



## TABLE OF CONTENTS

	Page
ACKNOWLEDGMENTS . . . . .	iii
DEDICATION . . . . .	iv
TABLE OF CONTENTS . . . . .	v
LIST OF TABLES . . . . .	vii
LIST OF FIGURES . . . . .	viii
ABSTRACT . . . . .	x
LIST OF ABBREVIATIONS . . . . .	xii
Chapter	
1. MYELOPEROXIDASE	
<i>Introduction</i> . . . . .	1
<i>Materials and Methods</i> . . . . .	12
<i>Results and Discussion</i> . . . . .	14
<i>References</i> . . . . .	38
2. EOSINOPHIL PEROXIDASE	
<i>Introduction</i> . . . . .	46
<i>Materials and Methods</i> . . . . .	48
<i>Results</i> . . . . .	49
<i>Discussion</i> . . . . .	57
<i>References</i> . . . . .	59

Chapter	Page
3. CYTOCHROME OXIDASE: THE HURST MODEL	
<i>Introduction</i> . . . . .	66
<i>Materials and Methods</i> . . . . .	72
<i>Results</i> . . . . .	83
<i>Discussion</i> . . . . .	104
<i>References</i> . . . . .	125
4. CYTOCHROME OXIDASE: SUBUNITS	
<i>Introduction</i> . . . . .	135
<i>Materials and Methods</i> . . . . .	137
<i>Results</i> . . . . .	138
<i>Discussion</i> . . . . .	141
<i>References</i> . . . . .	144
APPENDIX . . . . .	146
BIOGRAPHICAL NOTE . . . . .	152

## LIST OF TABLES

Table	Page
1. Biological Compounds Degraded by HOCl . . . . .	3
2. Selected Physical Properties of Myeloperoxidase . . . . .	8
3. Primary Sources of Resonance Raman Scattering . . . . .	31
4. Selected Hydroporphyrin-containing Proteins . . . .	33
5. Raman Frequencies of Eosinophil Peroxidase and Other Heme-containing Enzymes . . . . .	50
6. Unpaired Spin Densities for Methine Carbons . . . .	62
7. Raman Frequencies of Protoheme and Cu(I)-Protoheme . . . . .	90
8. Kinetic Parameters for Cu(I)-Protoheme Demetalation . . . . .	99
9. Raman Frequencies for the Vinyl Modes of Protoheme and Other Selected Olefins . . . . .	109
10. Raman Bands of Cytochrome Oxidase . . . . .	117

## LIST OF FIGURES

Figure	Page
1. Porphyrin and Chlorin Molecular Structures . . .	9
2. Resonance Raman Spectra of Canine Myeloperoxidase, High-Frequency Region . . .	15
3. Resonance Raman Spectra of Canine Myeloperoxidase, Low-Frequency Region . . .	17
4. Resonance Raman Spectra of Canine Myeloperoxidase, Temperature Dependence . . .	22
5. Relative Intensity Enhancement Profiles for Canine Myeloperoxidase . . . . .	28
6. Resonance Raman Spectra of Eosinophil Peroxidase, 406.7 nm Excitation . . . . .	52
7. Resonance Raman Spectra of Eosinophil Peroxidase, 514.5 nm Excitation . . . . .	54
8. Optical Absorption Maxima of Substituted Deuteroporphyrins As a Function of Vinyl Substituents . . . . .	67
9. Spectroelectrochemical Titrating Vessel . . . . .	76
10. Calibration Curve for Redox Electrode . . . . .	80
11. Resonance Raman Spectra of Protoheme and Cu(I)-protoheme, Room Temperature . . . . .	84
12. Resonance Raman Spectra of Protoheme and Cu(I)-protoheme, 90 K . . . . .	86
13. Resonance Raman Spectra of Protoheme and Cu(I)-protoheme, With Perchlorate . . . . .	88
14. Resonance Raman Spectra of Tetraprotonated Protoporphyrin . . . . .	85
15. Copper Dependence of Iron Loss from Cu(I)-Protoheme . . . . .	100

16.	Sodium Dodecyl Sulfate-Dependence of Iron Loss from Cu(I)-Protoheme . . . . .	102
17.	Rate Law Relationship Between Protoheme Reduction Potential and Kinetic Parameters for Iron Loss from Cu(I)-Protohem . . . . .	114
18.	Resonance Raman Spectra of Cytochrome Oxidase and Subunit Constituents . . . . .	139

## ABSTRACT

### A Resonance Raman Study of Myeloperoxidase, Eosinophil Peroxidase, and Cytochrome Oxidase

Scott S. Sibbett, Ph.D.  
Oregon Graduate Center, 1986

Supervising Professors: James K. Hurst and Thomas M. Loehr

Soret excitation of canine myeloperoxidase (MPO) produces complex resonance Raman (RR) spectra characterized by multiple bands in the core size and oxidation state marker regions. Spectra of dithionite-reduced and cyanide-coordinated derivatives are also reported. In the native and dithionite-reduced enzyme, there are no detectable bands between 1620 and 1700  $\text{cm}^{-1}$ , indicating that the hemes do not contain formyl substituents in conjugation with the macrocyclic ring. In the context of other physical measurements, it is concluded that MPO contains two equivalent or nearly equivalent chlorin prosthetic groups.

Resonance-enhanced Raman spectra of eosinophil peroxidase (EPO) from horse and human eosinophils is reported. Based upon the spectral energies, distribution and depolarization ratios of the high-frequency skeletal modes, and upon the presence of weak bands assignable to vinyl substituent groups, we

conclude that the heme prosthetic group is high-spin, six coordinate protoporphyrin. The Raman spectrum reveals clear differences from lactoperoxidase, an enzyme which appears nearly structurally isomorphous by other physical techniques; the data indicate a stronger axial sixth ligand in EPO.

Copper(I) addition to aqueous micellar suspensions of ferriprotoporphyrin or its dimethyl ester causes perturbations of resonance-enhanced Raman bands associated with vibrational motions of the vinyl group substituents at the pyrrolic 3 and 8 positions. No spectral perturbations occur upon adding cupric, zinc, or hexaquo chromic ions to these solutions, nor upon adding Cu(I) to ferrideuteroporphyrin. The data are interpreted to indicate Cu(I) coordination at the ring vinyl positions. Consistent with this view, intensity is lost in the vinyl carbon-carbon stretching region at  $1615\text{-}1630\text{ cm}^{-1}$  and a new band appears at  $1520\text{ cm}^{-1}$ , assignable to the carbon-carbon stretch of Cu(I)  $\pi$ -complexed olefin bonds. Similar changes occur in this region upon reduction of oxidized cytochrome oxidase, suggesting that peripheral vinyl substituents may assist the ligation of Cu(I) in the oxygen reductase site.

By preparative electrophoresis, enriched fractions of subunits I and II of mammalian cytochrome oxidase were prepared. The two heme chromophores appear to be divided *in vivo* between these two subunits. Soret excitation of the isolated subunits yields RR spectra which are nearly identical.

## LIST OF ABBREVIATIONS

Symbol -----	Equivalent -----
CCP	cytochrome c peroxidase
$\text{Co}(\text{bpy})_3^{3+}$	tris(2,2'-bipyridyl)cobalt(III)
EPO	eosinophil peroxidase
EPR	electron paramagnetic resonance
EXAFS	extended X-ray absorption fine structure
HRP	horseradish peroxidase
LPO	lactoperoxidase
MCD	magnetic circular dichroism
MPO	myeloperoxidase
P	porphyrin
PMS	phenazine methosulfate
SDS	sodium dodecyl sulfate
TFA	trifluoroacetic acid
UV	ultraviolet
$\rho$	polarization ratio



"It looks rather easy at a first glance,  
but you will notice that the further  
you get into it the more it widens out."

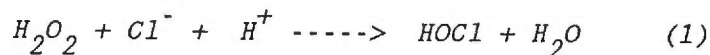
Mark Twain  
Early Tales & Sketches  
Volume 2, p 412

## Chapter 1

### *Myeloperoxidase*

Neutrophils in the bloodstream defend the body against microbial infection. The triggers for this defense are the host immune and complement systems, which release chemotactic signals that alert neutrophils to the presence and location of invading microbes. Once intercepted by a neutrophil, the microbe is entrapped within a specialized vacuole, the phagosome. The components of a potent microbicidal system then are injected into the phagosome, where subsequent development of a toxic environment leads to rapid bacterial killing. Since toxins inside the phagosome leak out, the antimicrobial activity of neutrophils is accompanied by inflammation of the surrounding host tissue. This inflammatory response provides a simple visual indicator of the extreme potency of the phagosomal environment.

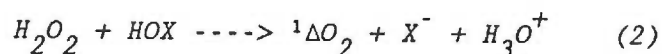
Myeloperoxidase (MPO) has been implicated in the antimicrobial and cytotoxic reactions of neutrophils.<sup>1</sup> This enzyme catalyzes the peroxidation of chloride ion to hypochlorous acid (HOCl):<sup>2</sup>



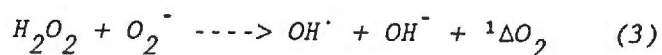
Hypochlorous acid efficiently degrades a wide variety of

biological substrates (Table 1), and can duplicate the cell-free MPO system in killing bacteria and modifying substrate analogs.<sup>3</sup> Consequently, HOCl has been suggested to be the ultimate MPO-generated toxin.<sup>4</sup>

A competing suggestion is that dioxygen excited to the first singlet electronic state ( $^1\Delta O_2$ ) constitutes the primary phagosomal microbicide.<sup>5</sup> This species, known commonly as "singlet oxygen", is formed by one or more secondary reactions,<sup>1,6</sup> such as reaction 2,



or the Haber-Weiss reaction:<sup>7</sup>



Circumstantial evidence supports singlet oxygen as the primary MPO-generated toxin,<sup>1</sup> but is based on the premise that the short-lived singlet oxygen intermediate is selectively trapped by certain exogenous reagents. Competition experiments contradict this notion, indicating instead that generation of singlet oxygen by MPO (reaction 2) is excluded in the physiological environment by preferential reaction of HOCl with organic substrates.<sup>4,8</sup> Moreover, reagents presumed to react only with singlet oxygen appear to be equally reactive with HOCl.

Chemiluminescence from the MPO- $H_2O_2$ - $Br^-$  system has been detected in recent studies by Kahn,<sup>9</sup> which he assigns to spontaneous emission from MPO-generated singlet oxygen upon

**Table 1**  
**Biological Compounds Degraded by HOCl**

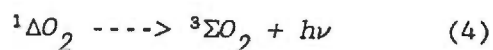
Compound	References (a)
<hr/>	
Enzymes with sulfhydryl functions	
Ferredoxin	b, f
Glyceraldehyde-3-phosphate dehydrogenase	b
Lactate dehydrogenase	b
Muscle aldolase	b
Papain	b
Yeast aldolase	b
Porphyrins and Porphyrin-containing Proteins	
2,4-diformyldeuteroporphyrin	b
2-formyl-4-vinyl-deuteroporphyrin	b
Cobalt(III) mesoporphyrin IX dimethyl ester	b
Ferridiacetyldeuteroporphyrin	b
Ferriprotoporphyrin IX	b, e
Ferriprotoporphyrin IX dimethyl ester	b
Mesoporphyrin IX dimethyl ester	b
Protoporphyrin IX	b, e
Cytochrome c heme undecapeptide	b
Cytochrome c	b, e
Myoglobin	b, e
Nucleotides and nucleic acids	
ADP	b
CDP	b
GMP	b
IDP	b
DNA	c
RNA	c
Other	
Aflatoxin	d, d
Beta-carotene	b
Beta-galactosidase	i, g
Biliverdin	-, e
Cytochalasin	-, h

- 
- a) A second citation indicates complementary studies with a cell-free MPO-halide-peroxide system.  
b) Albrich, J.M.; McCarthy, C.A.; Hurst, J.K. Proc. Natl. Acad. Sci. USA 1981, 78, 210-214.  
c) Odajima, T. Shika Kiso Igakkai Zasshi 1980, 22, 502-512.

Table 1, continued

- d) Odajima, T. Arch. Oral Biol. 1981, 26, 339-340.
- e) Odajima, T.; Onishi, M.; Sato, N. Shika Kiso Igakkai Zasshi 1982, 24, 243-248.
- f) Rosen, H.; Klebanoff, S.J. Infect. Immun. 1985, 47, 613-618.
- g) Hamers, M.N.; Sips, H.J. Adv. Exp. Med. Biol. 1982, 141, 151-160.
- h) Odajima, T.; Sato, N.; Onishi, M. Shika Kiso Igakkai Zasshi 1980, 22, 545-549.
- i) Albrich, J.M.; Gilbaugh, J.H., III; Callahan, K.B.; Hurst, J.K. J. Clin. Invest., 1986; *in press*.

decaying to the ground state triplet:



On the basis of measurements of quantum yield efficiency, he infers a significant production of singlet oxygen in neutrophil phagosomes by MPO. This inference is subject to several criticisms. 1. Quantum yields for MPO chemiluminescence were computed by Kahn relative to a hypochlorite-hydrogen peroxide inorganic system (reaction 2,  $X = Cl^-$ ). However, the measured enzyme system contained bromide as cosubstrate. Myeloperoxidase turnover rates are appreciably greater with bromide than with chloride,<sup>5,10</sup> hence the experimental protocol exaggerates quantum yields for the enzyme. 2. The MPO quantum yield is computed by Kahn from a visual estimation of emission band areas. By the cut-and-weigh method, our own estimates of these band areas indicate that the quantum yield is 0.3 or less, not 0.5 as reported. 3. Kahn's experimental system is cell-free. Kinetic data indicates rapid reaction between hypochlorous acid and various natural substrates.<sup>4,8</sup> Kahn's experiment excludes such side-reactions, and thus may permit singlet oxygen production by pathways which are kinetically insignificant under physiological conditions. Chemiluminescence quantum yields from the MPO- $H_2O_2$ - $Cl^-$  system have been reported by others to be less than 0.01 when measured at concentrations of hydrogen ion and ascorbic acid normally found in the bloodstream.<sup>11</sup> 4. The bloodstream contains only about  $5 \times 10^{-5}$  M bromide ion,<sup>12</sup>

whereas chloride ion is present at a concentration of about  $7 \times 10^{-2}$  M. Hence, experiments conducted by Kahn using bromide as cosubstrate for MPO reactions are probably physiologically irrelevant.

Myeloperoxidase contains two heme prosthetic groups.<sup>13</sup> In the absence of HOCl-reactive reagents,<sup>14</sup> catalytic turnover is accompanied by rapid bleaching of the hemes and by inactivation of the enzyme.<sup>15,†</sup> Neither chromophoric bleaching nor self-inactivation occurs when HOCl-reactive reagents are present. At the cellular level, bacteria present a large number of sites which are vulnerable to attack by HOCl. By furnishing ample substrate for HOCl, a newly phagocytized bacterium protects MPO against inactivation. This insures at the outset full enzymatic activity and maximum generation of HOCl. Eventually bacterial substrate becomes limiting, resulting in the inactivation of MPO. Hence, a "deadman brake" mechanism minimizes both overproduction of HOCl and consequent damage to surrounding host tissue. The regulation of MPO activity may occur primarily by this mechanism.

The MPO prosthetic groups are covalently linked to the protein.<sup>16,17</sup> Attempts to identify the molecular structure of

---

† Like MPO, lignin peroxidase<sup>95</sup> and the P-450 cytochromes<sup>96</sup> also undergo suicide inactivation. Numerous other non-heme enzymes are known to produce substrates which cause irreversible inactivation.<sup>97</sup>

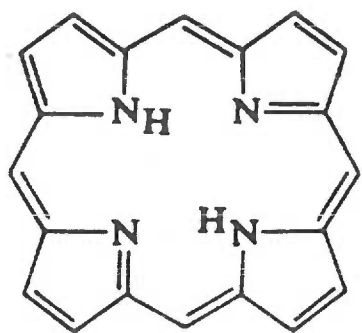
these groups by direct chemical means have been frustrated by their structural instability.<sup>16,18-22</sup> Under conditions examined thus far, extraction has resulted in hemes with physical properties that are distinctly altered from the native enzyme.<sup>16,20,21</sup> Hence structural identification has relied principally upon physical characteristics of the intact enzyme. A selection of these properties are presented in Table 2. Soret and visible absorption bands of the reduced form are dramatically red-shifted compared to protoheme<sup>23</sup> and c-type peroxidases.<sup>24</sup> Based upon spectral analogy of the reduced enzyme with ferrous sulfmyoglobin and other ferrochlorins, it has been suggested that the prosthetic groups are chlorins (Figure 1).<sup>18,19,25</sup> This idea is supported by the resemblance between MCD spectra of MPO and the chlorin-containing *Pseudomonas aeruginosa* nitrite reductase.<sup>26,27</sup>

Despite an early report that the intact MPO hemes test negatively for formyl substituents,<sup>19</sup> these hemes have been suggested to be formylporphyrins.<sup>16,20</sup> The primary evidence for this suggestion is a resemblance between pyridine hemochrome spectra of MPO and formyl-substituted heme a.<sup>18,19</sup> Studies on the reaction between extracted MPO heme and reagents capable of reducing formyl groups have been claimed to support this notion.<sup>20,28,29</sup> The products of these reactions show blue-shifted optical spectra, as anticipated for loss of an electrophilic substituent on the heme periphery. However, such data is probably irrelevant to the holoenzyme because the peripheral

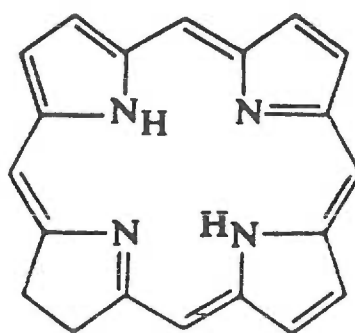


Table 2  
Selected Physical Properties of Myeloperoxidase

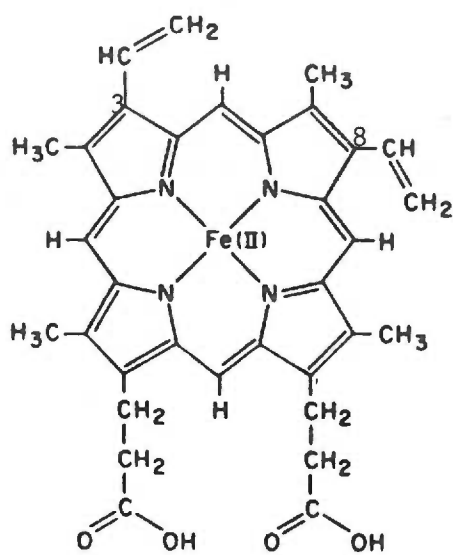
Property	Native enzyme	Reduced enzyme	Cyanide-derivative
<u>Soret</u>			
$\lambda_{\text{max}}$ , nm	428	468	456
$\epsilon$ , $\text{M}^{-1} \text{cm}^{-1} \text{heme}^{-1}$	$8.9 \times 10^4$	$9 \times 10^4$	$6.8 \times 10^4$
<u>Visible</u>			
$\lambda_{\text{max}}$ , nm	568	634	632
$\epsilon$ , $\text{M}^{-1} \text{cm}^{-1} \text{heme}^{-1}$	$1.5 \times 10^4$	$2.6 \times 10^4$	$1.6 \times 10^4$
$\mu_{\text{eff}}$ , B.M.	5.77	4.46	3.45
<u>Near-IR MCD</u>	high-spin ferric		low-spin ferric
<u>Visible MCD</u>			Chlorin- like
<u>EPR</u>	high-spin, g 7.09, 5.17		low-spin, g 2.58, 2.33, 1.81



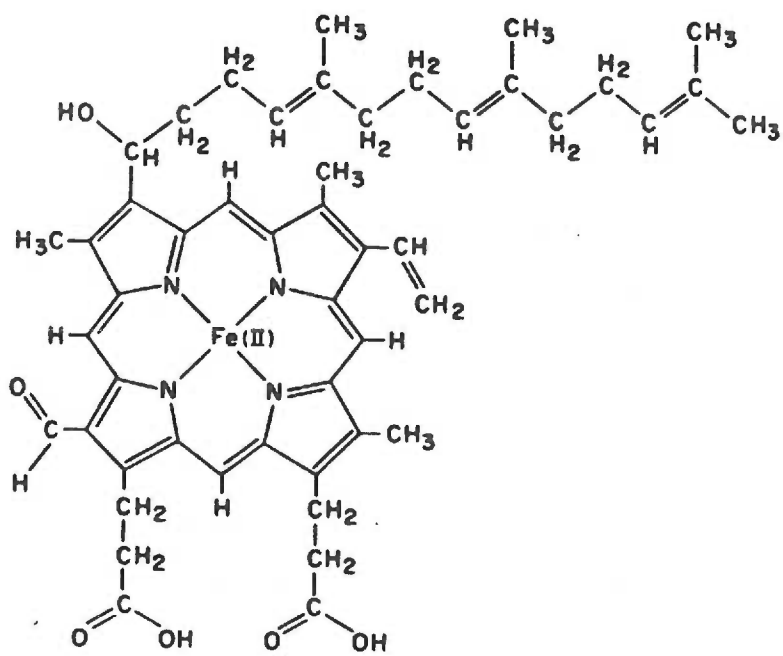
Porphin



Chlorin



Fe(II) protoporphyrin IX



heme a

substituents of the extracted MPO heme appear to be altered during extraction and isolation. This is indicated by the dissimilar pyridine hemochrome optical spectra of extracted and intact heme.<sup>20</sup>

Conversion of chlorins to formylporphyrins is known to occur under relatively mild conditions.<sup>28,30</sup> A conversion of the MPO chlorin to formylporphyrin provides a single explanation for (i) the dissimilarity of intact and extracted hemochrome spectra, (ii) the hypochromism of extracted heme on adding formyl-reactive reagents, and (iii) the negative test for formyl groups on the intact heme. At least one MPO heme-extraction study has been conducted in solutions which were relatively high in concentration of formaldehyde.<sup>20</sup> Experimental prudence would seem to dictate that such extractions be performed in the absence of free aldehyde.

The myeloperoxidase dimer contains two hemes, one per protomer.<sup>31,32</sup> There is no consensus on whether the hemes are equivalent. From experiments on extracted heme, binding inequivalence has been suggested,<sup>13,20</sup> but the recent separation of enzyme into apparently identical, fully active monomeric subunits<sup>31,33</sup> suggests otherwise. Electronic spectra, redox titrations,<sup>20</sup> and halide binding studies<sup>34</sup> do not detect differential behavior of two distinct hemes. The stoichiometry of the ferrimyeloperoxidase-cyanide complex has been reported to be 1:1<sup>29</sup> or 2:1 CN<sup>-</sup>/enzyme.<sup>27</sup> Cyanide binds to both hemes in ferromyeloperoxidase, and appears to

induce conformational distortion of the protein.<sup>35</sup>

Although reductive titration with dithionite is reported to require only one reducing equivalent per molecule,<sup>29</sup> integration of EPR signals suggests that the resting enzyme contains both iron atoms in the ferric oxidation state.<sup>27</sup> Oxidation of thiocyanate ion by MPO Compound II follows biphasic kinetics; each phase contributes about equally to the overall reaction.<sup>20</sup> Both catalytic and inhibitory anion binding sites are detected during halide<sup>34,36,37</sup> and pseudohalide peroxidation.<sup>38</sup> In summary, the data is insufficient to determine whether the two hemes are equivalent.

The curious physical properties of the MPO hemes signify unusual structural properties. For this reason, and because these hemes are integral to the function of MPO in disinfection<sup>39</sup> and the inflammatory response,<sup>40</sup> we have studied the enzyme by resonance Raman spectroscopy. This technique has proven useful in identifying heme oxidation and electronic spin states, as well as peripheral substituents such as formyl groups.<sup>41</sup>

## MATERIALS AND METHODS

Canine myeloperoxidase was provided by Professor Seymour J. Klebanoff (University of Washington, Seattle, WA). For the native enzyme, a value of 0.72 was measured for the absorbance ratio  $A_{430 \text{ nm}}/A_{280 \text{ nm}}$ . Typical values reported for highly purified enzyme are 0.7-0.8.<sup>15,31,42</sup> Samples were calculated to be  $1 \times 10^{-5} \text{ M}$  using  $\epsilon_{428 \text{ nm/mol dimer}} = 1.78 \times 10^5 \text{ M}^{-1} \text{ cm}^{-1}$ .<sup>43</sup> Absorption maxima were observed at 359, 428, 568, 626, and 684 nm. The reduced form of the enzyme was obtained by titration with solid, free-flowing sodium dithionite (BDH Chemicals Ltd., Poole, England) under an argon atmosphere. The progress of the reduction reaction was monitored spectrophotometrically until incremental addition of dithionite caused no further spectral change. Absorption maxima for the reduced enzyme were observed at 468 and 634 nm. The cyanide derivative of MPO was produced via titration with solid potassium cyanide (reagent grade, Baker, Phillipsburg, NJ) following the same procedure as the reductive titration. Absorption maxima were observed at 456 and 632 nm. All absorption spectra taken for MPO and its derivatives were in agreement with previous reports.<sup>15,27,31,39,44</sup> The perchlorate salt of tris(2,2'-bipyridyl)cobalt(III)  $[\text{Co}(\text{bpy})_3]^{3+}$ ,  $\epsilon_{307 \text{ nm}} = 3 \times 10^4 \text{ M}^{-1} \text{ cm}^{-1}$ ,<sup>45</sup> was prepared according to published methods.<sup>46</sup>

Sample excitation was provided by Spectra Physics ion lasers (164-05 argon, 164-01 krypton). The Raman spectrometer and computer interface have been described elsewhere;<sup>47</sup> the

scattered light was collected using a 90-degree geometry. Depolarization experiments were conducted with a polarizer situated between the laser head and sample. For experiments on non-frozen samples, a stream of cold dry  $N_2$  was used to control temperature at the sample such that freezing at the point of laser incidence was just prevented by internal heating due to laser light absorption. For low temperature studies, samples were mounted in a copper-rod cold finger immersed in liquid  $N_2$ .<sup>48</sup> In calculating excitation profiles, band intensities were measured relative to the symmetric sulfate stretching mode of  $(NH_4)_2SO_4$  (0.3 M). The average pathlength traveled through solution by Raman scattered photons was computed to be 0.44 mm. From this value, self-absorption was calculated to be negligible, and therefore neglected in calculating excitation profiles. For all Raman experiments, samples were contained in glass capillary tubes. Electronic spectra were obtained directly from these tubes with a Cary 16 spectrophotometer by placing them in the 2-5 °C water-filled chamber of a self-masked 1 cm cuvette. The baselines for these spectra were suitably flat between 400-800 nm, but subject to large background shifts. Hence for quantitative measurements, conventional spectroscopic methods were employed. No detectable photodecomposition of MPO hemes exposed to the laser beam was observed; electronic spectra were identical before and after each experiment and the Raman spectra remained constant over the 30-300 minute periods required for data collection.

## RESULTS AND DISCUSSION

Carbonyl Stretching Region. Figures 2 and 3 show the resonance Raman spectra of native, dithionite-reduced, and cyanide-complexed canine MPO under 454.5 nm excitation. A conspicuous feature of the resonance Raman spectra of native and reduced MPO is the absence of bands above  $1610\text{ cm}^{-1}$ . A formyl group on the periphery of heme typically adds a symmetric C=O stretching band in this region.<sup>49,50</sup> The strength of hydrogen bonding to carbonyl oxygen determines the frequency of this band within a  $30\text{ cm}^{-1}$  range between  $1670\text{-}1640\text{ cm}^{-1}$ .<sup>51</sup> With Soret excitation, the mode is Raman active for all formyl hemes and formyl heme proteins.

In resonance Raman spectra of mammalian cytochrome oxidase, a  $1610\text{ cm}^{-1}$  band has been assigned by Babcock and Callahan<sup>50</sup> to a formyl C=O stretching mode of one of the two hemes. To reconcile their assignment with a band frequency that is  $30\text{ cm}^{-1}$  outside the typical range, they postulated the perturbing influence of an exceptionally strong hydrogen bond between carbonyl oxygen and a protein residue. Like cytochrome oxidase, MPO also has a band at  $1610\text{ cm}^{-1}$ , but unlike cytochrome oxidase, the MPO band is essentially invariant with change in oxidation state of the heme iron (Figure 2). Since resonance interaction between central metal and formyl substituent renders local formyl modes sensitive to oxidation state changes,<sup>52</sup> we concluded earlier that the frequency-invariant  $1610\text{ cm}^{-1}$  band in MPO spectra could not be a formyl

---

Figure 2

Resonance Raman Spectra of Canine Myeloperoxidase, 900-1750  $\text{cm}^{-1}$ .

Upper spectrum, native enzyme; middle, dithionite-reduced;

lower, enzyme-cyanide complex. The spectra were obtained with 38-40 mW of 454.5 nm excitation and are accumulations of 8 to 15 scans; scan rate  $1.0 \text{ cm}^{-1} \text{ s}^{-1}$ , slit width  $\sim 8 \text{ cm}^{-1}$ . Upper

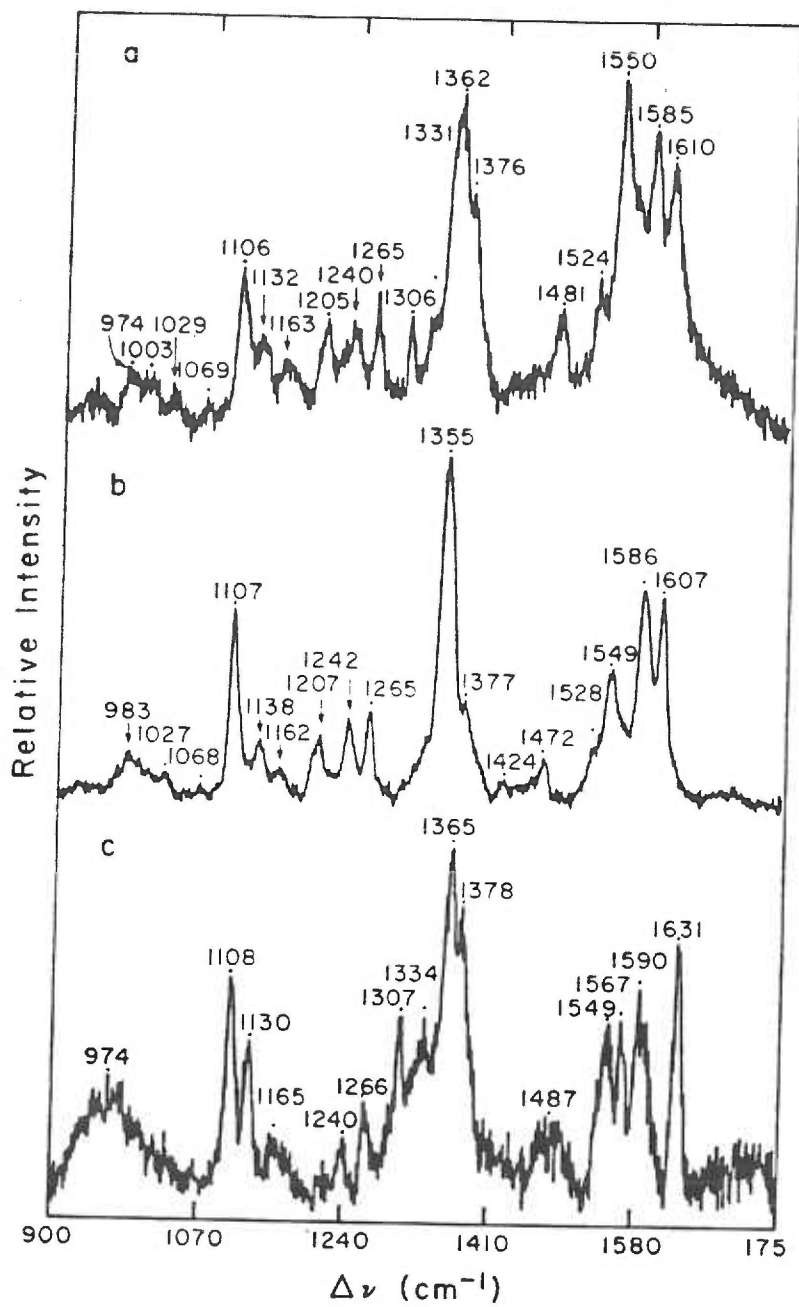
spectrum depolarization ratios [band frequency ( $\rho$ )]: 1585

(0.42); 1550 (0.46); 1362 (0.45); 1265 (0.46); 1242 (0.39); 1205

(0.35); 1161 (0.74); 1107 (0.57);  $\nu_1 \text{SO}_4^{=}$  982 (0.06).

---





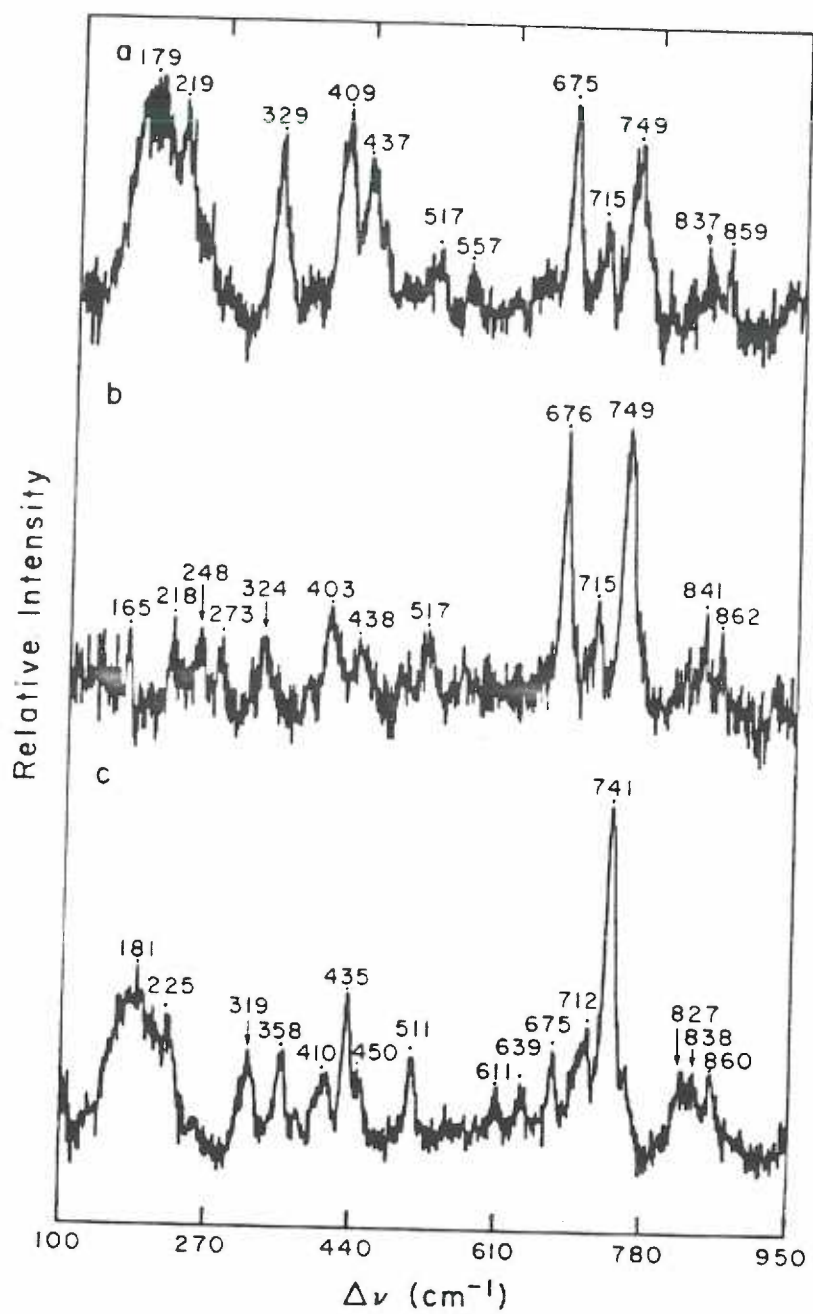
---

Figure 3

*Resonance Raman Spectra of Canine Myeloperoxidase, 100-950  $\text{cm}^{-1}$ .*

*Conditions and labels as in Figure 1.*

---



mode.<sup>53</sup> Recently, Kitagawa and coworkers have raised objections to the formyl mode assignment of Babcock and Callahan.<sup>54</sup> The Japanese group notes that spectra of heme *a* show bands at both  $1608\text{ cm}^{-1}$  and  $1660\text{ cm}^{-1}$ . Although vibronic coupling between formyl and porphyrin ring modes could produce two formyl bands, the invariance of the heme *a*  $1608\text{ cm}^{-1}$  band in both polar and apolar solvents eliminates this possibility. For this and other reasons,<sup>54</sup> the Babcock and Callahan assignment is questionable.

The absence of a formyl band in MPO spectra indicates that formyl substituents either are not present, or are not in conjugation with the macrocyclic ring. Conjugation may be broken either by attachment of formyl to a  $\beta$ -carbon on the pyrroline ring, or by severe tilting of the formyl group out of the plane of the macrocycle. Regardless of whether MPO contains no formyl or merely a nonconjugated formyl, the electronic spectrum of the enzyme will be largely unperturbed. Consequently, the most straightforward explanation for the red-shifted electronic spectrum of MPO (cf. Introduction) is that the chromophores are chlorins.<sup>25,55</sup>

Babcock and coworkers have recently argued that the magnitude of the MPO red-shift is too large in comparison to simple inorganic chlorins to be explained solely by the effects of a single pyrroline.<sup>56</sup> Although these workers overlook the spectral properties of heme  $d_1$  in asserting that large MPO-like red-shifts are not exhibited by inorganic chlorins,<sup>26,57</sup> it is

clear that the MPO spectrum is unusual. First, it lacks the dominant, well-resolved visible absorption band at ~600-650 nm ( $\epsilon \sim 50 \text{ mM}^{-1} \text{ cm}^{-1}$ ) that is typical of chlorins.<sup>58,59</sup> (This feature is also absent in spectra of *Pseudomonas aeruginosa* cytochrome oxidase, which contains heme  $d_1$ .<sup>60</sup>) Second, the Soret band appears either to be split (359, 428 nm) or flanked by an exceptionally active N band.<sup>58,61</sup> Third, the visible bands project above a relatively high underlying background.

The vibrational mode assignments calculated by Abe and coworkers for nickel(II) octaethylporphyrin are widely used to assign vibrational bands of various related porphyrins and metalloporphyrins.<sup>62</sup> All such assignments rely upon the assumption that the central metal atom and peripheral substituents may vary without substantially altering the normal coordinates of porphyrin vibration. In the following discussion, we rely upon a further assumption that the degree of saturation may vary at pyrrole  $C_b-C_b$  bonds without substantially altering the normal coordinates of porphyrin vibration. The presence of one or more pyrrolines in the macrocycle will lower the molecular symmetry and produce differences between porphyrin and chlorin vibrational assignments. As a first approximation, however, we regard the chlorin bands to be analogous to the porphyrin bands of nickel octaethylporphyrin. To date, all published assignments of chlorin Raman and infrared spectra have utilized the porphyrin assignments of Abe and coworkers.<sup>63-65</sup>

The MPO resonance Raman band at  $1610 \text{ cm}^{-1}$  (Fig. 1) is

probably the analogue of the  $\nu_{10}$  mode of nickel octaethylporphyrin.<sup>62</sup> Based upon published correlations between the frequency of  $\nu_{10}$  and the nature of the axial ligand to iron octaethylporphyrin,<sup>66</sup> we attribute the relatively low frequency of the  $1610\text{ cm}^{-1}$  band to an exceptionally weak axial field felt by the heme iron. Such weak field ligands might be  $\text{H}_2\text{O}$ , chloride ion, or carboxylate ion. Carboxylate has been shown to be an axial ligand to the hemes of lactoperoxidase<sup>67</sup> and *Pseudomonas aeruginosa* cytochrome c peroxidase.<sup>68</sup>

As suggested by Wever and coworkers, tyrosine is a plausible candidate as the weak field ligand.<sup>69</sup> The heme of catalase is coordinated by phenolate,<sup>70</sup> as are those of several mutant hemoglobins.<sup>71</sup> However, the resonance Raman spectra of MPO do not contain bands which are characteristic of iron-tyrosinate proteins ( $1600$ ,  $1500$ ,  $1270$ , and  $1170\text{ cm}^{-1}$ ).<sup>71,72</sup> Moreover, the MCD spectrum of MPO<sup>27</sup> bears no resemblance to that of catalase.<sup>73</sup> Hence, tyrosine does not appear to be an axial ligand of the MPO chlorin.

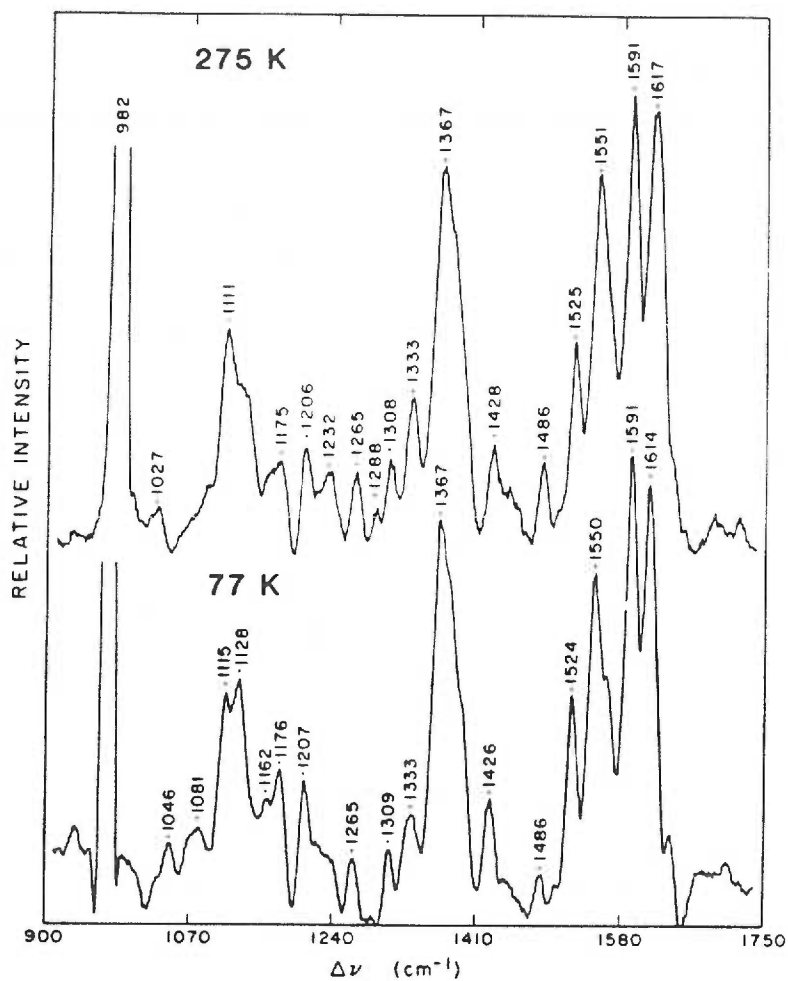
Core size and Oxidation State Marker Regions. Two resonance Raman bands appear in both the core size ( $1550$ ,  $1588\text{ cm}^{-1}$ ) and oxidation state marker regions ( $1362$ ,  $1376\text{ cm}^{-1}$ ) (Fig. 2a). Single hemes typically demonstrate only one band in these regions.<sup>41</sup> With an excitation wavelength of either  $406$  or  $454\text{ nm}$ , the relative intensities of these bands are unchanged upon freezing to  $90\text{ K}$  (Fig. 4). This temperature-insensitivity

---

**Figure 4**

*Resonance Raman Spectra of Canine Myeloperoxidase, Temperature Dependence. Upper spectrum, 275 K; lower, 90 K. The spectra were obtained with 406.7 nm excitation; scan rate  $1.0 \text{ cm}^{-1} \text{ s}^{-1}$ , slit width  $\sim 8 \text{ cm}^{-1}$ . The upper spectrum is the accumulation of 3 scans with 28-30 mW; the lower spectrum is the accumulation of 10 scans with 33-35 mW. After background subtraction, both spectra were subject to a 25-point smooth.*

---





indicates the two MPO hemes do not exist as an equilibrium distribution between different spin states.<sup>74</sup>

The doublets in MPO oxidation state and spin-state marker regions appear to dictate that either (i) the hemes are hydroporphyrins, for which ring reduction causes symmetry lowering, thereby increasing the number of totally symmetric, Raman allowed vibrational modes,<sup>75</sup> or (ii) the spectrum of the native enzyme consists of overlapping contributions from two vibrationally distinct hemes.

The distinct heme hypothesis (ii) is qualitatively consistent with changes in relative peak intensities upon dithionite reduction. The band at  $1376\text{ cm}^{-1}$  is substantially reduced in intensity, whereas the  $1362\text{ cm}^{-1}$  band increases in intensity relative to peaks such as those at  $1607\text{ cm}^{-1}$  and  $1107\text{ cm}^{-1}$ . Similarly, the band at  $1588\text{ cm}^{-1}$  increases in intensity at the expense of the  $1550\text{ cm}^{-1}$  (Fig. 2b). Thus, titration with dithionite suggests the simultaneous presence of high-spin ferriheme and low-spin ferroheme in the enzyme, with reduction converting high-spin ferriheme to a low-spin ferro species. According to this interpretation, the spectral shift from  $1610\text{ cm}^{-1}$  to  $1631\text{ cm}^{-1}$  that is observed upon titrating native MPO with potassium cyanide (Fig. 2c) is due to high-to-low spin conversion of the ferriheme. For six-coordinate ferrihemes, the band assigned to the  $\nu_{10}$  vibrational mode typically appears at  $1615\text{--}1625\text{ cm}^{-1}$  for the high-spin state<sup>66</sup> and at  $1638\text{--}1641\text{ cm}^{-1}$  for the low-spin state.<sup>76</sup> The resonance Raman

spectra of horseradish peroxidase,<sup>65</sup> intestinal peroxidase,<sup>77</sup> lactoperoxidase,<sup>78</sup> and cytochrome c<sup>66</sup> are consistent with these empirical rules. Cyanide titration of MPO has been shown by EPR, MCD<sup>27</sup> and magnetic susceptibility studies<sup>79</sup> to increase somewhat the content of low-spin heme.

Although such evidence supports the notion of two distinct hemes, this possibility is eliminated by the following observations. (1) The distinct heme hypothesis predicts that high-to-low spin conversion of the prosthetic groups should cause loss of the high-spin marker band at  $1549\text{ cm}^{-1}$ . Only slight loss of intensity is observed (Figs. 2a,c).<sup>†</sup> (2) The hypothesis cannot explain the apparent resistance of the native enzyme to undergo full reduction, as monitored by loss of the higher frequency oxidation state marker band ( $1376\text{ cm}^{-1}$ ), and intensification of the lower frequency band ( $1362\text{ cm}^{-1}$ ). (3) Nor can the hypothesis explain why the  $1362\text{ cm}^{-1}$  band shifts yet lower in frequency ( $1355\text{ cm}^{-1}$ ) upon reduction of the enzyme (Fig. 2a,b).<sup>††</sup> (4) The oxidation state marker band of native enzyme is insensitive to titration with  $\text{Co}(\text{bpy})_3^{3+}$  ion (data not shown). This reagent is sufficiently oxidizing

---

<sup>†</sup>Myeloperoxidase preparations contain several isozymes of differing kinetic behavior.<sup>98</sup> This heterogeneity also may contribute to the spectral complexity of the enzyme.

<sup>††</sup>Previous EPR and MCD studies have found that a fraction of the heme is resistant to cyanide-induced spin state changes.<sup>27</sup>

( $E^\circ = +310 \text{ mV}$  <sup>45</sup>) to convert ferrous MPO heme to the ferric state ( $E^\circ = +36 \text{ mV}$  <sup>20</sup>), and to cause the ferriheme component of a composite oxidation state marker band to intensify. This would shift the apparent oxidation state marker band to higher frequency, but is not observed.

The peculiar doublets in MPO resonance Raman spectra are more readily explained by assuming that the heme groups are chlorins. Our confidence in this conclusion was based initially on a comparison of MPO spectra with those of known inorganic chlorins, published by Kitagawa and coworkers, <sup>75</sup> and personally communicated to us by Drs. T.M. Loehr and L.A. Andersson (Oregon Graduate Center). Chlorin spectra are similar to analogous porphyrins, but demonstrate additional bands due to the effects of lower symmetry of the macrocycle. Such extra bands are observed in spectra of sulfmyoglobin, <sup>63</sup> iron octaethylchlorin, <sup>75</sup> *Pseudomonas aeruginosa* cytochrome oxidase, <sup>60</sup> iron deuterio-chlorin, <sup>64</sup> and copper(II) 2,6-di-n-pentyl-4-vinyl-7-hydroxy-8-acroleinyl-1,3,5,7-tetramethylchlorin. <sup>80</sup> Kitagawa and coworkers were first to suggest that the spectral richness of reduced porphyrins derives from the lower symmetry of the molecule. <sup>75</sup> The appearance of a relatively large number of bands in MPO spectra suggests the presence of one or more chlorin prosthetic groups.

Chlorin Raman spectra also differ from porphyrin spectra in the enhanced intensity of some modes, <sup>64,80</sup> and in a greater number of polarized bands. The increase in polarized

bands is especially conspicuous with visible excitation.<sup>81</sup> Myeloperoxidase spectra demonstrate these features (Figs. 2,3), as expected for a chlorin-containing protein.

Enhancement Profile. The excitation profile for oxidized MPO (Figure 5) provides further evidence that MPO contains chlorin. For all Raman bands, including those not listed in Figure 5, only negligible resonance enhancement is observed with laser excitation into the visible absorption bands. This contrasts with visible excitation of porphyrin-containing proteins, for which large increases in scattering occur as resonance is approached in the visible region. Oxyhemoglobin and methemoglobin show a 6- to 17-fold increase in scattering.<sup>82</sup>

Due to low signal-to-noise ratios in visible excitation MPO spectra, we were unable to quantify depolarization ratios. Qualitatively, we observed no inversely polarized bands. Within the limits of detection, most bands appeared polarized.

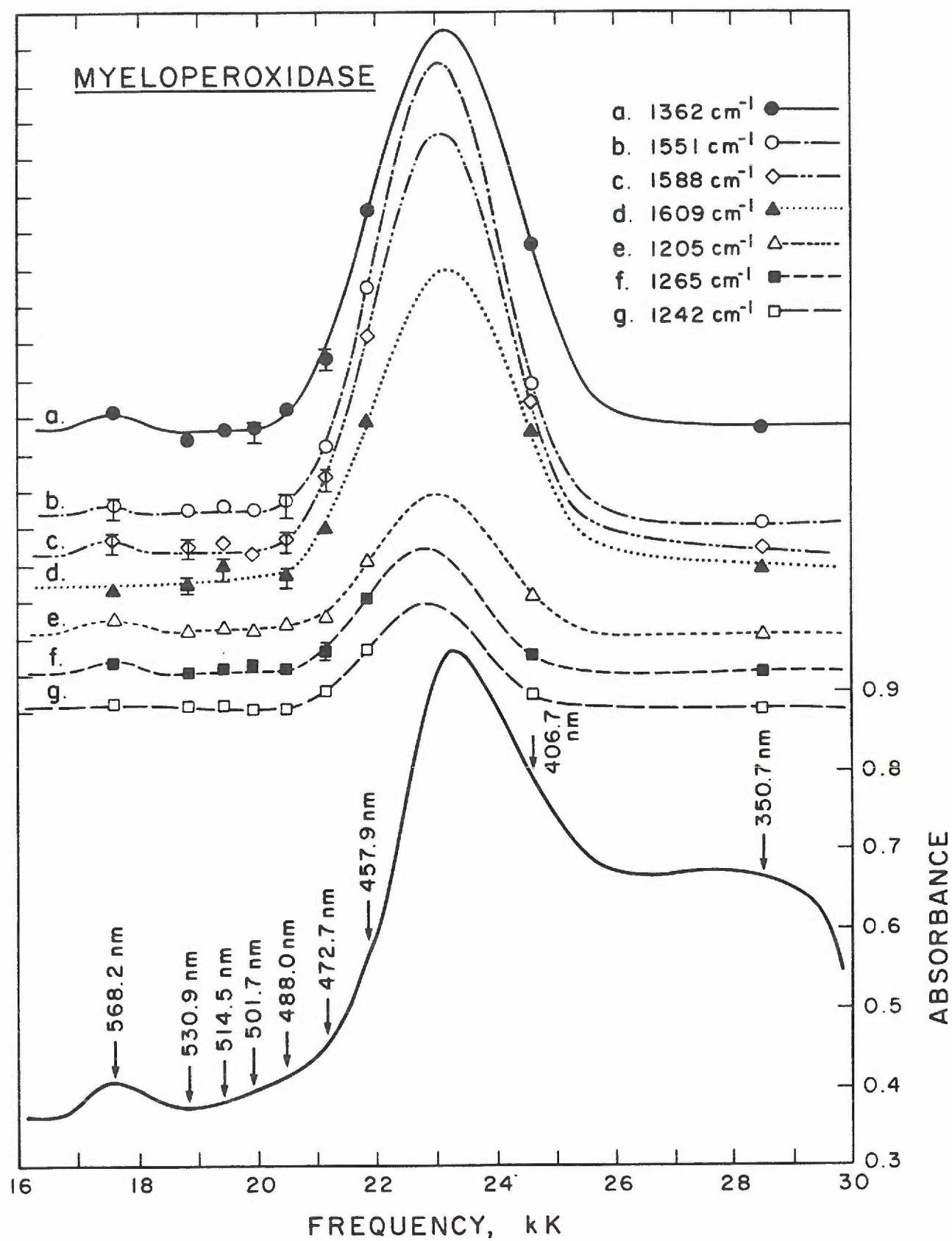
An explanation for these results follows a previous interpretation of the weakly resonance-enhanced Raman spectrum of horseradish peroxidase Compound I.<sup>83</sup> According to theoretical calculations:<sup>61</sup> (1) the lower molecular symmetry of a dihydroporphyrin lifts the degeneracy of the lowest unoccupied and highest occupied orbitals of the four-orbital model; (2) since the resulting excited states are non-identical, they do not undergo the sort of configuration interaction which leads, in the case of the porphyrins, to an intense Soret band and weak visible bands; and (3) the symmetry of the dihydroporphyrin molecular

---

**Figure 5**

Relative intensity enhancement profiles for canine myeloperoxidase. Intensities were measured relative to the  $982\text{ cm}^{-1}$  band of  $(\text{NH}_4)_2\text{SO}_4$  ( $\sim 0.5\text{ M}$ ). Error bars shown are those in the region below  $21.2\text{ kK}$  which exceeded the height of the symbol. Curves a-f between  $20\text{--}26\text{ kK}$  are shown as the gaussian fit to the data (Appendix). For clarity, each profile is displaced 10 units above the next lower profile (except curve a, which is displaced 20 units). The MPO absorption spectrum, given at the bottom of the Figure, is marked by arrows indicating laser excitation frequencies.

---



states thus permits transitions in the visible region which are directly allowed, and not vibronically mixed. If chlorin visible bands contain little or no vibronically-allowed component,<sup>83</sup> then B-term activity will be diminished and chlorin Raman spectra will consist primarily of A-term modes (Table 3). There are three practical consequences of this. (1) *Chlorin enhancement profiles will track chlorin electronic spectra.* Such tracking is not observed for higher-symmetry hemes and hemeproteins, which show instead comparable resonance enhancement upon exciting into either the strong Soret or the weak but vibronically-active visible bands. (2) *All observed Raman bands will be polarized.* Raman scattering from low symmetry porphyrins is permitted only by the A-term mechanism, hence all bands demonstrate A-term properties, including full polarization. (3) *When a chlorin visible band is relatively weak or unresolved, there may occur no detectable resonance enhancement of Raman bands.* Two examples illustrate these predictions.

*Example 1.* With excitation near the visible absorption bands of iron octaethylchlorin, high quality resonance Raman spectra are obtained.<sup>75</sup> The major octaethylchlorin visible band, at about 600 nm, is exceptionally intense ( $\epsilon_{\text{mM}}=24$ )<sup>59</sup> and well-resolved, and thus should allow relatively strong A-term scattering. Direct evidence for this is the increasing dominance of polarized bands as the excitation wavelength approaches the absorption maximum near 600 nm.<sup>81</sup>

*Example 2.* The visible absorption bands of MPO are

Table 3

Primary sources of porphyrin resonance Raman scattering (a)

	A TERM	B TERM
Intensity dependence	On allowedness of resonant electronic transitions	On extent of vibronic mixing between Q and B electronic states
Symmetry of sampled vibrations	Totally symmetric	Non-totally symmetric
Polarization properties	Polarized ( $\rho < 3/4$ )	Depolarized ( $\rho = 3/4$ ) and inversely polarized ( $\rho = \infty$ )
Contribution under Soret excitation	Dominant	Negligible
Contribution under visible excitation		Variable; in some cases, comparable to A term scattering

- a) The Raman scattering from a porphyrin has two basic sources.<sup>99</sup> The first source, A-term activity (Franck-Condon scattering), is indicated by the enhancement of the porphyrin's totally symmetric modes. The intensities of these A-term modes depend on the magnitude of the transition dipole moment of the resonant electronic state, and inversely upon bandwidth. Hence, large enhancement is observed with excitation into strongly allowed electronic bands. With Soret excitation, A-term scattering dominates a porphyrin Raman spectrum. The second source of Raman scattering is B-term activity (Herzberg-Teller scattering), characterized by resonance enhancement of vibrations involved in vibronic mixing of the Q and B electronic states. Theory predicts for a porphyrin macrocycle of  $D_{4h}$  symmetry that these modes are depolarized or anomalously polarized.<sup>100</sup> The intensities of these modes depend on the product of the transition dipole moments of the mixing states (i.e., the magnitude of the mixing integral). For some porphyrins, the visible excitation Raman spectrum is dominated by B-term scattering, whereas for other porphyrins the A- and B-term contributions are comparable.



relatively weak ( $\epsilon_{\text{mM}}=13$ )<sup>27</sup> and poorly resolved. Upon exciting into these bands, purely A-term resonance enhancement should be commensurately weak, as observed (Figure 5). We do not predict that it is *impossible* to obtain visible excitation spectra from MPO: this is a straightforward technical problem that can be met by long sampling times and optimally concentrated samples. We predict only that resonance enhancement will be weak. Our attempts to obtain high-quality MPO spectra with visible excitation were not successful. Our best spectrum was obtained using 35 mW of 568 nm excitation, and nine hours of sampling time. From this experiment, we achieved a signal-to-noise ratio of about 2 or less. Other attempts were less successful. For chlorins and chlorin-containing proteins (Table 4) which have weak or unresolved visible bands, we predict similar behavior.

Related Studies by Other Groups. Since first publishing our results,<sup>53</sup> two other groups have reported Raman spectra of MPO.<sup>56,84</sup> The interpretations of these groups conform to our own.<sup>†</sup> Except for minor discrepancies in some band frequencies ( $\pm 3 \text{ cm}^{-1}$ ), spectra reported by these other groups are virtually identical to our own. However, spectra of ferric myeloperoxidase obtained by Babcock and coworkers contain a band at  $1568 \text{ cm}^{-1}$ ,<sup>56</sup> which is not present in our spectra

---

<sup>†</sup>Priority is assignable.<sup>101</sup>

Table 4

Selected Proteins Which Contain Reduced Porphyrin (a)

Protein	References
Assimilatory nitrite/sulfite reductase	b, c, d, f
Coenzyme F430	e
<i>Escherichia coli</i> cytochrome b558-d complex	g
<i>Escherichia coli</i> cytochrome oxidase	h
Myeloperoxidase	i
<i>Neurospora crassa</i> catalase	j
<i>Nitrosomonas europaea</i> hydroxylamine oxidoreductase P-460	k, l
<i>Photobacterium phosphoreum</i> cytochrome bd	m
<i>Propionibacterium shermanii</i> cytochrome d630	n
<i>Pseudomonas aeruginosa</i> cytochrome oxidase	o, p
Sulfcatalase	q
Sulfhemoglobin	r
Sulflactoperoxidase	s
Sulfmyoglobin	t
Vitamin B12	u

a)	Also see: Poole, R.K. <u>Biochim. Biophys. Acta</u> 1983, <u>726</u> , 205-243; Lemberg, R.; Barrett, J. "The Cytochromes"; Academic Press: New York, 1973; pp 233-326.
b)	Vega, J.M.; Garrett, R.H.; Siegel, L.M. <u>J. Biol. Chem.</u> 1975, <u>250</u> , 7980-7989.
c)	Murphy, M.J.; Siegel, L.M.; Kamin, H.; Rosenthal, D. <u>J. Biol. Chem.</u> 1973, <u>248</u> , 2801-2814.
d)	Ondrias, M.R.; Carson, S.D.; Hirasawa, M.; Knaff, D.B. <u>Biochim. Biophys. Acta</u> 1985, <u>830</u> , 159-163.
e)	Shiemke, A.K.; Eirich, L.D.; Loehr, T.M. <u>Biochim. Biophys. Acta</u> 1983, <u>748</u> , 143-147.
f)	Timkovich, R.; Cork, M.S.; Taylor, P.V. <u>J. Biol. Chem.</u> 1984, <u>259</u> , 1577-1585.
g)	Kita, K.; Konishi, K.; Anraku, Y. <u>J. Biol. Chem.</u> 1984, <u>259</u> , 3375-3381.
h)	Poole, R.K.; Baines, B.S.; Hubbard, J.A.M.; Hughes, M.N.; Campbell, N.J. <u>FEBS Lett.</u> 1982, <u>150</u> , 147-150.
i)	Sibbett, S.S.; Hurst, J.K. <u>Biochemistry</u> 1984, <u>23</u> , 3007-3013.
j)	Jacobs, G.S.; Orme-Johnson, W.H. <u>Biochemistry</u> 1979, <u>18</u> , 2967-80.
k)	Unpublished data cited in footnote 5 of ref 1.
l)	Andersson, K.K.; Kent, T.A.; Lipscomb, J.D.; Hooper, A.B.; Munck, E. <u>J. Biol. Chem.</u> 1984, <u>259</u> , 6833-6840.
m)	Watanabe, H.; Kamita, Y.; Nakamura, T.; Takimoto, A.; Yamanaka, T. <u>Biochim. Biophys. Acta</u> 1979, <u>547</u> , 70-78.
n)	Asmundson, R.V.; Pritchard, G.G. <u>Arch. Microbiol.</u> 1983, <u>136</u> , 285-290.

*Table 4, continued*

- o) Cotton, T.M.; Timkovich, R.; Cork, M.S. FEBS Lett. 1981, 133, 39-44.
- p) Ching, Y.; Ondrias, M.R.; Rousseau, D.L.; Muhoberac, B.B.; Wharton, D.C. FEBS Lett. 1982, 138, 239-244.
- q) Nicholls, P. Biochem. J. 1961, 81, 374-383.
- r) Brittain, T.; Greenwood, C.; Barber, D. Biochim. Biophys. Acta 1982, 705, 26-32.
- s) Nakamura, S.; Nakamura, M.; Yamazaki, I.; Morrison, M. J. Biol. Chem. 1984, 259, 7080-7085.
- t) Andersson, L.A.; Loehr, T.M.; Lim, A.R.; Mauk, A.G. J. Biol. Chem. 1984, 259, 15340-15349.
- u) Salama, S.; Spiro, T.G. J. Ram. Spec. 1977, 6, 57-60.

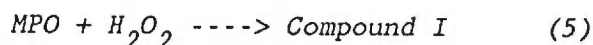
(Figure 2). They attribute the difference to low resolution, but this appears to be incorrect for two reasons. First, resolution of our spectra is equivalent to the Babcock spectra. Second, spectra reported by a third group also contain no band at  $1568\text{ cm}^{-1}$ ,<sup>84</sup> in conformity with our data. Since the anomalous band is absent in spectra of both canine and human forms of the enzyme, it cannot derive from differences in primary structure between species. In obtaining their MPO spectra, Babcock and coworkers employed laser powers of about 100 mW. Although such high powers reduce sampling times, they also tend to denature protein samples, and may be the origin of the anomalous extra band.

Heme equivalence. *Pseudomonas aeruginosa* cytochrome c peroxidase contains two structurally and functionally distinct c-type hemes. Physical characterization by a variety of techniques has shown that the resting enzyme contains one low-spin and one high-spin ferriheme.<sup>68,85</sup> Kinetic analysis suggests that the catalytically active form of the peroxidase is a one-electron reduced ferro-ferriheme; the high-spin ferriheme is thought to be the site of peroxidative action, while the low-spin ferroheme serves an electron transport function.<sup>24</sup> Since MPO is dimeric, similar bifunctional organization is possible. If the hemes have distinct electronic spectra, then they might be distinguished by selective enhancement of one or the other sets of resonance Raman bands as the excitation wavelength is varied across the Soret envelope. If the electronic spectra are

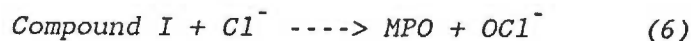
coincident, then the relative resonance Raman band intensities will be wavelength independent. The resonance Raman spectra of native MPO obtained with 454 nm and 406 nm excitation differ in some respects. Most notably, the asymmetric doublet peak ( $1362/1376\text{ cm}^{-1}$ ) in the oxidation state marker region under 454 nm excitation (Fig. 2) is seen as a broad asymmetric band centered at  $1367\text{ cm}^{-1}$  under 406 nm excitation (Fig. 4). Also, the intensity of the  $1550\text{ cm}^{-1}$  band is diminished slightly in the 406 nm spectrum relative to the other peaks in the core size marker region. Although this wavelength dependence might arise from inequivalent hemes, effects of similar character are apparent in the published spectra of iron octaethylchlorin which cannot be attributed to selective enhancement.<sup>75</sup> Hence, our data provide no evidence for heme inequivalence.

Functional Roles for Chlorin in Chloride Peroxidation.

The peroxidation of chloride ion by MPO begins with formation of MPO Compound I:<sup>37,86</sup>



Compound I contains two oxidizing equivalents more than the resting enzyme, and rapidly oxidizes chloride ion in a concerted two-electron step to hypochlorite:



By analogy with other peroxidases, MPO Compound I is probably an oxo-bound ferryl chlorin  $\pi$ -cation radical.<sup>39,87</sup> This species

is inactivated by one-electron reduction to ferryl chlorin Compound II.

Inorganic metallochlorins undergo one-electron oxidation to the  $\pi$ -cation radical at reduction potentials about 300 mV less positive than analogous porphyrins.<sup>59,88</sup> In other words, the energetics of oxidation are more favorable for chlorins than porphyrins. Consequently the reverse process, which occurs in the formation of  $\text{OCl}^-$  by reaction 6, probably is disfavored for chlorins relative to porphyrins. Hence, in comparison to the conventional porphyrin group, there does not appear to be a thermodynamic advantage to the unusual chlorin prosthetic group of MPO.

Since the disrupted  $\pi$ -conjugation of hydroporphyrin enhances structural flexibility of the macrocycle, adjustments in core size are more easily achieved than porphyrins.<sup>89</sup> Based on this observation, we suggested that the MPO chlorin possibly has a preferred role in the axial binding of weak-field chloride ion.<sup>53</sup> However, recent studies indicate that MPO activity is competitively inhibited by chloride with respect to hydrogen peroxide,<sup>86</sup> which renders the suggestion unlikely.

Alternatively, we suggested that the ring charge asymmetry of chlorin ferryl  $\pi$ -cations<sup>90</sup> may provide an unusually reactive peripheral site for chloride ion oxidation.<sup>53</sup> The dominant reaction between chloride ion and metalloporphyrin  $\pi$ -cations<sup>91</sup> and other aromatic  $\pi$ -cations<sup>92</sup> appears to be electron transfer, not nucleophilic addition leading to ring chlorination.

Since reduction of HOCl is highly sensitive to the nucleophilic character of the reductant,<sup>93</sup> incipient bond formation must precede electron transfer. Ferryl  $\pi$ -cation chlorins in the electronic ground state are calculated to have  $a_2$  symmetry, for which certain methine positions are relatively electron deficient.<sup>90</sup> These sites may serve as the unique peripheral sites for chloride oxidation by MPO Compound I. Other attractive features of this suggestion are the relative proximity of chloride to a putative axially-bound oxygen, and the feasibility of rapid intramolecular electron transfer between chlorin ring and ferryl iron.<sup>94</sup> Discussion of the functional importance of a chlorin prosthetic group continues in the following chapter.

# REFERENCES

1. a) Klebanoff, S.J.; Clark, R.A. "The Neutrophil: Function and Clinical Disorders"; North-Holland, Amsterdam, 1978. b) Klebanoff, S.J. Annals Int. Med. 1980, 93, 480-489.
2. Harrison, J.E.; Schultz, J. J. Biol. Chem. 1976, 251, 1371-1374.
3. a) Agner, K. Abstr. 4th Intl. Congr. Biochemistry 1958, p64, Abstract 5-58. b) Agner, K. In: "Structure and Function of Oxidation-Reduction Enzymes"; (Akeson, A.; Ehrenberg, A., Eds.); Pergamon Press: Oxford, 1972; pp 329-335. c) Lee, C.W.; Lewis, R.A.; Tauber, A.I.; Mehrotra, M.; Corey, E.J.; Austen, K.F. J. Biol. Chem. 1983, 258, 15004-15019.
4. Albrich, J.M.; McCarthy, C.A.; Hurst, J.K. Proc. Natl. Acad. Sci. USA 1981, 78, 210-214.
5. a) Rosen, H.; Klebanoff, S.J. J. Biol. Chem. 1977, 252, 4803-4810. b) Allen, R.C. Biochem. Biophys. Res. Commun. 1975, 63, 675-683.
6. a) Arnold, S.J.; Ogryzlo, E.A.; Witzke, H. J. Chem. Phys. 1964, 40, 1769-1770. b) Kahn, A.U.; Kasha, M. J. Chem. Phys. 1963, 39, 2105-2106.
7. Wilshire, J.; Sawyer, D.T. Acc. Chem. Res. 1979, 12, 105-132.
8. a) Held, A.M.; Hurst, J.K. Biochem. Biophys. Res. Comm. 1978, 81, 878-885. b) Harrison, J.E.; Watson, B.D.; Schultz, J. FEBS Lett. 1978, 92, 327-332.
9. Kahn, A.U. Biochem. Biophys. Res. Comm. 1984, 122, 668-675.
10. Klebanoff, S.J. J. Bacteriol. 1968, 95, 2131-2138.
11. Kanofsky, J.R.; Wright, J.; Tauber, A.I. FEBS Lett. 1985, 187, 299-301.
12. Diem, K.; Lentner, C. In: "Scientific Tables"; (Basle, J.R., Ed.); Geigy S.A., 1970; pp 562-563.
13. Agner, K. Acta Chem. Scand. 1958, 12, 89-94.
14. Naskalski, J.W. Biochim. Biophys. Acta 1977, 485, 291-300.
15. Matheson, N.R.; Wong, P.S.; Travis, J. Biochemistry 1981, 20, 325-330.



16. Wu, N.C.; Schultz, J. FEBS Lett. 1975, 60, 141-144.
17. Schultz, J.; Wu, N.C.; Marti, R. Biochemistry 1983, 22(15), 14A.
18. Newton, N.; Morell, D.B.; Clarke, L. Biochim. Biophys. Acta 1965, 96, 463-475.
19. Newton, N.; Morell, D.B.; Clarke, L.; Clezy, P.S. Biochim. Biophys. Acta 1965, 96, 476-486.
20. Harrison, J.E.; Schultz, J. Biochim. Biophys. Acta 1978, 536, 341-349.
21. Nichol, A.W.; Morell, D.B.; Thomson, J. Biochem. Biophys. Res. Commun. 1969, 36, 576-581.
22. Odajima, T.; Yamazaki, I. Biochim. Biophys. Acta 1972, 284, 368-374.
23. Adar, F. Porphyrins, 1978, 3, 167-209.
24. Ronnberg, M.; Araiso, T.; Ellfolk, N.; Dunford, H.B. Arch. Biochem. Biophys. 1981, 207, 197-204.
25. Morell, D.B.; Chang, Y.; Hendry, I.; Nichol, A.W.; Clezy, P.S. In: "Structure and Function of Cytochromes"; (Okunuki, K.; Kamen, M.D.; Sekuzu, I., Eds.); University Park Press: Baltimore, 1968; pp 563-571.
26. Walsh, T.A.; Johnson, M.K.; Barber, D.; Thomson, A.J.; Greenwood, C. J. Inorg. Biochem. 1980, 14, 15-31.
27. Eglinton, D.G.; Barber, D.; Thompson, A.J.; Greenwood, C.; Segal, A.W. Biochim. Biophys. Acta 1982, 703, 187-195.
28. Inhoffen, H.H.; Jager, P.; Mahlhof, R. Justus Liebigs Ann. Chem. 1971, 749, 109-116.
29. Odajima, T. J. Biochem. (Tokyo) 1980, 87, 379-391.
30. a) Barrett, J. Biochem. J. 1956, 64, 626-639. b) Barrett, J.; Clezy, P. Nature 1958, 184, 1988-1990.
31. Andrews, P.C.; Krinsky, N. J. Biol. Chem. 1980, 256, 4211-4218.
32. a) Harrison, J.E.; Pabalan, S.; Schultz, J. Biochim. Biophys. Acta 1977, 493, 247-259. b) Olsson, I.; Olofsson, T.; Odeberg, H. Scand. J. Haematol. 1972, 9, 483-491.

33. Andrews, P.C.; Parnes, C.; Krinsky, N.I. Arch. Biochem. Biophys. 1984, 228, 439-442.
34. Bakkenist, A.R.J.; DeBoer, J.E.G.; Plat, H.; Wever, R. Biochim. Biophys. Acta 1980, 613, 337-348.
35. Harrison, J.E. J. Biol. Chem. 1979, 254, 4536-4539.
36. Andrews, P.C.; Krinsky, N.I. J. Biol. Chem. 1982, 257, 13240-13245.
37. Harrison, J.E. Miami Winter Symp. 1976, 12, 305-317.
38. Wever, R.; Kast, W.M.; Kasinoedin, J.H.; Boelens, R. Biochim. Biophys. Acta 1982, 709, 212-219.
39. Harrison, J.E.; Araiso, T.; Palcic, M.M.; Dunford, H.B. Biochem. Biophys. Res. Commun. 1980, 94, 34-40.
40. a) Henderson, W.R.; Klebanoff, S.J. J. Biol. Chem. 1983, 258, 13522-13527. b) Weiss, S.J.; Lampert, M.B.; Test, S.T. Science 1983, 222, 625-628.
41. Spiro, T.G. In: "Iron Porphyrins", Part 2; (Lever, A.B.P.; Gray, H.B., Eds.); Addison-Wesley: Reading, MA, 1983; pp 91-159.
42. Schultz, J.; Schmukler, H.W. Biochemistry 1964, 3, 1234-1238.
43. Olsen, R.L.; Little, C. Biochem. J. 1983, 209, 781-787.
44. a) Agner, K. Acta Phys. Scand. 1941, Vol. II, Suppl. VIII, 5-61. b) Odajima, T.; Yamazaki, I. Biochim. Biophys. Acta 1972, 284, 360-367. c) Wever, R.; Bakkenist, A.R.J. Biochim. Biophys. Acta 1980, 612, 178-184.
45. Ciana, A.; Crescenzi, V. Gazz. Chim. Ital. 1978, 108, 519-522.
46. Berkoff, R.; Krist, K.; Gafney, H.D. Inorg. Chem. 1980, 19, 1-7.
47. Loehr, T.M.; Keyes, W.E.; Pincus, P.A. Anal. Biochem. 1979, 96, 456-463.
48. Sjoberg, B-M.; Loehr, T.M.; Sanders-Loehr, J. Biochemistry 1982, 21, 96-102.
49. a) Tsubaki, M.; Nagai, K.; Kitagawa, T. Biochemistry 1980, 19, 379-385. b) Van Steelandt-Frentrup, J.; Salmeen, I.; Babcock, G.T. J. Am. Chem. Soc. 1981, 103, 5981-5982.

50. Callahan, P.M.; Babcock, G.T. Biochemistry 1983, 22, 452-461.
51. Choi, S.; Lee, J.J.; Wei, Y.H.; Spiro, T.G. J. Am. Chem. Soc. 1983, 105, 3692-3707.
52. Chang, C.K. In: "Biochemical & Clinical Aspects of Oxygen"; (Caughey, W.S.; Caughey, H., Eds.); Academic Press: New York, 1979; pp 437-454.
53. Sibbett, S.S.; Hurst, J.K. Biochemistry 1984, 23, 3007-3013.
54. Ogura, T.; Sone, N.; Tagawa, K.; Kitagawa, T. Biochemistry 1984, 23, 2826-2831.
55. Nicholls, P. Biochem. J. 1961, 81, 374-383.
56. Babcock, G.T.; Ingle, R.T.; Oertling, W.A.; Davis, J.C.; Averill, B.A.; Hulse, C.L.; Stufkens, D.J.; Bolscher, B.G.J.M.; Wever, R. Biochim. Biophys. Acta 1985, 828, 58-66.
57. Chang, C.K. J. Biol. Chem. 1985, 260, 9520-9522.
58. a) Gouterman, M. Porphyrins, 1978, 3, 1-165. b) Petke, J.D.; Maggiora, G.M.; Shipman, L.L.; Cristoffersen, R.E. J. Mol. Spectrosc. 1973, 73, 311-331.
59. Stolzenberg, A.M.; Strauss, S.H.; Holm, R.H. J. Am. Chem. Soc. 1981, 103, 4763-4778.
60. Ching, Y.; Ondrias, M.R.; Rousseau, D.L.; Muhoberac, B.B.; Wharton, D.C. FEBS Lett. 1982, 138, 239-244.
61. Weiss, C. Porphyrins, 1978, 3, 211-223.
62. Abe, M.; Kitagawa, T.; and Kyogoku, Y. J. Chem. Phys. 1978, 69, 4526-4534.
63. Andersson, L.A.; Loehr, T.M.; Lim, A.R.; Mauk, A.G. J. Biol. Chem. 1984, 259, 15340-15349.
64. Andersson, L.A.; Loehr, T.M.; Chang, C.K.; Mauk, A.G. J. Am. Chem. Soc. 1985, 107, 182-191.
65. Teraoka, J.; Kitagawa, T. J. Biol. Chem. 1981, 256, 3969-3977.
66. Teraoka, J.; Kitagawa, T. (1980) J. Phys. Chem. 84, 1928-1935.
67. Sievers, G.; Gadsby, P.M.A.; Peterson, J.; Thomson, J.A. Biochim. Biophys. Acta 1983, 742, 659-668.

68. Ronnberg, M.; Osterlund, K.; Ellfolk, N. Biochim. Biophys. Acta 1980, 626, 23-30.
69. Bolscher, B.G.J.M.; Plat, H.; Wever, R. Biochim. Biophys. Acta 1984, 784, 177-186.
70. Reid, T.J., III; Murthy, M.R.N.; Sicignano, A.; Tanaka, N.; Musick, W.D.L.; Rossmann, M.G. Proc. Natl. Acad. Sci. USA 1981, 78, 4767-4771.
71. Nagai, K.; Kagimoto, T.; Hayashi, A.; Taketa, F.; Kitagawa, T. Biochemistry 1983, 22, 1305-1311.
72. a) Keyes, W.E.; Loehr, T.M.; Taylor, M.L. Biochem. Biophys. Res. Commun. 1978, 83, 941-945. b) Que, L. Coord. Chem. Rev. 1983, 50, 73-108.
73. Browett, W.R.; Stillman, M.J. Biochim. Biophys. Acta 1979, 577, 291-306.
74. Maltempo, M.M.; Moss, T.H. Q. Rev. Biophys. 1976, 9, 181-215.
75. Ozaki, Y.; Kitagawa, T.; Ogoshi, H. Inorg. Chem. 1979, 18, 1772-1776.
76. Rakshit, G.; Spiro, T.G. Biochemistry 1974, 13, 5317-5323.
77. Kimura, S.; Yamazaki, I.; Kitagawa, T. Biochemistry 1981, 20, 4632-4638.
78. Kitagawa, T.; Hashimoto, S.; Teraoka, J.; Nakamura, S.; Yajima, H.; Hosoya, T. Biochemistry 1983, 22, 2788-2792.
79. a) Dunford, H.B.; Stillman, J.S. Coord. Chem. Rev. 1976, 19, 187-251. b) Ehrenberg, A. Arkiv Kemi 1962, 19, 119-128.
80. Hanson, L.K.; Chang, C.K.; Ward, B.; Callahan, P.M.; Babcock, G.T.; Head, J.D. J. Am. Chem. Soc. 1984, 106, 3950-3958.
81. See footnote 5 of reference 53.
82. a) Strekas, T.C.; Packer, A.J.; Spiro, T.G. J. Ram. Spec. 1973, 1, 197-206. b) Strekas, T.C.; Spiro, T.G. J. Ram. Spec. 1973, 1, 387-392.
83. Felton, R.H.; Romans, A.Y.; Yu, N.T.; Schonbaum, G.R. Biochim. Biophys. Acta 1976, 434, 82-89.
84. Ikeda-Saito, M.; Argade, P.V.; Rousseau, D.L. FEBS Lett. 1985, 184, 52-55.

85. Aasa, R.; Ellfolk, N.; Ronnberg, M.; Vanngard, T. Biochim. Biophys. Acta 1981, 670, 170-175.
86. Bolscher, B.G.J.M.; Wever, R. Biochim. Biophys. Acta 1984, 788, 1-10.
87. Palmer, G. In: "The Iron Porphyrins", Part 2; (Lever, A.B.P.; Gray, H., Eds.); Addison-Wesley: Reading, PA, 1983; pp 43-88.
88. Fuhrhop, J.H. Z. Naturforsch. 1970, 25b, 255-265.
89. a) Strauss, S.H.; Silver, M.E.; Ibers, J.A. J. Am. Chem. Soc. 1983, 105, 4108-4109. b) Strauss, S.H.; Silver, M.E.; Long, K.M.; Thompson, R.G.; Hudgens, R.A.; Spartalian, K.; Ibers, J.A. J. Am. Chem. Soc. 1985, 107, 4207-4215.
90. Hanson, L.K.; Chang, C.K.; Davis, M.S.; Fajer, J. J. Am. Chem. Soc. 1981, 103, 633-670.
91. Smith, K.M.; Barnett, G.H.; Evans, B.; Martynenko, Z. J. Am. Chem. Soc. 1979, 101, 5953-5961.
92. Ristagno, C.V.; Shine, H.J. J. Org. Chem. 1971, 36, 4050-4055.
93. a) Held, A.M.; Halko, D.J.; Hurst, J.K. J. Am. Chem. Soc. 1978, 100, 5732-40. b) Hurst, J.K.; Carr, P.A.G.; Hovis, F.E.; Richardson, R.J. Inorg. Chem. 1981, 20, 2435-2438.
94. Johnson, E.C.; Niem, T.; Dolphin, D. Can. J. Chem. 1978, 56, 1381-1388.
95. Personal communication from Dr. V. Renganathan (Oregon Graduate Center).
96. Ortiz de Montellano, P.R.; Correia, M.A. Ann. Rev. Pharmacol. Toxicol. 1983, 23, 481-503.
97. Abeles, R.H. Chem. Eng. News 1983, Sept. 19, pp 48-56.
98. a) Feldberg, N.T.; Schultz, J. Arch. Biochem. Biophys. 1972, 148, 407-413. b) Kinkade, J.M., Jr.; Pember, S.O.; Barnes, K.C.; Shapira, R.; Spitznagel, J.K.; Martin, L.E. Biochem. Biophys. Res. Comm. 1983, 114, 296-303. c) Pember, S.O.; Fuhrer-Krusi, S.M.; Barnes, K.C.; Kinkade, J.M., Jr. FEBS Lett. 1982, 140, 103-107. d) Yamada, M.; Mori, M.; Sugimura, T. J. Biochem. 1983, 93, 1661-1668.

99. Albrecht, A.C.; Hutley, M.C. J. Chem. Phys. 1971, 55, 4438-4443.
100. Spiro, T.G.; Strekas, T.C. Proc. Natl. Acad. Sci. USA 1972, 69, 2622-2626.
101. a) Sibbett, S.S.; Loehr, T.M.; Hurst, J.K. Abstr. Pap. Am. Chem. Soc. INOR. 1984, 187, 27. b) Bolscher, B.G.J.M.; Wever, R.; Babcock, G.T. Symp. Pap. 8th Int. Biophys. Congr. 1984, p 135. c) Ikeda-Saito, M.; Prince, R.C.; Argade, P.V.; Rousseau, D.L. Fed. Proc. 1984, 43, 1561.

## Chapter 2

### *Eosinophil peroxidase*

The capability for catalyzing a two-electron peroxidation of chloride ion to hypochlorous acid is not unique to myeloperoxidase (MPO), but also a property of eosinophil peroxidase (EPO).<sup>1</sup> Hypochlorous acid appears to be the primary toxin in microbicidal reactions of both MPO and EPO.<sup>2,3</sup> The active MPO system is effective against bacteria, viruses, fungi, mycoplasma and tumor cells,<sup>4,5</sup> whereas the EPO system appears to be targeted primarily against protozoa,<sup>6</sup> nematodes,<sup>3</sup> and other blood-inhabiting parasites.<sup>7</sup> The two enzymes are isolated from white blood cells (leukocytes) having cytoplasmic granules and bi-lobed nuclei, but from different subfractions distinguished by granule texture. Eosinophilic leukocytes have coarse granules and contain EPO; neutrophilic leukocytes have fine granules and contain MPO.

Although functionally similar, EPO and MPO have different optical and electron paramagnetic resonance (EPR) spectra,<sup>8</sup> different chromatographic and electrophoretic behavior, and no antigenic similarity.<sup>9</sup> The spectral differences of the two enzymes are probably due to different molecular structures of the incorporated prosthetic groups. Resonance Raman and MCD spectra demonstrate that MPO contains iron chlorin.<sup>10,11</sup> In contrast,

the optical spectra of EPO have been interpreted to originate from protoheme.<sup>1,8,12,13</sup> This interpretation is based upon the resemblance between optical spectra of EPO and lactoperoxidase (LPO), an enzyme known to contain protoheme.<sup>†</sup> To clarify the functional requirement for chlorin in halide peroxidation, we conducted a study of EPO by resonance Raman spectroscopy.

---

<sup>†</sup>Lactoperoxidase is isolated from bovine milk and human colostrum,<sup>42</sup> but not human milk.<sup>43</sup> The enzyme catalyzes peroxidation of bromide, iodide, and thiocyanate ion ( $\text{SCN}^-$ ), but not chloride ion.<sup>44</sup>



# MATERIALS AND METHODS

Horse EPO was provided by Prof. Seymour J. Klebanoff (University of Washington, Seattle, WA). The purification procedures have been described previously.<sup>13</sup> Enzymes samples contained 1.0 M NaCl and 0.05 M sodium acetate buffer at pH 4.7. A value of 1.05 was determined for the absorbance ratio  $A_{415 \text{ nm}}/A_{280 \text{ nm}}$ .

Human EPO was provided by Dr. Gerald Gleich. The enzyme was obtained as the void volume of a Sephadex G-50 chromatographic separation of granules from a subject with eosinophilia.<sup>14</sup> Samples contained 0.15 M NaCl and 0.05 M sodium acetate buffer at pH 4.3. Based on the reported molar extinction coefficient,  $\epsilon_{413 \text{ nm}} = 1.1 \times 10^5 \text{ M}^{-1} \text{ cm}^{-1}$ ,<sup>8</sup> the concentration of the human enzyme was calculated to be  $1.8 \times 10^{-5} \text{ M}$ . The measured absorbance ratio  $A_{413 \text{ nm}}/A_{275 \text{ nm}}$  was 0.38.

Raman spectra were obtained on the suspensions by procedures described in the preceding chapter. No evidence of sample degradation was observed in successive scans. Cyanide derivatives were prepared by spectrophotometric titration with solid potassium cyanide (Baker reagent grade).<sup>10</sup> The Soret maximum of the cyanide-derivative of human EPO was observed at 431 nm, which compares favorably with a reported value of 432.5 nm.<sup>8</sup>

## RESULTS

Resonance Raman spectra of chlorins are typified by relatively large numbers of bands,<sup>15</sup> many of which are intense.<sup>16-18</sup> Raman spectra of horse and human EPO (Figures 6,7) do not contain such bands, but instead are similar to known protoporphyrin-containing proteins, such as hemoglobin,<sup>19</sup> intestinal peroxidase,<sup>20</sup> horseradish peroxidase,<sup>21</sup> and lactoperoxidase (Table 5).<sup>22</sup> In the oxidation state marker region, for example, EPO spectra obtained with Soret excitation demonstrate a single intense band in the oxidation state marker region, at  $1365\text{ cm}^{-1}$ . This feature is typical of spectra from protoheme-containing proteins. In MPO spectra, however, at least two bands are observed in the region between  $1355$  and  $1375\text{ cm}^{-1}$ . A second conspicuous feature of the ferric EPO spectrum is the low intensities of bands between  $1545$  and  $1615\text{ cm}^{-1}$  relative to the  $1365\text{ cm}^{-1}$  band. This feature is typical of protoheme-containing proteins, but not observed in resonance Raman spectra of MPO in which at least three bands are present, each with an intensity comparable to bands in the oxidation state marker region.

Several anomalously polarized vibrational bands ( $\rho > 3/4$ ) are observed with excitation into the EPO visible absorption bands. With  $514.5\text{ nm}$  laser excitation, these bands are found at  $1560$ ,  $1423$ ,  $1389$ ,  $1337$ , and  $1302\text{ cm}^{-1}$  (Figure 7). The appearance of anomalously polarized bands indicates that the EPO heme is a relatively high-symmetry porphyrin.<sup>23,24</sup> This

Table 5  
Raman Frequencies of Ferric Eosinophil Peroxidase  
and Other Heme-containing Enzymes (a)

EPO	Hb	IPO	HRP	LPO	MPO
	1622	1622	1630	1622	
1613	1610		1608		1610
1581	1585	1586	1575	1593	1585
	1564	1564		1560	
	1550		1548		1550
1512	1515	1526		1527	1524
1477	1480	1485	1500	1484	1481
1442	1454				
1418	1427		1430		
	1392		1405		
1365	1372	1375	1374	1373	1376
					1362
1336	1345	1344		-	1331
1281	1312	1306	1302	-	1306
					1265
	1224		1238	-	1240
1207	1216			-	1205
1167	1173		1170	-	1163
	1133	-	1140	-	1132
1116		-		-	1106
		-		-	1069
		-		-	1029
	1008	-		-	1003
988	999	-	990	-	974
927	-	-		-	
841	-	-		-	859
816	-	-		-	837
789	-	-		-	
750	-	-	755	-	749
706	-	-		-	715

(continued)

Table 5, continued

675	-	677	675	-	675
	-		592	-	
545	-			-	557
	-			-	517
489	-	488		-	
475	-		441	-	437
408	-	416	408	-	409
	-		380	-	
	-		350	-	
335	-	329		-	329
324	-		321	-	
275	-		292	-	
258	-	260	274	-	
	-	223		-	219
	-			-	179

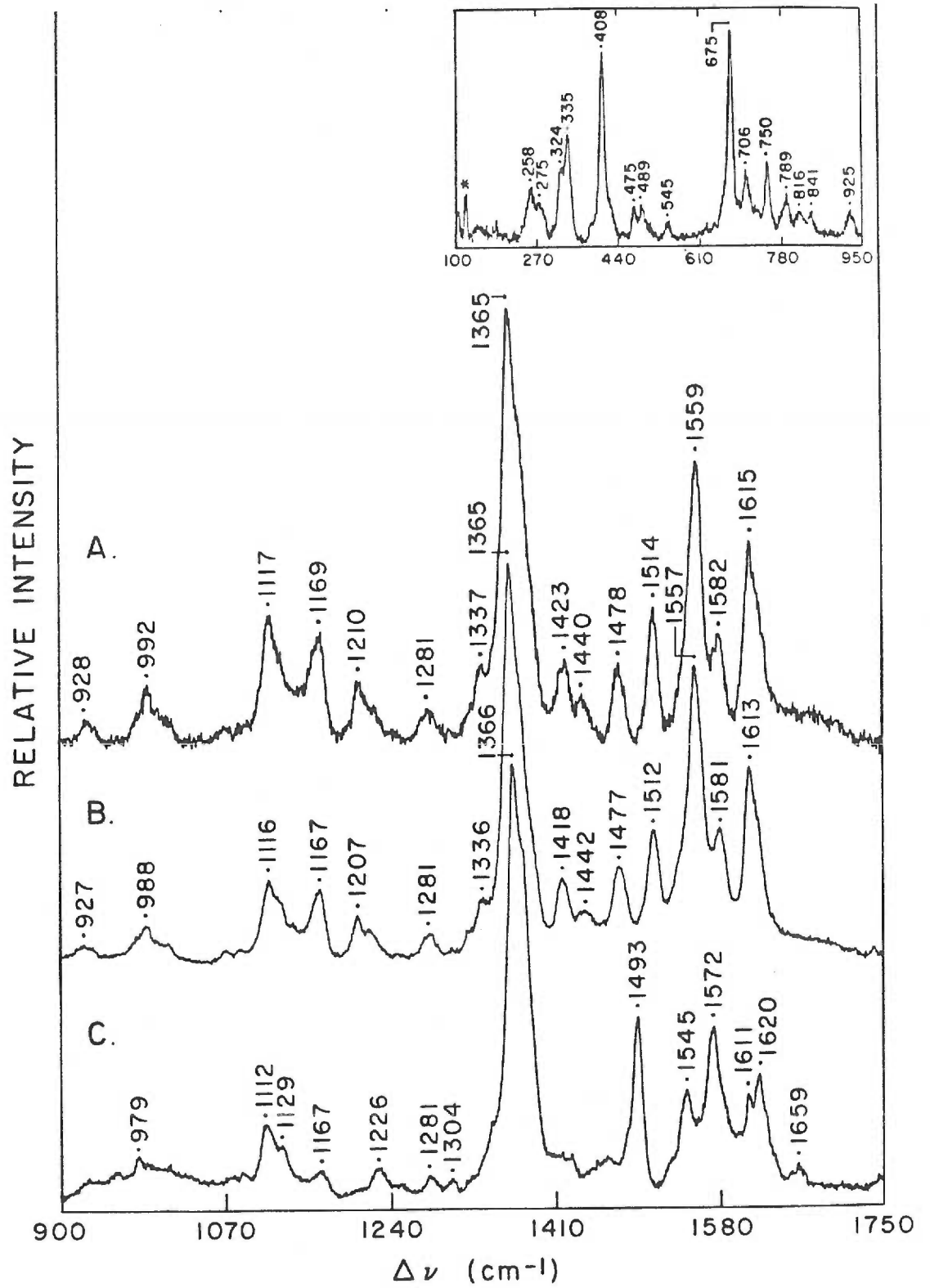
(a) Tabulated data is from the following sources: EPO, this work; Hb (ferrihemoglobin fluoride), ref. 19; IPO (intestinal peroxidase), ref. 20; HRP (horseradish peroxidase), ref. 21; LPO (lactoperoxidase), ref. 22; MPO, this work. A hyphen denotes an absence of reported data.

---

Figure 6

Resonance Raman Spectra of Eosinophil Peroxidase under 406.7 nm Excitation. 90 degree scattering geometry,  $\sim 4^\circ\text{C}$ , scan rate  $1\text{ cm}^{-1}\text{ s}^{-1}$ . Upper spectrum a: oxidized horse enzyme, 14 mW incident power, 6 scans. Lower b: oxidized human enzyme, 32 mW, 9 scans. Inset: oxidized human enzyme, low-frequency region, conditions as in B. Asterisk indicates laser plasma emission line. Oxidized human enzyme band frequencies and depolarization ratios ( $\rho$ ): 1613 (0.3); 1581 (0.3); 1557 (0.2); 1512 (0.2); 1477 (0.3); 1418 (0.7); 1365 (0.3); 1207 (0.3); 1167 (0.5); 1116 (0.3); 988 (0.5).

---

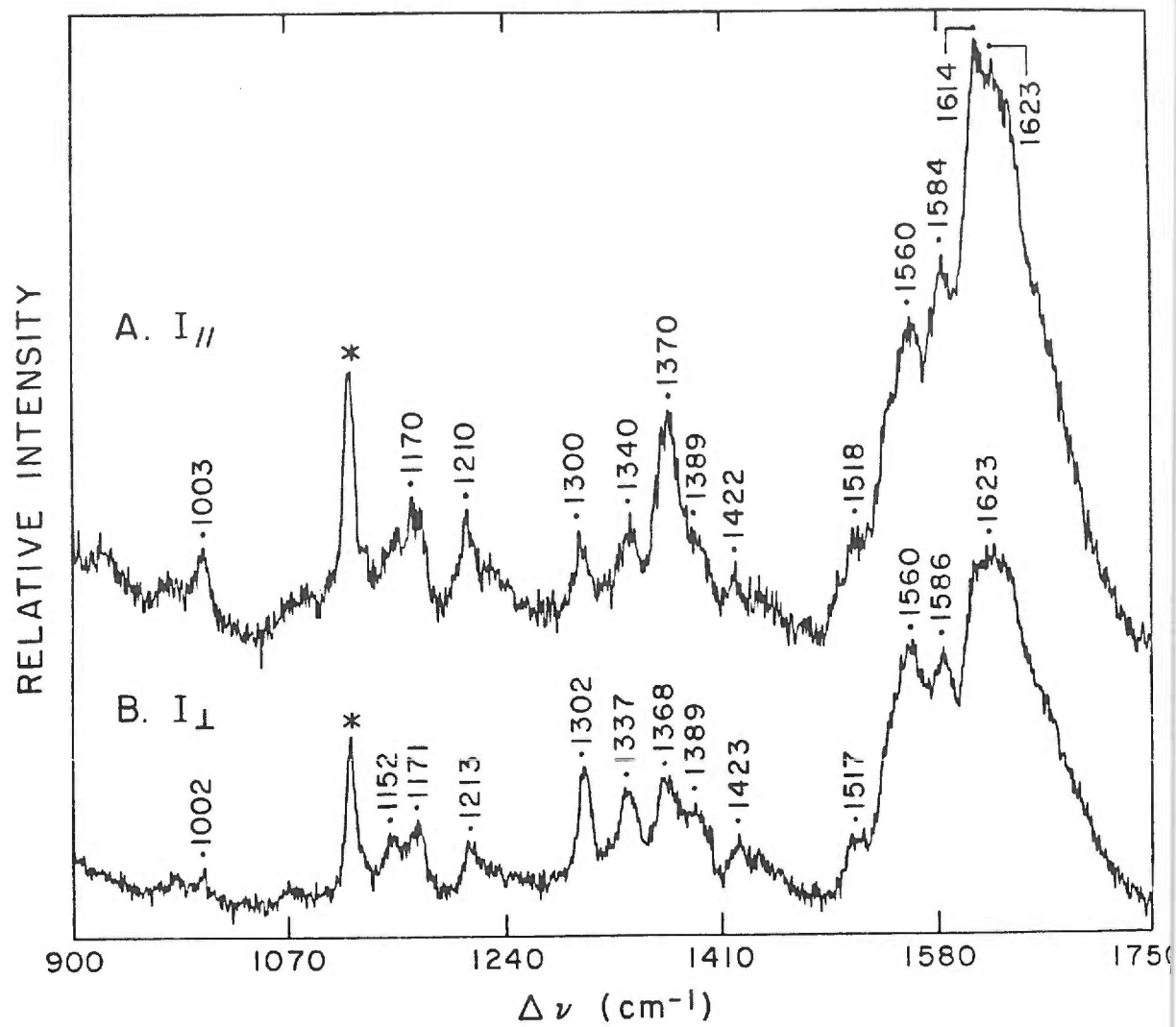


---

Figure 7

*Resonance Raman Spectra of Human Eosinophil Peroxidase under 514.5 nm Excitation. Upper spectrum a: oxidized enzyme, parallel polarized light, ~4 °C, 75 mW incident power, 17 scans, scan rate  $1\text{ cm}^{-1}\text{ s}^{-1}$ , 90 degree scattering geometry. Lower spectrum b: Same as A except perpendicular polarized light. Asterisk indicates an emission line (435.8 nm) of the external fluorescent room lighting. Band frequencies and depolarization ratios ( $\rho$ ): 1623 (0.6); 1422 (1.3); 1389 (1.0); 1370 (0.4); 1300 (1.2); 1210 (0.4); 1170 (0.6); 1003 (0.3).*

---





excludes chlorin, which exhibits only polarized modes  
 $(\rho < 3/4)$ .<sup>10,17,18</sup>

The oxidation state marker band ( $\nu_4$ ) of the resting enzyme appears at  $1365\text{ cm}^{-1}$  (Figures 6A,B), and at  $1366\text{ cm}^{-1}$  in the cyano derivative (Figure 6C). Although somewhat low, these frequencies probably indicate that the central iron is ferric. Based on the frequency of  $\nu_{10}$  at  $1614\text{ cm}^{-1}$  (Figures 6A,B), the heme appears to be six-coordinate.<sup>25,26</sup> The shift in the core-size marker band ( $\nu_{11}$ ) from  $1557$  to  $1572\text{ cm}^{-1}$  accompanying cyanide addition indicates ligation occurs with high-to-low spin conversion of the ferric electronic configuration. With Soret excitation (Figure 6B), the presence of vinyl substituents on the porphyrin ring is inferred from weak bands at  $1620\text{ cm}^{-1}$  [ $\nu_{\text{C}=\text{C}}$ (2)],  $1336\text{ cm}^{-1}$  [ $\delta_{\text{S}}(\text{=CH}_2)$ (2)],  $1304\text{ cm}^{-1}$  [ $\delta(\text{CH=})$ ], and  $1167\text{ cm}^{-1}$  [ $\nu_{\text{C}_\beta-\text{C}_\alpha}$ (1)], or with visible excitation (Figure 7B) at  $1423\text{ cm}^{-1}$  [ $\delta_{\text{S}}(\text{=CH}_2)$ (1)], and  $1337\text{ cm}^{-1}$  [ $\delta_{\text{S}}(\text{=CH}_2)$ (2)]. Band assignments in brackets correspond to those determined from frequency shifts upon deuteration of protoheme vinyl carbons.<sup>19,27</sup>

### DISCUSSION

Raman spectra of eosinophil peroxidase exhibit none of the spectral features which distinguish the MPO chlorin, such as additional bands and enhanced band intensities. Furthermore, EPO spectra contain anomalously polarized vibrational bands which can originate only from a high-symmetry porphyrin. From this evidence, we conclude that EPO does not contain chlorin. As judged from the qualitative resemblance of EPO resonance Raman spectra with other known protoheme-containing proteins, the enzyme appears to contain protoheme. The appearance of characteristic vinyl-related bands corroborates this conclusion.

Since both protoheme-containing EPO and chlorin-containing MPO are able to use chloride ion in catalyzing halogenation reactions, the unusual hydroporphyrin of MPO is not obligatory for such activity.

Heme coordination geometries for EPO, MPO, and LPO are strikingly similar. The ligand field parameters of LPO and EPO are nearly identical, so the two enzymes probably possess the same axial ligands; these have been determined for LPO to be a histidine imidazole and most likely a carboxylate.<sup>28</sup> Hyperfine splitting of the EPR signal from ferrous nitrosyl derivatives of EPO confirms that this enzyme has nitrogen as one of the axial ligands.<sup>29</sup> A study of MPO by this technique yields the same conclusion.<sup>29</sup> Resonance Raman studies indicate that the MPO chlorin, like EPO and LPO protoheme, is six-coordinate with one nitrogenous and one weak-field axial ligand.<sup>10</sup>

Eosinophil peroxidase and LPO possess the same protoheme prosthetic group, with similar if not identical coordination geometries, yet they exhibit different activities: EPO can catalyze chloride peroxidation, whereas LPO cannot. The molecular basis for this difference is not clear at present. However, resonance Raman spectra provide an important clue. Skeletal vibrational modes of human EPO (Figure 6B) are all shifted 5 to 10  $\text{cm}^{-1}$  to lower energies than the corresponding LPO modes.<sup>21</sup> Frequencies of horse EPO are somewhat intermediate (Figure 6A). Since band energies in the high frequency region are inversely correlated with porphyrin core size,<sup>27</sup> the core size of the EPO porphyrin is presumed to be larger than the LPO porphyrin. An expanded core can originate from the influence of a strong sigma-donating sixth ligand which induces an in-plane alignment of the central iron.<sup>30</sup>

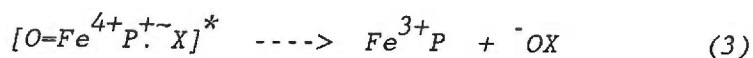
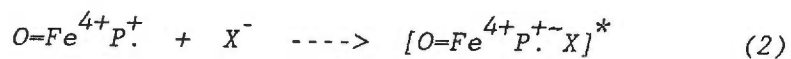
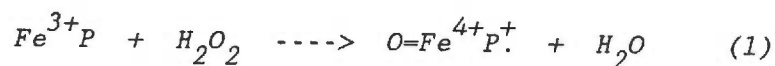
The energy of the  $\nu_4$  Raman band has been shown to monitor the extent of  $\pi$ -delocalization in the porphyrin ring.<sup>21,31</sup> Because the frequency of this band is 8  $\text{cm}^{-1}$  lower for EPO than LPO, we suggest that the electronic density of the porphyrin ring is greater for EPO. This suggestion is consistent with the notion that EPO contains a sixth ligand with a field strength greater than the corresponding LPO ligand. It is also possible that the 8  $\text{cm}^{-1}$  difference in  $\nu_4$  indicates differences in the interaction between protein and heme<sup>32</sup>, perhaps involving  $\pi$ -overlap of aromatic residues and the heme macrocycle.<sup>33</sup>

Except for one reduced pyrrole, the hemes of EPO and MPO have nearly identical structures. The approximate functional equivalence of these two enzymes therefore excludes any obligatory role for a pyrroline in MPO activity. However, there may be some kinetic or halide-specific advantage for the MPO chlorin. The cellular toxicity of the  $\text{EPO-H}_2\text{O}_2\text{-Cl}^-$  system is substantially less than the corresponding MPO system.<sup>7</sup> Moreover, EPO exhibits greater selectivity for iodide and bromide over chloride than MPO, and the efficiency of chloride ion peroxidation by EPO is diminished relative to MPO.<sup>7,34,35</sup>

It has been reported that EPO cannot catalyze certain chlorination reactions that are facile for MPO, such as amino acid decarboxylations.<sup>36</sup> More recent data indicates that this is only true for studies undertaken in certain buffers.<sup>37</sup> Hence, failure to observe EPO-mediated decarboxylation may be due to buffer-dependent enzyme inactivation, or to depressed substrate affinity. Similarly, it has been observed that bacterial killing by the EPO system is inhibited by albumin and gelatin,<sup>34</sup> which may reflect incidental scavenging of  $\text{HOCl}$  by extraneous protein.

The rate of reaction of  $\text{HOCl}$  with various oxidants has been shown to be controlled by the electrophilic character of the electron-accepting site of the oxidant.<sup>38</sup> Thus, a bond of at least partial character must form between  $\text{HOCl}$  and the oxidant prior to electron transfer. For the reverse process, which occurs in the reaction between chloride ion and MPO Compound I,<sup>39</sup>

bonding of at least a transient nature must also occur. In the enzymatic production of hypohalite,  $\text{OX}^-$ , nucleophilic attack of halide ion on Compound I (reaction 2) is postulated to be rate-limiting. In other words, slow reaction between halide and Compound I forms a precursor complex, followed by rapid electron transfer from chloride to oxygen and then rapid rupture of the iron-oxygen bond (reaction 3).



With increasing halide nucleophilicity, the attack by halide on Compound I should become more avid, resulting in a greater rate of hypohalite production. The postulate thus predicts that the relative effectiveness of microbial killing will follow trends in halide nucleophilicity, i.e.,  $\text{I}^- > \text{Br}^- > \text{Cl}^-$ .<sup>40</sup> Although precisely this behavior is observed for MPO<sup>5</sup> and EPO,<sup>3,34</sup> the actual basis for such trends is uncertain without more complete information on mechanisms of microbial killing and on rates of primary product scavenging as a function of halide cosubstrate.

The notion of rate-limiting halide attack on Compound I permits a rationalization of the greater effectiveness of chloride peroxidation by MPO than EPO. This rationalization

assumes that there is no difference in the catalytic mechanisms of these two enzymes, and is based on computed values of electronic densities of the  $\pi$ -cation radicals of ferrylchlorin and ferrylporphyrin.<sup>41</sup> For chlorin-containing peroxidases, electrons are probably abstracted from the  $a_2$  orbital.<sup>41</sup> For this species, two of the four methine carbons are calculated to be electron deficient (Table 6). In the case of MPO Compound I, one or both of these carbons should be reactive toward nucleophilic chloride ion. In contrast, electronic density on the methine carbons of porphyrin radical is either exceptionally deficient or exceptionally rich, depending on the symmetry of the orbital from which the electron is abstracted (Table 6). The electron-rich species corresponds to Compound I of horseradish peroxidase (HRP I), whereas the electron-deficient species corresponds to Compound I of catalase.<sup>41</sup> Provided EPO Compound I is like HRP I, then relatively high electron density on the methine carbons will retard halide attack on EPO in comparison to MPO. As the rate-determining step, this would render EPO less reactive toward a given halide than MPO. In this manner, the MPO chlorin may provide some kinetic advantage in microbial killing.

Table 6

Calculated unpaired spin densities for methine carbons  
of heme  $\pi$ -cation radical with imidazole ligand (a)

Compound (symmetry)	Position (b)			
	5	10	15	25
Protoporphyrin ( $a_{1u}$ )	.000	.003	.003	.002
Chlorin ( $a_2$ )	.050	.005	.005	.050
Protoporphyrin ( $a_{2u}$ )	.104	.106	.104	.108
Chlorin ( $b_2$ )	.108	.103	.103	.108

(a) Data taken from reference 41.

(b) Numbering conforms to the recommendations of Bonnett, R.,  
Porphyrins 1978, 1, 9-14.

# REFERENCES

1. Wever, R.; Plat, H.; Hamers, M.N. FEBS Lett. 1981, 123, 327-331.
2. Albrich, J.M.; McCarthy, C.A.; Hurst, J.K. Proc. Natl. Acad. Sci. USA 1981, 78, 210-214.
3. Buys, J.; Wever, R.; van Stigt, R.; Ruitenberg, E.J. Eur. J. Immunol. 1981, 11, 843-845.
4. Klebanoff, S.J. Semin Hematol. 1975, 12, 117-142.
5. Klebanoff, S.J.; Clark, R.A. "The Neutrophil: Function and Clinical Disorder"; North-Holland: Amsterdam, 1978.
6. Nogueira, N.M.; Klebanoff, S.J.; Cohn, Z.A. J. Immunol. 1982, 128, 1705-1708.
7. Klebanoff, S.J.; Henderson, W.R.; Jong, E.C.; Jorg, A.; Locksley, R.M. In: "Immunobiology of the Eosinophil"; (Yoshida, T.; Torisu, M., Eds.); Elsevier: Amsterdam, 1983; pp 261-282.
8. Bolscher, B.G.J.M.; Plat, H.; Wever, R. Biochim. Biophys. Acta 1984, 784, 177-186.
9. Desser, R.K.; Himmelhoch, S.R.; Evans, W.H.; Januska, M.; Mage, M.; Shelton, E. Arch. Biochem. Biophys. 1972, 148, 452-465.
10. Sibbett, S.S.; Hurst, J.K. Biochemistry 1984, 23, 3007-3013.
11. Eglinton, D.G.; Barber, D.; Thompson, A.J.; Greenwood, C.; Segal, A.W. Biochim. Biophys. Acta 1982, 703, 187-195.
12. a) Archer, G.T.; Air, G.; Jackas, M.; Morell, D.B. Biochim. Biophys. Acta 1965, 99, 96-101. b) Olsen, R.L.; Little, C. Biochem. J. 1983, 209, 781-787 c) Ohtaki, S.; Nakagawa, H.; Nakamura, S.; Nakamura, M.; Yamazaki, I. J. Biol. Chem. 1985, 260, 441-448.
13. Jorg, A.; Pasquier, J.M.; Klebanoff, S.J. Biochim. Biophys. Acta 1982, 701, 185-191.
14. Gleich, G.J.; Loegering, D.A.; Mann, K.G.; Maldonado, J.E. J. Clin. Invest. 1976, 57, 633-640.



15. Ozaki, Y.; Kitagawa, T.; Ogoshi, H. Inorg. Chem. 1979, 18, 1772-1776.
16. Hanson, L.K.; Chang, C.K.; Ward, B.; Callahan, P.M.; Babcock, G.T.; Head, J.D. J. Am. Chem. Soc. 1984, 106, 3950-3958.
17. Andersson, L.A.; Loehr, T.M.; Lim, A.R.; Mauk, A.G. J. Biol. Chem. 1984, 259, 15340-15349.
18. Andersson, L.A.; Loehr, T.M.; Chang, C.K.; Mauk, A.G. J. Am. Chem. Soc. 1985, 107, 182-191.
19. Choi, S.; Spiro, T.G.; Langry, K.C.; Smith, K.M.; Budd, D.L.; La Mar, G.N. J. Am. Chem. Soc. 1982, 104, 4345-4351.
20. Kimura, S.; Yamazaki, I. and Kitagawa, T. Biochemistry 1981, 20, 4632-4638.
21. Turner, J.; Reed, D.E. Biochim. Biophys. Acta 1984, 789, 80-86.
22. Kitagawa, T.; Hashimoto, S.; Teraoka, J.; Nakamura, S.; Yajima, H.; Hosoya, T. Biochemistry 1983, 22, 2788-2792.
23. Albrecht, A.C.; Hutley, M.C. J. Chem. Phys. 1971, 55, 4438-4443.
24. Spiro, T.G.; Strekas, T.C. Proc. Natl. Acad. Sci. USA 1972, 69, 2622-2626.
25. Spiro, T.G.; Stong, J.D.; Stein, P. J. Am. Chem. Soc. 1979, 101, 2648-2655.
26. Teraoka, J.; Kitagawa, T. J. Chem. Phys. 1980, 84, 1928-1935.
27. Choi, S.; Spiro, T.G. J. Am. Chem. Soc. 1983, 105, 3683-3692.
28. Sievers, G.; Gadsby, P.M.A.; Peterson, J.; Thomson, A.J. Biochim. Biophys. Acta 1983, 742, 659-668.
29. Bolscher, B.G.J.M.; Wever, R. Biochim. Biophys. Acta 1984, 791, 75-81.
30. Scheidt, W.R.; Reed, C. Chem. Rev. 1981, 81, 543-555.
31. Spiro, T.G.; Strekas, T.C. J. Am. Chem. Soc. 1974, 96, 338-345.
32. Wever, R.; Plat, H. Biochim. Biophys. Acta 1981, 661, 235-239.

33. Mohr, P.; Scheler, W. Eur. J. Biochem. 1969, 8, 444-449.
34. Jong, E.C.; Henderson, W.R.; Klebanoff, S.J. J. Immunol. 1980, 124, 1378-1382.
35. Jong, E.C.; Mahmoud, A.A.F.; Klebanoff, S.J. J. Immunol. 1981, 126, 468-471.
36. Migler, R.; DeChatelet, L.R.; Bass, D.A. Blood 1978, 51, 445-456.
37. Cramer, R.; Soranzo, M.R.; Patriarca, P. Blood 1981, 58, 1112-1118.
38. a) Held, A.M.; Halko, D.J.; Hurst, J.K. J. Am. Chem. Soc. 1978, 100, 5732-5740. b) Hurst, J.K.; Carr, P.A.G.; Hovis, F.E.; Richardson, R.J. Inorg. Chem. 1981, 20, 2435-2438.
39. Bolscher, B.G.J.M.; Wever, R. Biochim. Biophys. Acta 1984, 788, 1-10.
40. March, J. "Advanced Organic Chemistry", 2nd ed.; McGraw-Hill: New York; pp 322-325.
41. Hanson, L.K.; Chang, C.K.; Davis, M.S.; Fajer, J. J. Am. Chem. Soc. 1981, 103, 663-670.
42. Tenovuo, J.A. In: "The Lactoperoxidase System: Chemistry and Biological Significance", (Pruitt, K.M.; Tenovuo, J.O., Eds.), Marcel Dekker: New York, 1985, pp 101-122.
43. Moldoveanu, Z.; Tenovuo, J.; Mestecky, J.; Pruitt, K.M. Biochim. Biophys. Acta 1982, 718, 103-109.
44. Thomas, E.L. In: "The Lactoperoxidase System: Chemistry and Biological Significance", (Pruitt, K.M.; Tenovuo, J.O., Eds.), Marcel Dekker: New York, 1985, pp 31-53.

### Chapter 3

#### *Cytochrome Oxidase: The Hurst Model*

Protoporphyrin IX has two peripherally-bound vinyl groups. The influence of these groups on the physical chemistry of the porphyrin core is illustrated by a series of deuteroporphyrins with zero, one or two vinyl substituents. Continuous red-shifting of electronic bands is observed for the series as a function of increasing substitution (Figure 8).<sup>1</sup> Incremental shifts of this sort indicate that both vinyls conjugate with the porphyrin aromatic system; bathochromism indicates that the vinyl groups influence porphyrin electronic states in the expected  $\pm E$  electromeric manner.<sup>2</sup>

In addition to electronic effects, substituted vinyls also perturb the vibrational properties of the porphyrin, causing chiefly an increase in the number of detectable bands. Three mechanisms separately add bands. 1) Local vinyl vibrations are vibronically active in porphyrin electronic transitions. Laser excitation within these transitions therefore produces resonance Raman enhancement of local vinyl vibrations, in addition to the well-characterized skeletal vibrations.<sup>3</sup> Protoporphyrin vinyl modes, for example, appear as additional bands otherwise absent in spectra of the non-vinyl porphyrins.<sup>4,5</sup> 2) Symmetry-equivalent vinyl and porphyrin fundamental modes undergo

---

Figure 8

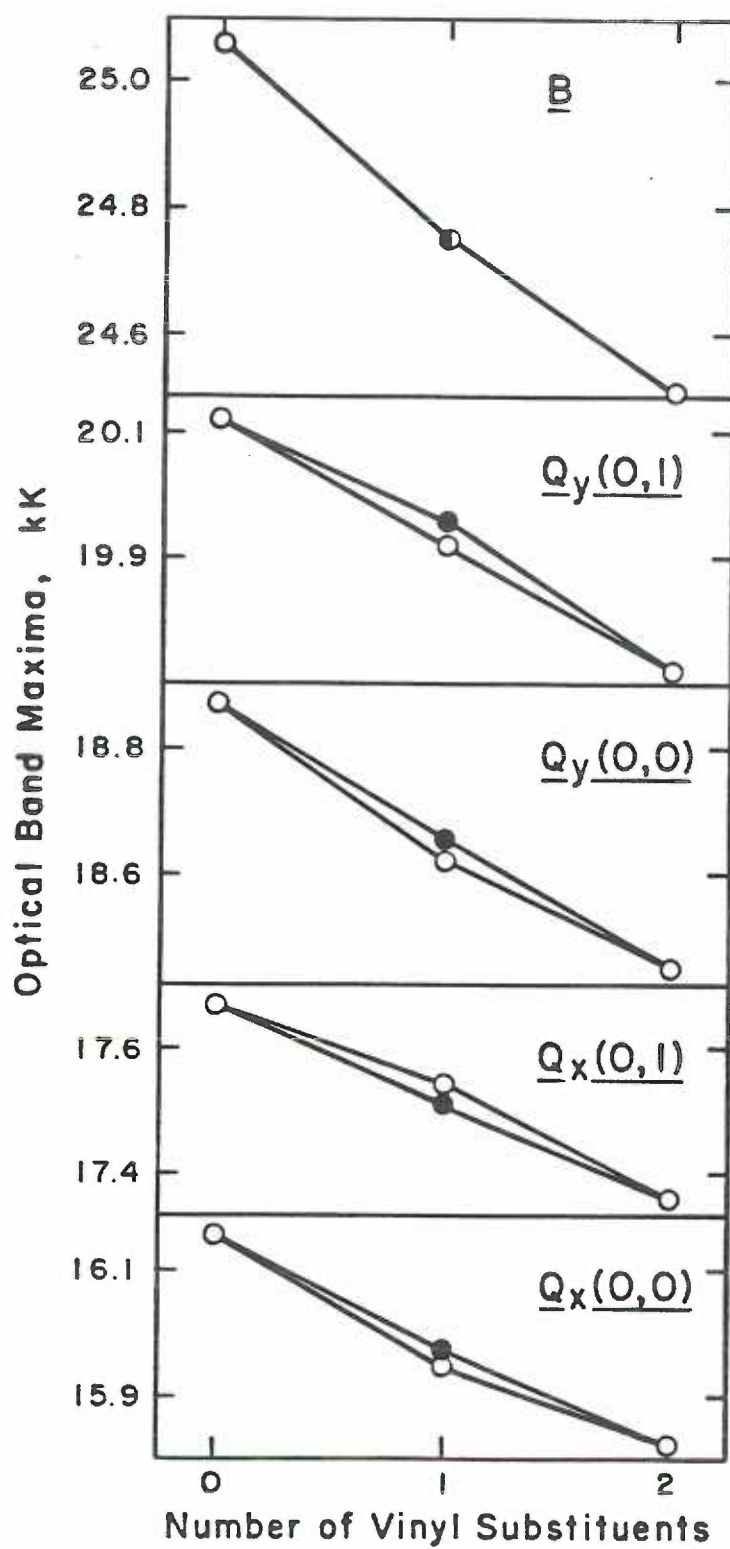
Optical absorption maxima of substituted deuteroporphyrin dimethyl esters in  $\text{CHCl}_3$  as a function of the number of vinyl substituents. Open circles (monovinyl): 3-vinyldeuteroporphyrin (nomenclature depicted on p 9). Closed circles: 8-vinyldeuteroporphyrin. By treating the effects of peripheral substituents on visible band energies as a sum of perturbation elements (PE) influencing the spectra of reference octaalkylporphyrins (OAP),<sup>117</sup>

$$[E(Q_x) + E(Q_y)] = [\Sigma(\text{PE})] + [E(Q_x) + E(Q_y)]_{\text{OAP}}$$

we calculate from the (0,0) and (0,1) data that  $\text{PE}_{\text{vinyl}} = -332 \text{ cm}^{-1}$ . Since substitution of a second vinyl group on an adjacent ring gives a spectral shift of nearly identical magnitude, the experimental data are an exception to the empirical rule that only substituents on opposite pairs of pyrrole rings should be included in the summation.<sup>117</sup>

Monovinyldeuteroporphyrin data from: Grigg, R.; Johnson, A.W.; Roche, M. J. Chem. Soc. C, 1970, 1928-1934. Deuteroporphyrin and protoporphyrin data from: Caughey, W.S.; Fujimoto, W.Y.; Johnson, B.P. Biochemistry 1966, 5, 3830-3843.

---



resonance coupling.<sup>6</sup> This may introduce to a spectrum two bands in place of one.<sup>5,7,8</sup> 3) Attachment of vinyls at the asymmetric 3,8 positions<sup>†</sup> lowers the formal  $D_{4h}$  symmetry of the porphyrin macrocycle. One consequence is an activation of porphyrin  $E_u$  modes that otherwise are Raman forbidden.<sup>8-10</sup>

Modification of porphyrin physical properties by vinyl substituents may contribute to the catalytic function of some hemeproteins. Previous studies indicate a role for vinyl groups in modulating the ligand affinities of oxygen-binding proteins (Hb,<sup>11-14</sup> Mb,<sup>12-16</sup> legHb<sup>16,17</sup>), the reactivity of a P-450 cytochrome,<sup>18</sup> and the redox properties of cytochromes<sup>19</sup> and peroxidases (CCP,<sup>20</sup> HRP<sup>16,21</sup>). In addition, Caughey and coworkers have speculated that the single vinyl group of heme *a* provides a binding site for Cu(I) in mammalian cytochrome oxidase.<sup>22</sup> Their suggestion is based on the observation that terminal olefins strongly coordinate Cu(I).<sup>23</sup>

The interest of Hurst and coworkers in Cu(I)-olefin electron transfer<sup>24</sup> prompted them to obtain information on simple heme-copper(I) complexes which might model structural features of the oxygen binding site of cytochrome oxidase.<sup>25</sup> To evaluate the potential for coordination of copper(I) by the vinyl group of heme *a*, they studied various vinyl-substituted

---

<sup>†</sup>Nomenclature conforms to Bonnett's recommendations (cf. p 9).<sup>118</sup>

and non-vinyl porphyrins.<sup>†</sup> In the absence of vinyl substituents, it was found that added Cu(I) does not perturb porphyrin optical spectra.<sup>25</sup> However, new UV bands appear when Cu(I) is added to vinyl-substituted porphyrins. These new bands are not induced by other aquo metal ions. Such bands are assignable to Cu(d)--->olefin( $\pi^*$ ) metal-to-ligand charge-transfer,<sup>25-27</sup> and commonly are used as a criterion of Cu(I)-olefin  $\pi$ -bonding.<sup>23</sup> Copper(I) also perturbs the porphyrin Soret and visible bands.

The coordination of Cu(I) to olefin affects not only electronic properties of the olefin, but also vibrational properties. For instance,  $\pi$ -bonding between a metal and an olefin causes a large decrease in frequency of the C=C symmetric stretching vibration.<sup>23</sup> This well-known decrease is due to greater electron density in olefin  $\pi^*$  orbitals, and concomitant loss in  $\pi$ -bonding orbitals.<sup>††</sup> Resonance Raman spectra reported here demonstrate such a frequency shift for the vinyl stretching mode of protoheme. Also, we find that Cu(I) binding perturbs

---

<sup>†</sup>Isoprenoid units of the 3-(1'-hydroxy)farnesyl substituent of heme *a* also are potentially capable of binding Cu(I).

<sup>††</sup> $\pi$ -complex theory postulates two synergic components of metal-olefin bonds,<sup>119</sup> (1) the donation of electron density from olefin  $\pi$  orbitals into empty metal sigma orbitals, and (2) the donation of electron density from metal d-orbitals into empty olefin  $\pi^*$  orbitals. Metal-->olefin back-bonding compensates olefin-->metal delocalization, and vice versa. The strength of both bonding components is thereby reinforced.

virtually all of the other vibrational modes that are thought to contain some component of vinyl vibration, whereas non-vinyl modes remain largely unaffected. A similar change can be identified in resonance Raman spectra of reduced and semi-reduced forms of cytochrome oxidase, suggesting that Cu(I) may coordinate to the heme periphery of the oxidase.



## MATERIALS AND METHODS

Except as indicated, all chemicals were reagent grade and used without further purification. Water was purified by reverse osmosis-ion exchange followed by all-glass distillation. Reagent solutions of Cu(I) were prepared by reduction of Cu(II) using either chromous<sup>26</sup> or europous ions.<sup>28</sup> Cu(I)-protoheme solutions were prepared according to previous methods.<sup>25</sup> The concentration of hemin  $\mu$ -oxo dimer solutions (pH 12.6) were determined spectrophotometrically according to  $\epsilon_{384 \text{ nm}} = 105 \text{ mM}^{-1} \text{ cm}^{-1}$  per molecule of dimer.<sup>†</sup> Copper(I)-protoheme solutions were prepared by adding the Cu(I) reagent to micellar protoheme solutions using anaerobic syringe transfer techniques. By the criteria of optical and Raman spectra, the two preparative methods generate chemically identical heme-Cu(I) solutions. To minimize disproportionation of Cu(I), glassware was soaked in concentrated nitric acid prior to use.<sup>29</sup> It is necessary to remove oxygen from all reactant solutions to prevent both oxidation of Cu(I)<sup>30,31</sup> and photooxidation of heme.<sup>32-34</sup> Argon was bubbled through solutions to purge oxygen. To remove contaminant oxygen from the purging gas, argon was passed through BASF Catalyst R 3-11 just prior to passing through reagent solutions.<sup>35</sup>

Sodium dodecyl sulfate (SDS) was obtained from Aldrich

---

<sup>†</sup>This corrects a previous misprint.<sup>25</sup>

and BDH; the Aldrich material was triply recrystallized from ethanol to remove impurities,<sup>36</sup> whereas the "specially purified" BDH material was used without further treatment. Sodium dodecyl sulfate was added to aqueous acidic solutions at concentrations above the critical micelle concentration of the detergent. Under these conditions, hemin is solubilized in a monomer form<sup>37,38</sup> within the hydrophobic region of the micelle.<sup>39</sup> This environment bears some resemblance to the physiological environment of hemes within proteins. Upon freezing, the SDS micellar structure is maintained.<sup>40</sup> Acidities and ionic strength were adjusted by adding trifluoroacetic acid (TFA) or its sodium salt.<sup>41,42</sup>

Room temperature optical and Raman spectra were obtained from samples in a 1 cm optical cuvette. To minimize introduction of adventitious oxygen, the cuvette was fitted with a degassable antechamber bounded by septum-stoppered outer and inner ports. On piercing the outer septum with a transfer needle, introduced oxygen was purged before penetration of the inner septum. The bottom face of the cuvette was polished, permitting Raman spectra to be obtained in a 90-degree scattering geometry by laser illumination from beneath the cell. To reduce self-absorption,<sup>43</sup> the distance of travel of scattered light through solution was minimized by focusing the laser beam near the cuvette sampling window. Low temperature Raman spectra were obtained from samples in 4 mm outer diameter septum-sealed electron paramagnetic resonance (EPR) tubes. Temperature was

controlled by placing these tubes in the quartz dewar insert of a Varian E-257 Variable Temperature Controller. Scattered light was sampled from the top-forward quadrant of the frozen solution in a sample tube aligned perpendicular to the scattering plane. This configuration approximates a 90 degree scattering geometry. The computer-controlled Raman spectrometer has been described previously.<sup>44</sup>

The electrochemical measurement of protoheme was performed by spectrophotometric redox potentiometry.<sup>45</sup> Although numerous attempts to measure the ferric/ferrous protoheme redox couple have been reported,<sup>46-51</sup> there has been no successful measurement of the potential of monomeric five-coordinate protoheme.<sup>†</sup> There are two chief obstacles to this measurement.

(1) *Ferroprotoheme in aqueous solution is chemically degraded by O<sub>2</sub>.*<sup>††</sup> The titration of aerobic SDS-micellar solutions of ferriprotoheme by aqueous Eu(II) was found by us to exhaustively bleach the protoheme spectrum in a completely isosbestic manner. The resulting spectrum is featureless between 340 and 700 nm, except for very weak bands at 404 and 493 nm.

---

<sup>†</sup>Loach and coworkers report a value for the redox potential of protoheme in phosphatidylcholine vesicles, but provide no experimental or statistical detail.<sup>61</sup>

<sup>††</sup>In surprising contrast, ferroprotoheme in neat N,N-dimethylformamide has been reported to be stable in the presence of dioxygen.<sup>120</sup>

Titrant was observed to cause full spectral conversion within 1 s of mixing. Identical results are obtained when anaerobic ferroprotoheme is titrated with aerobic aliquots of micellar SDS. In both cases, chemical degradation of the porphyrin macrocycle is presumed to occur by oxidative coupling.<sup>52,53,†</sup>

Since a rigorously anaerobic system is essential to conducting accurate potentiometric titrations of protoheme, a standard Dutton vessel<sup>55</sup> was modified to permit a complete incorporation of the redox electrode (Orion Model 96-78 Platinum Electrode) within the titrating vessel (Figure 9). This approach eliminates the redox electrode as a portal for adventitious oxygen, and was found, among a variety of configurations, to give superior results. The electrode is fitted to the Dutton vessel by a silicone stopper in contact with the upper vinyl cap of the electrode. Deoxygenation of the electrode filler solution occurs by atmospheric exchange between the purged vessel and the electrode interior, through a small port on the electrode body. The port also allows isobaric equilibrium to be maintained between filler and analyte solutions. This insures that the rate of flow of filling solution through the sleeve-type liquid

---

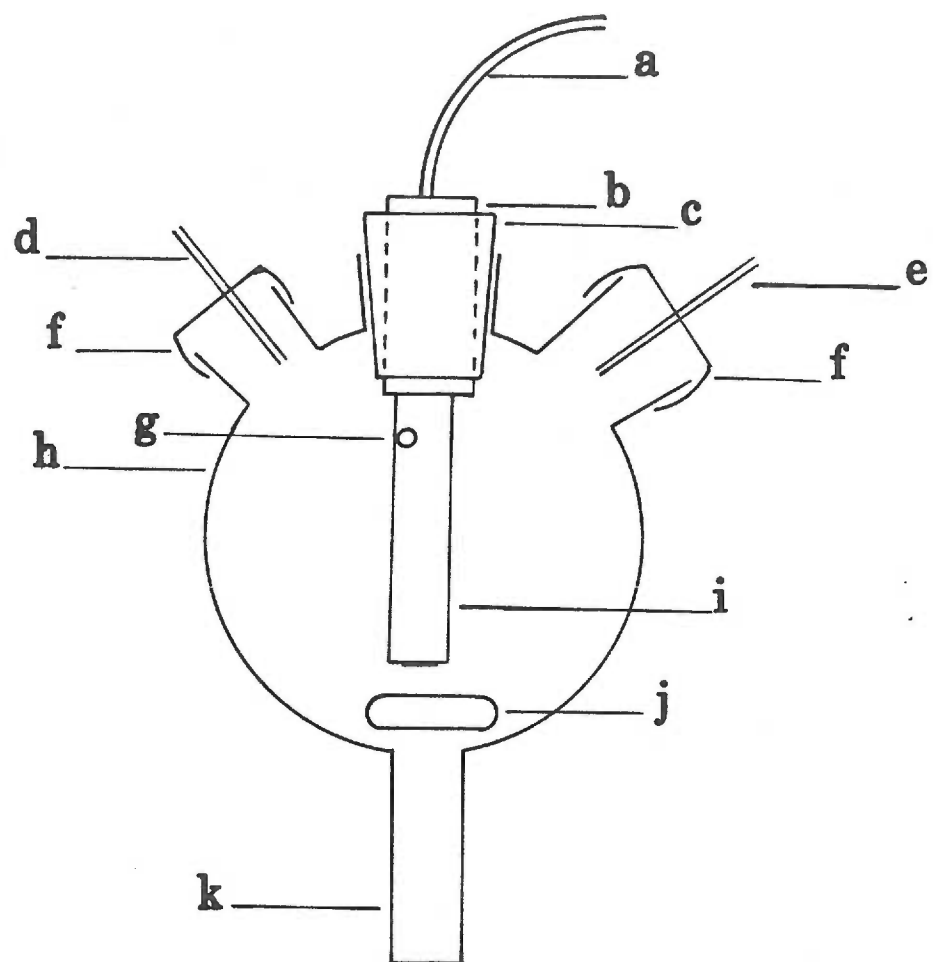
† Kinetic studies by Swallow and coworkers on the pulse radiolytic reduction of protoheme in SDS revealed a fast and a slow step.<sup>59</sup> These workers report that the rate of the slow step varied with the purgant gas (Ar or nitrous oxide.) Since they describe no special precautions against interference by oxygen, their results may be due to differing amounts of residual oxygen in the purgant gasses.

---

Figure 9

Spectroelectrochemical Titrating Vessel. (a) Cable to pH meter with millivolt scale; (b) upper vinyl cap of electrode; (c) silicone stopper; (d) argon inlet; (e) argon outlet; (f) white-rubber septum; (g) small port on electrode body; (h) titrating vessel; (i) electrode body; (j) magnetic stirring bar; (k) quartz spectrophotometer cuvette attached to titrating vessel through a graded seal.

---



junction is determined solely by hydrostatic pressure, as necessary for proper functioning of the electrode.<sup>60</sup>

All titrations were preceded by purging the assembled vessel for at least 8 h. During this period, the loss of filling solution into the heme solution was found to be significant unless hydrostatic pressure was minimized by fixing the vessel in a near-horizontal position. During titrations, purging was maintained without interruption. Sample temperature was maintained at 25°C ( $\pm 1$ ) by a jacketed cuvette holder. Solutions were not stirred except immediately following the addition of titrant.

(2) *In aqueous media, protoheme tends to aggregate.*<sup>38,56,57</sup> This introduces additional equilibria which transform the relatively simple problem of measuring the ferric/ferrous protoheme couple into something much more complicated.<sup>46</sup> The recognition of this<sup>47</sup> prompted the development of alternate strategies to measure the protoheme potential, in which aggregation is prevented either by the use of non-aqueous solvents<sup>50</sup> or by strongly coordinating ligands.<sup>48,49,58</sup> But both approaches have drawbacks. The strong ligand approach does not provide a suitable model for hemes in a protein environment, while the use of non-aqueous solvents greatly limits the number and variety of porphyrins which may be solubilized. The strategy which we have employed exploits the ability of aqueous SDS to monomerize protoheme and a wide variety of other porphyrins within a protein-like

hydrophobic environment.

There are obstacles to performing redox titrations in SDS. The first of these is the insolubility of SDS in the presence of potassium ion. To our knowledge, all commercially available filling solutions contain potassium ion. Titrations conducted with commercial filling solutions resulted in the precipitation of SDS at the sleeve junction, or, in more extreme cases, precipitation throughout the micellar heme solution. Such precipitate obstructs the free flow of filling solution into the solution being titrated, and thereby disables the electrode. We used saturated  $\text{NH}_4\text{Cl}$  as an alternate to potassium-containing commercial filling solutions. Ammonium and chloride ions are more nearly equitransferant than  $\text{K}^+$  and  $\text{Cl}^-$ ,<sup>58,†</sup> and thus excellent species for minimizing junction potentials.<sup>55</sup> With  $\text{NH}_4\text{Cl}$  as the filling solution, calibration of observed potentials to the normal hydrogen electrode was achieved by measuring potentials of pH 7 quinhydrone redox buffer and various ferricyanide/ferrocyanide systems of known potential (Figure 10).

Upon adding Eu(II) to micellar heme solutions, the observed potential requires about 15 minutes to reach a stable value. The approach to this value is asymptotic. Although electrode response is sluggish, heme reduction is not. By optical analysis, we observe reduction to occur within 1 s of

---

†Cf. reference 121, p237.



---

Figure 10

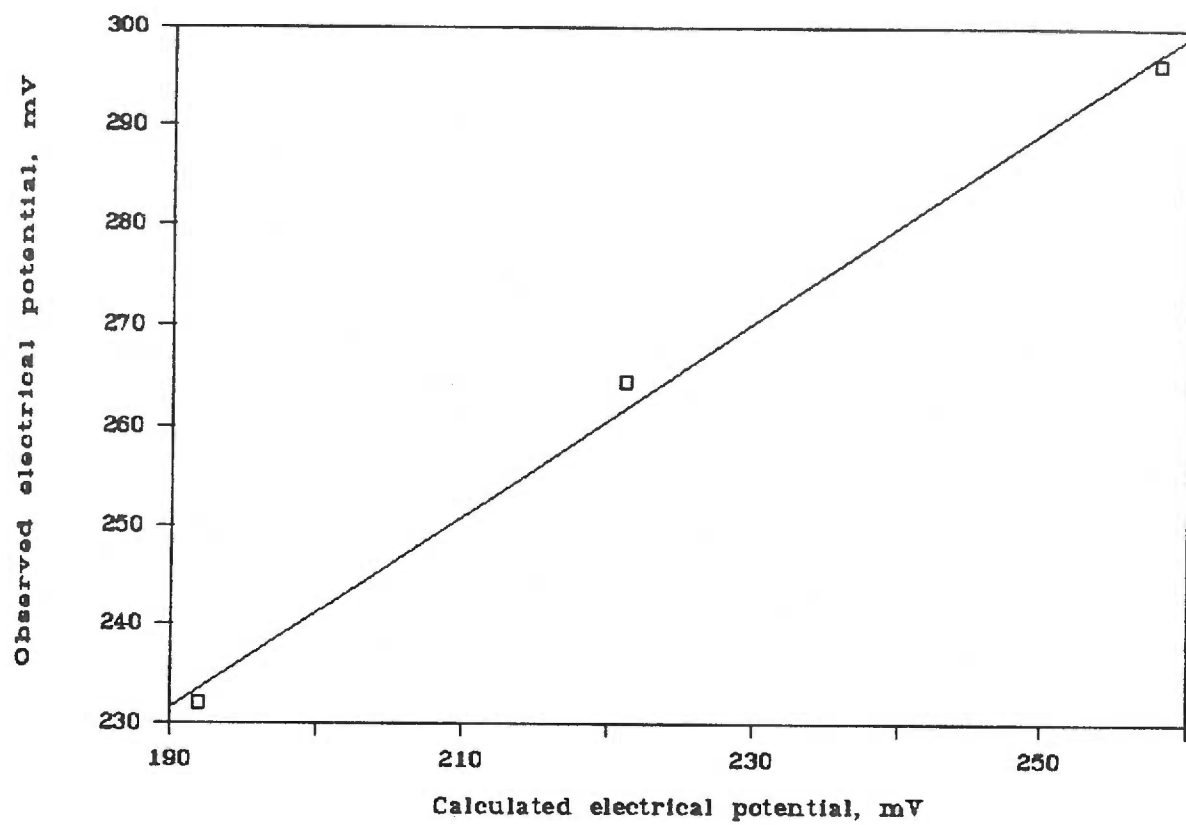
*Calibration of Saturated Ammonium Chloride Redox Electrode, 25°C.*

To relate the observed potential of the ammonium chloride redox electrode to a calomel redox electrode, potentials were measured for three redox buffers of known standard potential (versus the saturated calomel electrode). These buffers are:

1. 0.1 M potassium ferrocyanide and 0.05 M potassium ferricyanide, 192 mV (versus the saturated calomel electrode).
2. Saturated quinhydrone at pH 4.00, 221 mV.
3. 0.01 M potassium ferrocyanide and 0.36 M potassium fluoride, 258 mv.

The least squares line, shown in Figure 10, has a slope of 0.968, an intercept at 47.7 mV, and a correlation coefficient of 0.99. To obtain potentials versus the normal hydrogen electrode, 48 mV was subtracted from the observed potential (to account for differences arising from the ammonium chloride filling solution), then 241 mV was added to this value (to account for differences between the saturated calomel and normal hydrogen electrodes). The quinhydrone datum was obtained from a single measurement; the other two data are plotted as the average of three measurements each.

---



mixing. Micellar protoheme is reduced by pulse radiolysis at diffusion controlled rates.<sup>59</sup> Similar rates have been observed for  $\text{IrCl}_6^-$  oxidation of micelle-solubilized silver(II) protoporphyrin.<sup>60</sup> A slow electrode response has been observed by others studying protoheme in aqueous solution;<sup>46,49,58</sup> iron tetraphenylporphyrin in phosphatidylcholine vesicles;<sup>61</sup> and heme *a* in SDS.<sup>62</sup> Slow electrode response appears to be a general phenomenon of the electrochemistry of molecules solubilized in surfactant solutions. The effect probably originates in the slow diffusion of electroactive species across micelle layers.<sup>63</sup> To increase the rate of redox equilibration during protoheme measurements, phenazine methosulfate (PMS) was added to a final concentration of about  $1 \times 10^{-7}$  M. We found PMS to be essential for obtaining Nernstian behavior.

Another problem of micellar solutions is the sensitivity of potentials to the micelle concentration.<sup>63</sup> This complication was avoided by conducting all measurements at a single SDS concentration (2.2%).

At low pH, ferroprotoheme undergoes demetalation. This was prevented during redox titrations by buffering solutions at pH 3.0

Data from redox titrations was analyzed by the method of non-linear least squares. A program for this analysis was written by the author based on several published expositions (Appendix).<sup>64</sup> A modification of the program was used to analyze kinetic parameters of heme demetalation reactions.

## RESULTS

When measured at room temperature, the Raman spectrum of aqueous Cu(I) in 0.1 M trifluoroacetic acid is featureless except for a single band at  $1434\text{ cm}^{-1}$ .<sup>65</sup> On freezing to  $\sim 90\text{ K}$ , this band disappears to yield a completely blank spectrum. From these observations, we consider the resonance Raman spectra of frozen heme-copper solutions reported below to contain no direct contribution from Cu(I) or trifluoroacetic acid.

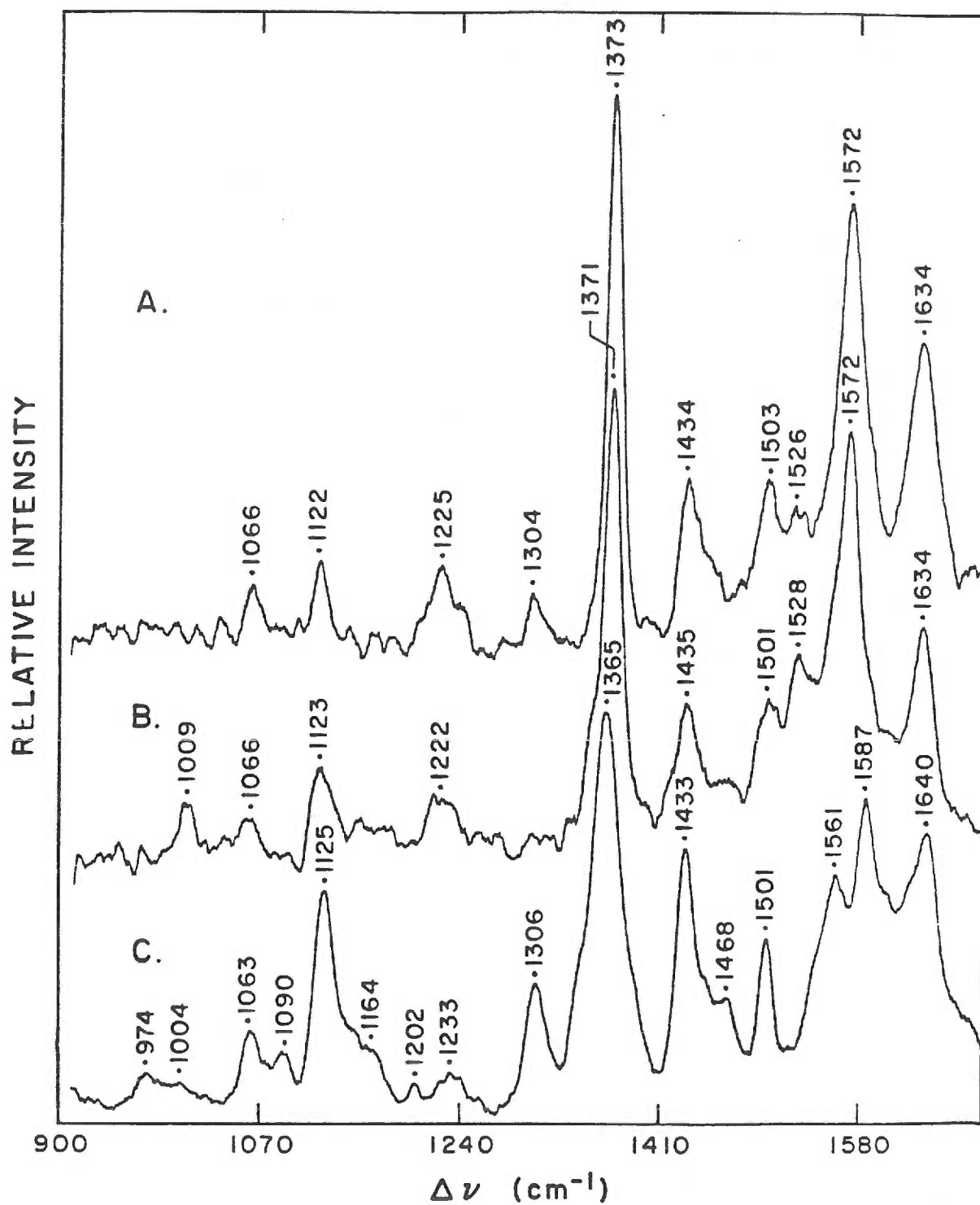
The resonance Raman spectra of monomeric ferri- and ferroprotoporphyrin are shown in Figures 11 and 12. The ferriprotoporphyrin spectrum is typical of high-spin heme, as indicated by the positions of the vibrational bands in the core size marker region ( $1550\text{-}1600\text{ cm}^{-1}$ ). Low temperature EPR studies confirm this assignment.<sup>66</sup> Ferriprotoporphyrin bands shown in Figures 11-13 are listed in Table 7, following assignments of Spiro and coworkers.<sup>8,10</sup> The  $\nu_{10}$  and vinyl symmetric stretching modes apparently are not well resolved. Assuming that  $\nu_{10}$  contributes to the band at  $1634\text{ cm}^{-1}$ , the positions of the skeletal modes  $\nu_{10}$ ,  $\nu_2$  ( $1572\text{ cm}^{-1}$ ), and  $\nu_3$  ( $1503\text{ cm}^{-1}$ ) are consistent with five-coordinate ligation of the SDS-solubilized ferriheme.<sup>67</sup> The band at  $418\text{ cm}^{-1}$  that we assign to a vinyl bending mode may also contain a pyrrole folding mode.<sup>10</sup> We do not observe bands reported<sup>10</sup> at  $1260$  ( $\nu_5+\nu_9$ ),  $694$  ( $\nu_{47}$ ), and  $373\text{ cm}^{-1}$  ( $2\nu_{35}$ ). Also, the glass band obscures bands reported at  $555$  ( $\nu_{49}$ ) and  $492\text{ cm}^{-1}$  (pyrrole

---

Figure 11

Resonance Raman Spectra of Iron Protoporphyrin in 2.2% SDS, 0.1M HTFA at 296 K. Laser excitation was 406.7 nm excitation. Upper spectrum A:  $1.4 \times 10^{-5}$  M Fe(III) protoporphyrin(Cl),  $6 \times 10^{-4}$  M Cu(II)<sub>aq</sub>, 1 scan at  $1 \text{ cm}^{-1} \text{ s}^{-1}$ , 32 mW incident power. Middle spectrum B: same as A except  $3.8 \times 10^{-4}$  M Cu(II),  $2.2 \times 10^{-4}$  M Cu(I),  $2.2 \times 10^{-4}$  M Cr(III)<sub>aq</sub>. Lower spectrum C: Fe(II) protoporphyrin(Cl) obtained by addition of slight stoichiometric excess of Eu(II)<sub>aq</sub> to  $2.4 \times 10^{-5}$  M Fe(III) protoporphyrin(Cl), in 0.11 M glycine, pH 2.60, 4 scans, 19 mW incident power. A 25-point smooth was applied to each spectrum.

---

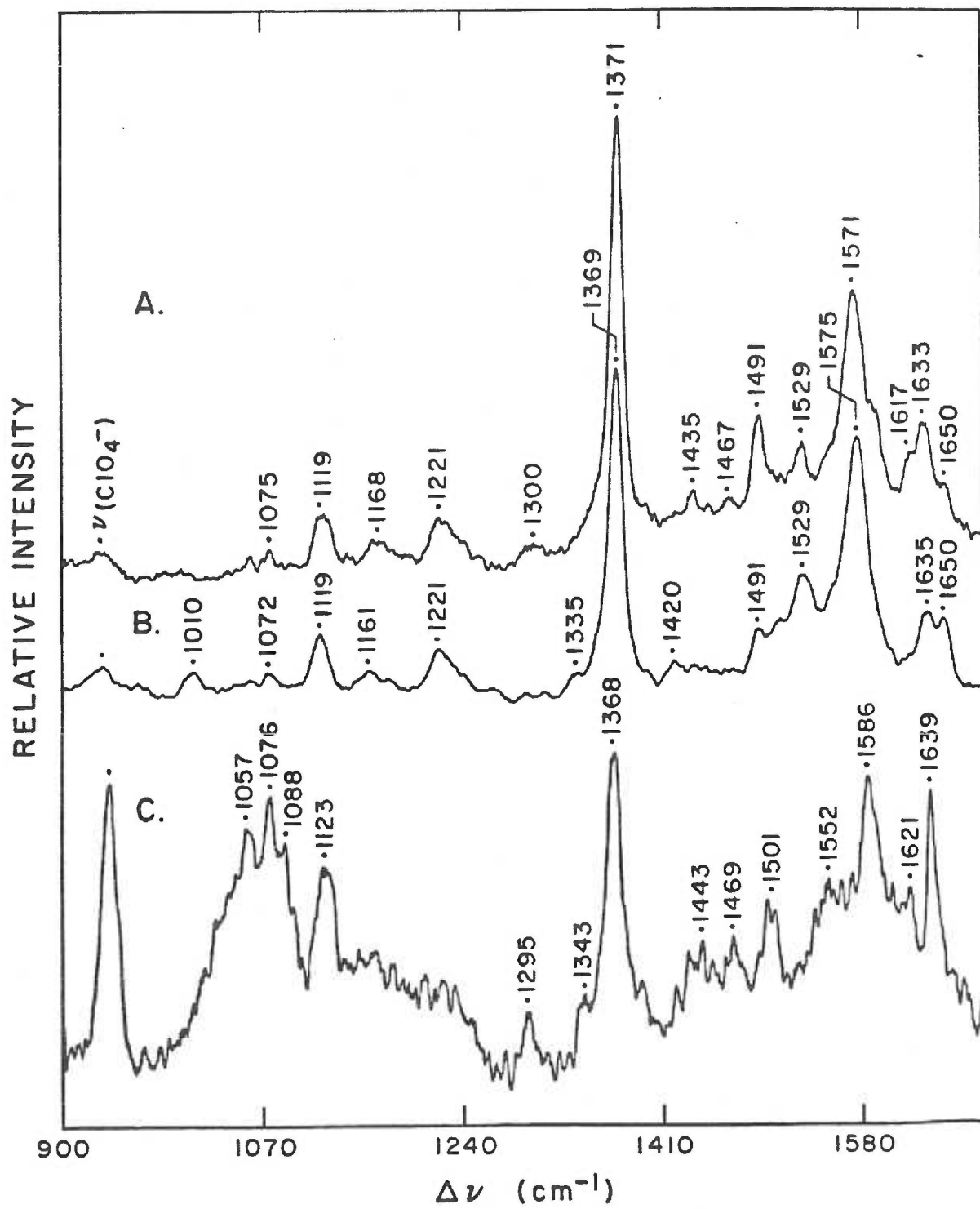


---

Figure 12

Resonance Raman spectrum of Iron Protoporphyrin in 2.2% SDS using 406.7 nm Excitation,  $\sim 77$  K. Upper spectrum A:  $1.0 \times 10^{-4}$  M Fe(III) protoporphyrin(Cl),  $1.9 \times 10^{-3}$  M Cu(II), 0.1 M TFA, 0.06 M  $\text{ClO}_4^-$ , 8 scans, 34 mW incident power. Middle spectrum B: same as A except  $1.7 \times 10^{-3}$  M Cu(II),  $1.9 \times 10^{-4}$  M Cu(I),  $1.9 \times 10^{-4}$  M  $\text{Eu(III)}_{\text{aq}}$ . Lower spectrum C: Fe(II) protoporphyrin(Cl) obtained by addition of slight stoichiometric excess of  $\text{Eu(II)}_{\text{aq}}$  to  $4.8 \times 10^{-5}$  M Fe(III) protoporphyrin(Cl) in 0.3 M  $\text{ClO}_4^-$ , TFA (pH 3.0), 8 scans, 30 mW incident power. A 9-point smooth was applied to each spectrum.

---





---

Figure 13

Resonance Raman Spectrum of Iron Protoporphyrin in 2.2% SDS using 406.7 nm Excitation, ~77 K. Upper spectrum A: same as Figure 12A except 0.3 M  $\text{ClO}_4^-$ . Middle spectrum B: same as Figure 12B except 0.3 M  $\text{ClO}_4^-$ . Lower spectrum C: subtraction of upper spectrum minus middle spectrum. Spectra are presented without smoothing.

---

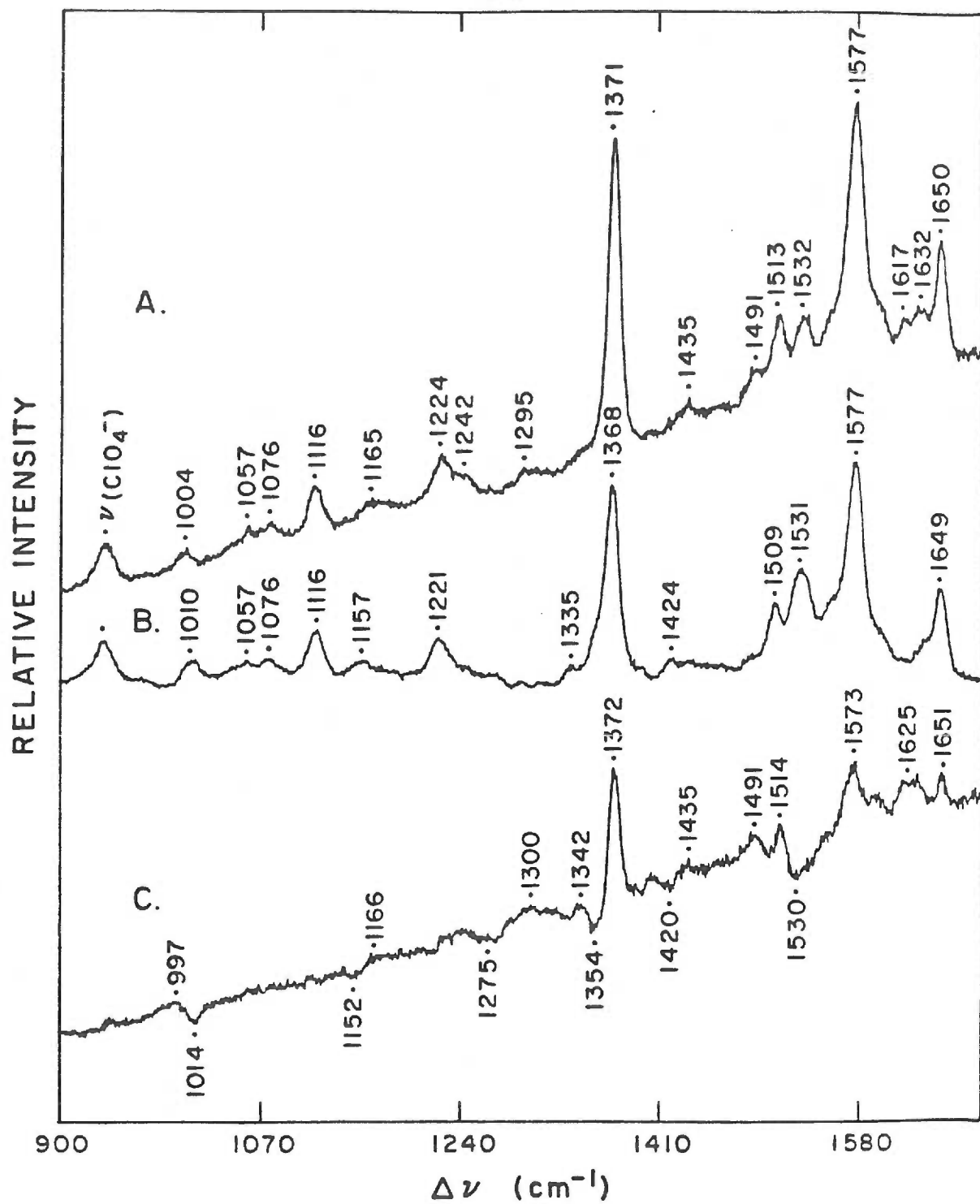


Table 7  
Raman Frequencies of Protoheme and Cu(I)-Protoheme

Assignment (a)	298 K		90 K		90 K, +ClO <sub>4</sub> <sup>-</sup>	
	-----		-----		-----	
	-Cu(I)	+Cu(I)	-Cu(I)	+Cu(I)	-Cu(I)	+Cu(I)
-----						
$\nu_{10}$	1634 m	1634 m	1650 m 1633 sh	1650 m 1636 sh	1650 m	1649 m
$\nu(\text{C}=\text{C})(1)$	* 1634 m	1634 m	1633 m	1636 m	1632 w	~1630 vw
$\nu(\text{C}=\text{C})(2)$	n.o.	n.o.	~1617 sh	n.o.	1617 vw	n.o.
$\nu_2$	* 1572 s	1572 s	1571 s	1575 s	1577 s	1577 s
$\nu(\text{Cu}-\text{C}=\text{C})$ (b)		1528 w		1529 m		1531 m
$\nu_{38}$	1526 vw		1529 w		1532 w	
$\nu_3$	1503 w	1501 w	1491 m	1491 w	1513 w	1509 w
$\delta_s(\text{=CH}_2)(1)$	* 1434 m	1435 m	1435 vw	1420 vw	1435 vw	1424 vw
$\nu_4(\text{Fe}^{3+})$	1373 vs	1371 vs	1371 vs	1369 s	1371 s	1368 s
$\nu_4(\text{Fe}^{2+})$		~1360 sh				~1365 sh
$\delta_s(\text{=CH}_2)(2)$	* n.o.	n.o.	n.o.	~1335 vw	n.o.	1335 vw
$\nu_{21}, \delta(\text{CH=})$	* 1304 w	n.o.	1300 vw	n.o.	1295 vw	n.o.
$\nu_{13}$	1225 w	1222 w	1221 w	1221 w	1224 w	1221 w
$\nu(\text{C}_b-\text{C}_\alpha)(1)$	* n.o.	n.o.	1168 w	1161 vw	1165 vw	1157 vw
$\nu_6 + \nu_8$	1122 w	1123 w	1119 w	1119 w	1116 w	1116 w

(continued)

Table 7, continued

$\delta_{as}(-CH_2)$	*	1066 w	1066 w	1075 vw	1072 vw	1076 vw	1076 vw
$\gamma(CH=)$	*	n.o.	1009 w	n.o.	1010 w	1004 vw	1010 vw
		756 m	756 m	752 m	~752 m	752 w	752 w
	*	~722 vw	~722 vw	~726 vw	n.o.	714 w	714 w
$\nu_7$	*	681 m	681 m	677 m	679 w	676 m	676 w
$\nu_{48}$	*	n.o.	n.o.	604 m	604 m	603 w	603 w
$\delta_{C_b C_\alpha C_\beta}^{(1)}$	*	n.o.	n.o.	418 vw	n.o.	n.o.	n.o.
$\gamma_{C_b S}$		n.o.	n.o.	~380 vw	~380 vw	n.o.	n.o.
$\nu_8$		~339 vw	~339 vw	~346 w	~346vw	345 vw	345 vw
$\delta_{C_b C_\alpha C_\beta}^{(2)}$	*	n.o.	n.o.	310 w	~310 vw	313 w	294 w
$\nu_9$		n.o.	n.o.	251 m	250 w	~251 w	~251 w

(a) Assignments taken from references 8 and 10. Asterisks indicate bands that shift upon vinyl deuteration (references 8, 10, 74, 75). Band not observed = n.o.

(b) Attributed to Cu(I)-coordinated vinyl stretching mode.

fold). The ferroprotoporphyrin spectra (Figures 11C, 12C) are very nearly identical to the previously reported spectrum taken in aqueous cetyltrimethylammonium micelles.<sup>68</sup> Positions of the bands at 1640, 1501 and 1365  $\text{cm}^{-1}$  are consistent with the SDS-solubilized ferroheme existing as a tetracoordinate intermediate spin ( $S=1$ ) species.<sup>68</sup> Mossbauer studies of aqueous alkaline ferroprotoheme support this assignment.<sup>69</sup>

At room temperature, Soret excitation Raman spectra of ferriprotoporphyrin (Figure 11A) are perturbed upon adding Cu(I) (Figure 11B). Although ferriheme remains high spin, intensity is lost in the vinyl stretching mode at 1634  $\text{cm}^{-1}$ , and gained at 1528  $\text{cm}^{-1}$ ; the vinyl rocking mode at 1304  $\text{cm}^{-1}$  disappears, while the vinyl trans wagging motion appears at 1009  $\text{cm}^{-1}$ ; and the oxidation state marker band loses intensity at 1373  $\text{cm}^{-1}$ , but gains a shoulder at approximately 1360  $\text{cm}^{-1}$ . No changes are detected in low frequency bands. Oxygenation of the solution causes reversion to the original ferriprotoporphyrin spectrum.<sup>†</sup>

Copper(I)-protoheme spectra obtained in frozen suspensions at ~90 K demonstrate other perturbations in addition to those noted above (Figures 12A, 12B). With added Cu(I), a shoulder at ~1617  $\text{cm}^{-1}$  is resolved. This appears to be a

---

<sup>†</sup>Oxygenation of Cu(I)-protoheme solutions also diminishes overall Raman scattering. This is probably due to degradation of the porphyrin chromophore by coupled oxidation<sup>52</sup> or photooxidation.<sup>33,34</sup>

consequence of the loss of a weak shoulder at  $\sim 1617\text{ cm}^{-1}$  and loss of intensity at  $\sim 1633\text{ cm}^{-1}$ . In addition, the core size marker at  $1571\text{ cm}^{-1}$  ( $\nu_2$ ) shifts  $+4\text{ cm}^{-1}$ , the vinyl-ring stretch at  $1168\text{ cm}^{-1}$  shifts  $-7\text{ cm}^{-1}$  and loses intensity, the vinyl asymmetric rocking mode at  $1075\text{ cm}^{-1}$  shifts  $-3\text{ cm}^{-1}$ , and intensity is lost in a vinyl bending mode ( $310\text{ cm}^{-1}$ ) and in three fundamentals [ $\nu_7$  ( $677\text{ cm}^{-1}$ ),  $\nu_8$  ( $\sim 346\text{ cm}^{-1}$ ),  $\nu_9$  ( $251\text{ cm}^{-1}$ )]. Since at liquid nitrogen temperature interference from the  $1434\text{ cm}^{-1}$  TFA solvent band is eliminated, the influence of Cu(I) on the weak vinyl scissors mode<sup>8,10</sup> is detected as a  $-15\text{ cm}^{-1}$  shift. The additional changes which appear upon lowering temperature may be due to linewidth narrowing. Identical spectral shifts are obtained with the dimethyl ester of ferriprotoporphyrin.

To obtain an accurate difference spectrum, aqueous perchloric acid was added to heme solutions. Spectra of these solutions were recorded at  $\sim 90\text{ K}$  in the presence or absence of Cu(I) (Figures 13A, 13B). The symmetric stretching band of perchlorate ion at  $\sim 930\text{ cm}^{-1}$  is not resonance enhanced and was expected to serve as an internal reference of intensity. The ferriprotoporphyrin minus ferriprotoporphyrin-Cu(I) difference spectrum (Figure 13C) was obtained by subtracting the corresponding Raman spectra normalized to  $\nu_1(\text{ClO}_4^-)$ . At room temperature, the ferriheme spectrum is unchanged upon addition of  $0.3\text{ M NaClO}_4^-$ , but when these solutions are frozen, several spectral shifts occur in the high frequency region.

Specifically, below 180 K intensity is lost in the  $1634\text{ cm}^{-1}$  region, a new band appears at  $1650\text{ cm}^{-1}$ , and the bands at 1572, 1526, and  $1503\text{ cm}^{-1}$  shift to slightly higher frequencies (1577, 1532 and  $1513\text{ cm}^{-1}$ , respectively). The  $\text{ClO}_4^-$ -modified protoheme can also be detected in the  $\sim 90\text{ K}$  spectrum of solutions containing  $0.06\text{ M ClO}_4^-$  ion (Figures 12A, 12B).

Although high concentrations of perchlorate alter protoheme spectra, the difference spectrum (Figure 13C) demonstrates a set of Cu(I) perturbations similar to those in the absence of perchlorate ion. Most prominently, intensity is lost in the region of the vinyl symmetric stretching band ( $\sim 1630\text{ cm}^{-1}$ ) and gained at  $\sim 1530\text{ cm}^{-1}$ . Negative shifts also occur for components of the vinyl scissors ( $1435\text{ cm}^{-1}$ ) and vinyl group stretching modes ( $\sim 1168\text{ cm}^{-1}$ ). Also, the vinyl wagging mode ( $\sim 1300\text{ cm}^{-1}$ ) and a component of the vinyl stretching mode ( $\sim 1617\text{ cm}^{-1}$ ) both lose intensity, whereas a component of the vinyl scissors mode ( $1335\text{ cm}^{-1}$ ) gains intensity.

Solutions of Cu(I)-protoheme are unstable, undergoing slow demetalation as indicated by changes in Raman spectra from Figure 11B to that of tetraprotonated protoporphyrin dication (Figure 14A). Parallel changes occur in the heme optical absorption spectrum, also leading to the spectrum of the dication.<sup>25</sup> Heme demetalation is prevented by freezing Cu(I)-protoheme solutions. Samples stored at  $\sim 90\text{ K}$  appear to be stable indefinitely, as judged from Raman spectra.

No change occurs in the resonance Raman spectrum of

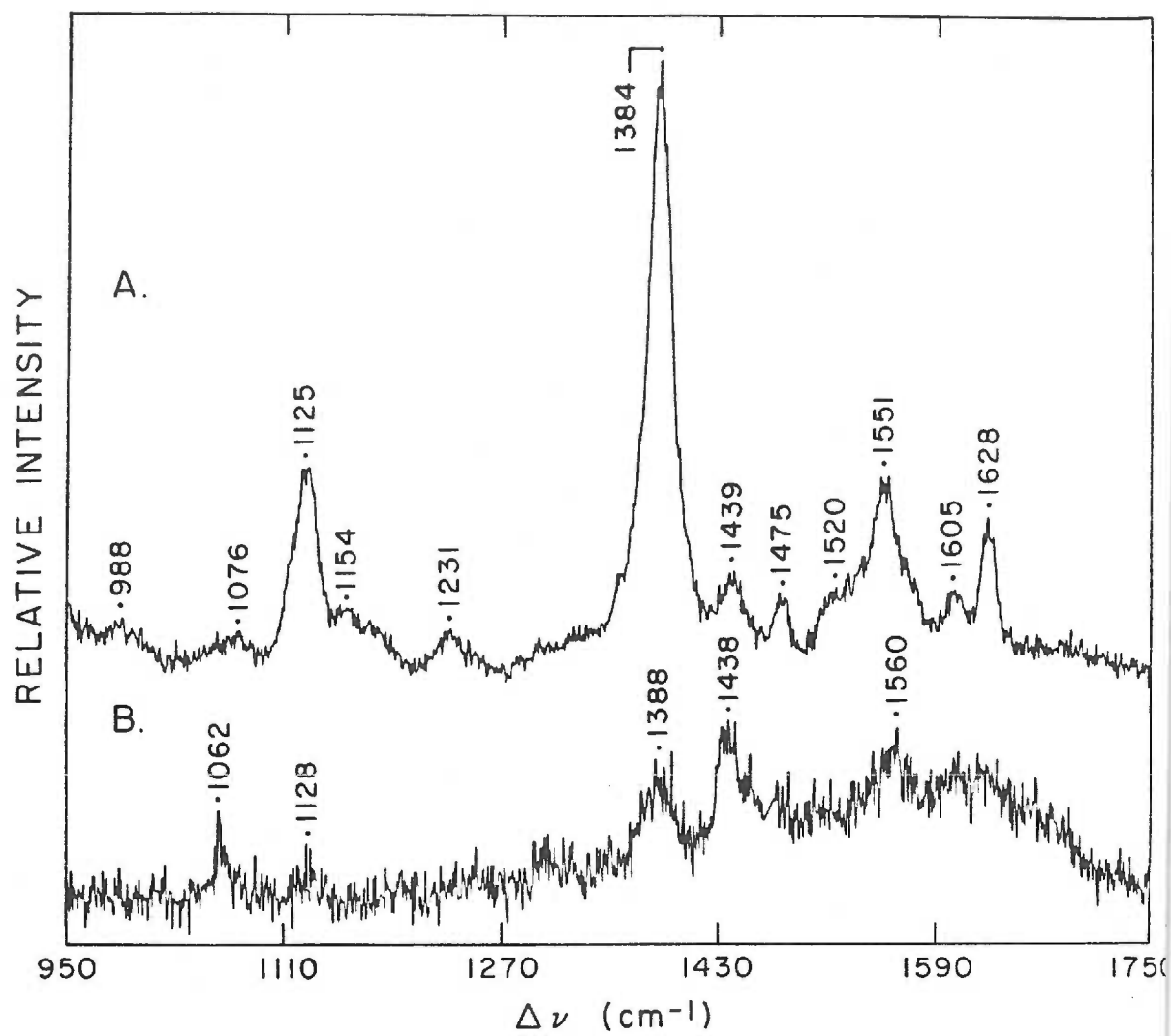
---

Figure 14

*Resonance Raman Spectra of Tetraprotonated Protoporphyrin in 1% SDS at 298 K. Upper spectrum A:  $4.8 \times 10^{-4}$  M Cu(II), 0.1 M HTFA, 1 scan at  $1 \text{ cm}^{-1} \text{ s}^{-1}$ , 25 mW incident power at 406.7 nm excitation. Lower spectrum B: Same as A except  $3.8 \times 10^{-4}$  Cu(II),  $2.2 \times 10^{-4}$  M Cu(I). Spectra are presented without smoothing at the correct relative scattering intensities.*

---





ferriprotoporphyrim upon adding Cu(II). Moreover, no change occurs in the resonance Raman spectrum of 3,8-diethyldeuterothene with added Cu(I). However, dramatic changes occur in the Raman spectrum of tetraprotonated protoporphyrim upon adding Cu(I). The multibanded porphyrim spectrum (Figure 14A) is converted to one with few bands that is qualitatively uncharacteristic of a porphyrim spectrum (Figure 14B). Bands are observed at 1560, 1388, 1128, and 1062  $\text{cm}^{-1}$ . These changes are largely reversed upon adding ferricyanide except that there is no return in intensity of the 1628  $\text{cm}^{-1}$  band, and there occurs a -9  $\text{cm}^{-1}$  shift in the 1560  $\text{cm}^{-1}$  band.

The magnitude of Cu(I)-induced optical shifts is relatively small for protoporphyrim,<sup>25</sup> hence an extensive change in vibrational properties is not expected. The origin of these changes is not metalation of the porphyrim core, as evident from the constant tetraprotonated character of the optical spectrum and from the undiminished intensity of fluorescence emission. (High acidity of the porphyrim solution (~pH 1) precludes metalation.) The mechanism by which Cu(I) extensively but reversibly perturbs the Raman spectrum of protoporphyrim remains puzzling.

By spectroelectrochemical titration, the standard reduction potential of protothene in a 2.2% SDS solution (pH 3.0) was determined to be +92 mV ( $\pm 5$  mV; average of 3 runs; 25°C;  $7.2 \times 10^{-5}$  M protothene). Nernstian behavior for a one-electron redox process was observed.

Heme demetalation rates for Cu(I)-ferriheme solutions were measured. Demetalation rates were found to be inversely dependent on Cu(II) concentration (Table 8, Figure 15), as noted previously.<sup>25</sup>

A minor discrepancy in demetalation rates was observed between our measurements and those of Dr. Eugene A. Deardorff (laboratory of Professor James K. Hurst, Oregon Graduate Center). This discrepancy prompted us to examine the laboratory notebooks of Deardorff, which indicate that demetalation rates had been computed from averages of data obtained at three different SDS concentrations (2.0%, 0.9%, 0.18%). Deardorff's original data appears to reveal, however, a dependence of demetalation rates on SDS concentration (Figure 16). Hence in this case, data averaging appears to have introduced slight inaccuracies to the reported demetalation rates and thermodynamic constants.<sup>25</sup> Based on experiments conducted at a single SDS concentration (2.2%), we report here improved values. These values are close to those we compute from data obtained by Deardorff at 2.0% SDS.

Table 8  
Kinetic Parameters for Cu(I)-Protoheme Demetalation (a)

[Cu(II)], M	[Cu(I)], M	[SDS], %	$10^{-4}/k_{\text{obs}}, \text{ s}$
-----	-----	-----	-----
$7.33 \times 10^{-5}$	$1.92 \times 10^{-3}$	2.2	6.39
$7.33 \times 10^{-5}$	$1.02 \times 10^{-3}$	2.2	3.67
$7.33 \times 10^{-5}$	$8.87 \times 10^{-5}$	2.2	0.52
$2.20 \times 10^{-4}$	$1.32 \times 10^{-2}$	2.0	6.94
$2.20 \times 10^{-4}$	$5.19 \times 10^{-3}$	2.0	2.27
$2.20 \times 10^{-4}$	$3.41 \times 10^{-4}$	2.0	0.67
$6.60 \times 10^{-4}$	$8.00 \times 10^{-4}$	2.2	0.38
$6.60 \times 10^{-4}$	$1.73 \times 10^{-2}$	2.2	3.46
$6.60 \times 10^{-4}$	$4.42 \times 10^{-2}$	2.2	8.40

a) Conditions: ferriprotoheme =  $1.2 \times 10^{-5}$ ; 0.1 M TFA; 23°C.

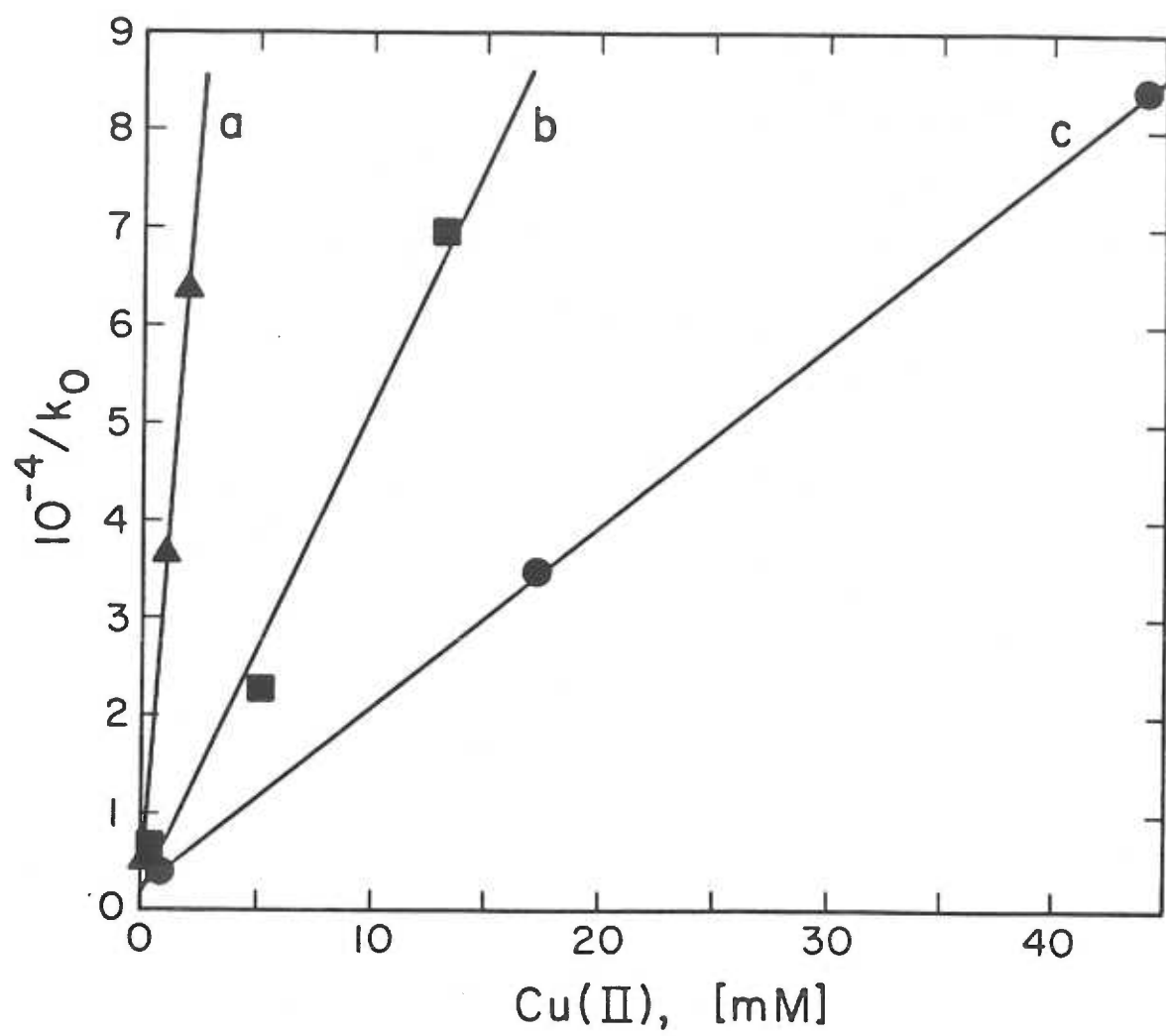
---

**Figure 15**

*Copper Dependence of Iron Loss from Cu(I)-Protoheme. Conditions:  
 $1.2 \times 10^{-5}$  M Fe(III)protoporphyrin IX, 0.1 M TFA, 23 C.*

*Triangles:  $7.33 \times 10^{-5}$  M Cu(I). Squares:  $2.20 \times 10^{-4}$  M  
Cu(I). Circles:  $6.60 \times 10^{-4}$  M Cu(I). Solid lines are the  
least squares fits to the data; computed correlation coefficients  
were greater than 0.99 for the three lines shown (N-1 weighting).*

---

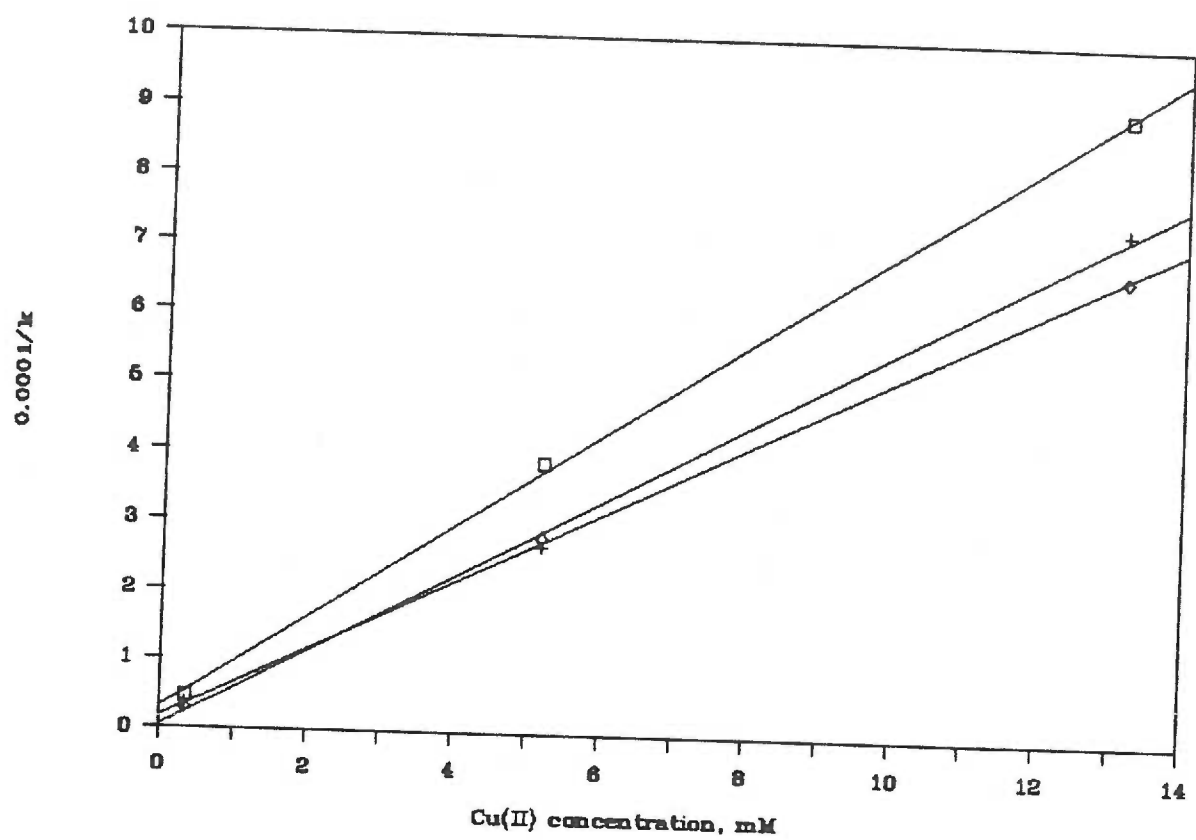


---

Figure 16

SDS Dependence of Iron Loss from Cu(I)-Protoheme. Conditions:  
 $1.2 \times 10^{-5}$  M Fe(III)protoporphyrin IX,  $2.2 \times 10^{-4}$  M Cu(I),  
0.1 M TFA, 23 C. Triangles: 2.0% SDS. Squares: 0.9% SDS.  
Circles: 0.18% SDS. Solid lines are the least squares fits to  
the data; computed correlation coefficients were greater than  
0.99 for the data obtained at 2.0% and 0.18% SDS.

---

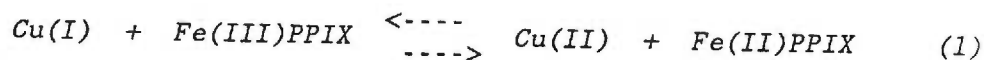




### DISCUSSION

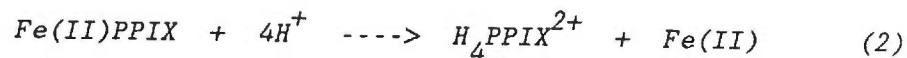
Resonance Raman spectra of protoheme solutions are perturbed by Cu(I) (Figure 11). Previous optical studies<sup>25</sup> suggest these perturbations originate predominately from a  $\pi$ -bonding interaction between Cu(I) and vinyl substituents. An additional minor perturbation is caused by the reduction of a small fraction of ferriheme by Cu(I).

Heme reduction by Cu(I). When Cu(I) is added to protoheme, the ferriheme oxidation state marker band at  $1373\text{ cm}^{-1}$  loses intensity and shifts to slightly lower energy (Figure 11B). Also, a weak shoulder develops at  $\sim 1365\text{ cm}^{-1}$ . By comparison with the spectrum of ferroprotoporphyrin (Figure 11C), which shows an oxidation state marker band at  $1365\text{ cm}^{-1}$ , these spectral changes are attributed to the reduction of a minor portion of the total ferriheme. This reduction is governed by the equilibrium:



Establishment of equilibrium is indicated by the following:

1. Manipulating the Cu(II)/Cu(I) ratio of protoheme solutions varies the intensities of the ferriheme and ferroheme oxidation state marker bands in a reciprocal manner.
2. In acidic media, solutions of ferriheme are stable, whereas ferroheme is unstable toward demetallation:



The demetalation of ferroheme to tetraprotonated porphyrin dication (reaction 2) drives reaction 1 from left to right. Provided Cu(I) is initially in excess over heme, all of the heme eventually undergoes demetalation. A Raman spectrum of the final product from such an experiment is identical to one of tetraprotonated porphyrin dication (Figure 14A). The rate law for demetalation is quantitatively in accord with a mechanism comprising reactions (1) and (2):<sup>25,66</sup>

$$k_{obs}^{-1} = ((K_{eq\ 1})(k_2)([Cu(I)]))^{-1}[Cu(II)] + (k_2)^{-1} \quad (3)$$

From data shown in Figure 15, a mean value for the equilibrium constant of reaction 1 was computed to be 1.5; a mean value for the rate constant of demetalation, reaction 2, was computed to be  $4.2 \times 10^{-4} \text{ s}^{-1}$ .

Upon adding Cu(I) to protoheme, the vibrational spectra undergo several changes in addition to those in the oxidation state marker region. At room temperature (Figure 11), Cu(I) perturbs bands at 1634, 1526, 1304, and 1009  $\text{cm}^{-1}$ ; at liquid nitrogen temperature (Figure 12), additional bands are perturbed at 1571, 1168, 1075, 677, ~346, 310, and 251  $\text{cm}^{-1}$ . The extent to which Cu(I) perturbs the protoheme spectrum is illustrated by the difference spectrum given in Figure 13C. Although the entire set of perturbations can be reversed by oxygen, the new Cu(I)-induced features do not resemble those of ferroheme (Figures 11C, 12C), and so cannot be attributed to heme reduction. This conclusion is consistent with the measured value for  $K_{eq\ 1}$ ,

from which we calculate, for the experimental conditions of Figures 12B and 13B, that ferroheme comprises less than 20% of the total heme. Although ferroheme is a minor constituent, it may introduce features in the oxidation state marker region ( $\sim 1365\text{ cm}^{-1}$ ) where Raman scattering is exceptionally efficient; it should not, however, contribute significantly at other frequencies.

It is also incorrect to attribute the other spectral changes to interactions involving non-vinyl heme substituents, e.g., propionyl groups,<sup>†</sup> or incidental constituents of the Cu(I)-protoheme solutions, e.g., Cu(II) associated with SDS micelles.<sup>70-73</sup> This can be deduced from the tendencies of related systems to demonstrate a protoheme-like Cu(I)-sensitivity. With added Cu(I), esterified protoheme shows the same Raman spectral changes as protoheme, but not 3,8-diethyl-deuterothene, which is spectrally unperturbed. Also, protoheme spectra are unperturbed by Cu(II), whether added as an authentic solution, or as the oxygenated product of Cu(I)-containing solution. The foregoing circumstantial evidence suggests that the various protoheme spectral changes are due to specific interaction between Cu(I) and porphyrin vinyl substituents. This

---

<sup>†</sup>Carboxylate coordination of Cu(II) and Cu(I) is known.<sup>122,123</sup> However, carboxylic acids with olefinic groups preferentially bind Cu(I) at the olefin rather than the carboxylate.<sup>25</sup>

conclusion is in accord with previous arguments based on optical studies.<sup>25</sup>

Cu(I)-vinyl bonding. Direct evidence for Cu(I)-vinyl bonding is provided by the Cu(I) perturbation of vinyl-related modes. From the frequency shifts which accompany deuteration of vinyl carbons, vinyl modes have been identified by resonance Raman studies on protoheme and reconstituted protoheme proteins.<sup>8,10,74,75,†</sup> These modes are denoted by asterisks in Table 7. Nearly all of the modes perturbed by Cu(I) are also vinyl-related modes.<sup>††</sup> Conversely, the modes not perturbed by Cu(I) contain neither local nor porphyrin-coupled vinyl vibrational components.

---

<sup>†</sup>Three deuteration-sensitive modes of Ni(II) protoporphyrin ( $\nu_{38}$ ,  $\nu_{29}$ ,  $\nu_{20}$ )<sup>9</sup> and one of myoglobin(F<sup>-</sup>) ( $\nu_{44}$ )<sup>8,10</sup> do not appear to be resonance enhanced in Soret excitation spectra of iron protoporphyrin. The glass band obscures two deuteration-sensitive modes which have been reported for myoglobin(F<sup>-</sup>) ( $\nu_{49}$ , pyrrole fold at 472 cm<sup>-1</sup> and 501 cm<sup>-1</sup>) and for the bis-imidazole complex of iron protoporphyrin (pyrrole fold at 488 cm<sup>-1</sup> and 507 cm<sup>-1</sup>).

<sup>††</sup>There appear to be only a few exceptions to this generalization. Cu(I) addition shifts the oxidation state marker band by  $\sim -3$  cm<sup>-1</sup>, presumable due to partial reduction of heme. In addition,<sup>1</sup> intensity changes are observed in bands at 346 and 251 cm<sup>-1</sup>, neither of which are known to be associated with vinyl modes. However, these intensity changes are not reproduced in spectra obtained at higher perchlorate concentrations (0.3 M), possibly due to axial ligation effects. On the other hand, a dramatic shift of the 310 cm<sup>-1</sup> vinyl bending mode ( $-19$  cm<sup>-1</sup>) was observed only at higher perchlorate concentrations (Table 7).

Vibrational data on several Cu(I)-olefins are collected in Table 9. On binding Cu(I), a large negative shift in frequency of the C=C stretching mode is observed. For many metal-olefins, this shift is diagnostic of  $\pi$ -complex bond formation.<sup>23</sup> When Cu(I) is added to protoheme solutions, there occurs a loss of intensity at 1615-1630  $\text{cm}^{-1}$  and a concomitant increase at  $\sim 1530 \text{ cm}^{-1}$  (Table 9, Figures 12, 13). The intensity increase occurs atop an underlying weak band ( $\nu_{38}$ ) at  $1526 \text{ cm}^{-1}$ , but appears as a prominent feature in the difference spectrum (Figure 13C). By analogy to the simple olefins (Table 9), the intensity increase at  $1530 \text{ cm}^{-1}$  is anticipated if  $\pi$ -bonding occurs to  $\beta$ -pyrrolic vinyl substituents on the porphyrin. The change in intensity does not correlate with any Cu(I)-induced spin state changes since EPR spectra of protoheme and Cu(I)-protoheme solutions indicate ferric high-spin heme as the predominant species.<sup>66</sup>

In earlier studies,<sup>25</sup> it was shown that Cu(I) complexation occurs with 1:1 binding stoichiometry. This means that only one of the two potential olefinic coordination sites is occupied, and may explain the apparent splitting of the vinyl  $1633 \text{ cm}^{-1}$  band into two bands ( $1635 \text{ cm}^{-1}$  and  $1650 \text{ cm}^{-1}$ ) (Figure 12B). An alternate explanation is that lower temperature diminishes the intensity of the C=C symmetric stretching mode to reveal an underlying contribution at  $1650 \text{ cm}^{-1}$ . The frequency of the  $1650 \text{ cm}^{-1}$  band is somewhat high for assignment to vinyl C=C stretching modes, and instead may be  $\nu_{10}$ .<sup>8-10,76</sup> The

Table 9

Raman Frequencies for Vinyl Modes of Protoheme and  
Other Selected Olefins (a)

	$\nu(\text{C}=\text{C})$		$\delta_s(=\text{CH}_2)$		$\delta(\text{CH}=\text{)}$	
	-Cu(I)	+Cu(I)	-Cu(I)	+Cu(I)	-Cu(I)	+Cu(I)
Protoheme	1633 w	1529 w	1435 vw	1420 vw	1300 vw	n.o.
			n.o.	1335 vw		
( $\text{H}_2\text{O}$ ) <sub>5</sub> Cr(III)- fumarate (b)	1660 m	1526 m	1436 vw	n.o.	1275 w	1236 m
Allylpyridine (c)	1640 m	1553 m	1435 vs	1445 s 1420 s	1297 w	n.o.
Allyl alcohol (d)	1645 w	1550 w	1425 m	1420 m	1235 w	1230 w
Acrolein (e)	1620 m	1530 s	1425 m	1430 m	1275 m	1240 w

(continued)

Table 9, continued

	$\delta_{as}(=CH_2)$		$\gamma(CH=)$	
	-Cu(I)	+Cu(I)	-Cu(I)	+Cu(I)
Protoheme	1074 vw	1072 vw	n.o.	1010 w
$(H_2O)_5Cr(III)$ - fumarate (b)	n.r.	n.r.	n.r.	n.r.
Allylpyridine (c)	1110 m	1095 m	993 s	1016 ms 1007 w
Allyl alcohol (d)	1115 m	1107 m	995 s	995 s
Acrolein (e)	1160 s	1150 s	975 s	960 s

(a) See also: Thompson, J.S.; Swiatek, R.M. Inorg. Chem. 1985, 24, 110-113, and references therein. Not observed = n.o.; not reported = n.r.

(b) References 25 and 66.

(c) Yingst, R.E.; Douglas, B.E. Inorg. Chem. 1964, 3, 1177-1180.

(d) Ogura, T.; Furuno, N.; Kawaguchi, S. Bull. Chem. Soc. Jpn. 1967, 40, 1171-1174.

(e) Kawaguchi, S.; Ogura, T. Inorg. Chem. 1966, 5, 844-846.

$\text{ClO}_4^-$  concentration and temperature dependence observed in the resonance Raman spectra suggest that axial  $\text{ClO}_4^-$  ligation of the heme can occur at lower temperatures. A band assigned to  $\nu_{10}$  has been observed at  $\sim 1650 \text{ cm}^{-1}$  in an intermediate spin ( $S=3/2$ ) five-coordinate perchloratoferri-octaethylporphyrin complex;<sup>77</sup> the  $\text{ClO}_4^-$ -induced shift from  $1503 \text{ cm}^{-1}$  to  $1513 \text{ cm}^{-1}$  in the  $\nu_3$  band (Figures 11A, 13A) and the insensitivity of the  $\nu_4$  band ( $1373 \text{ cm}^{-1}$ ) are also consistent with assignment of the new species as a perchlorate-bound five-coordinate intermediate spin heme.

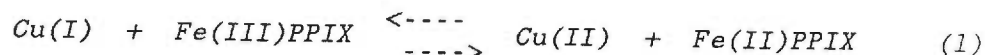
Vibrational coupling. The involvement of protoheme in  $\pi$ -bonding may be expected to perturb the vibrational doublets derived from coupling<sup>6</sup> between vinyl modes and other degenerate vibrations of like symmetry.<sup>7,78</sup> The porphyrin macrocycle probably contributes these degenerate vibrations. Although vinyl-vinyl coupling is also conceivable,<sup>9</sup> it is not likely since seven bonds intervene between the two protoporphyrin vinyl groups. A similar separation in non-porphyrin polyenes disallows vibrational coupling between such groups.<sup>79</sup> Self-consistent HMO calculations also predict a rapid decrease in vibrational coupling between two groups as the number of intervening bonds increases.<sup>80</sup>

The notion of vinyl-porphyrin coupling is consistent with a report by Macor and Spiro<sup>81</sup> on the Raman spectrum of a monovinyl porphyrin obtained electrochemically from nickel(II) protoporphyrin. Upon saturating one of the protoporphyrin



vinyls, these workers observe that a weak band at  $1634\text{ cm}^{-1}$  loses intensity, but without shifting in frequency. If the observation is correct,<sup>†</sup> then the  $1634\text{ cm}^{-1}$  band is possibly the Raman-active half of a doublet derived from coupling-induced splitting of the vinyl symmetric stretching mode. Were such splitting to originate in vinyl-vinyl resonance, then a loss of coupling on reducing the number of vinyl groups from one to two would eliminate the splitting. This would cause a shift in the vinyl stretching band to the frequency expected for the non-coupled condition. Yet as expected for vinyl-porphyrin coupling, splitting appears instead to occur for both monovinyl and divinyl porphyrin, with a second vinyl simply adding intensity to the Raman-active half-doublet band. Similar evidence for substituent-porphyrin coupling is to be found in the vibrational data of Willems and Bocian on a nickel(II) deuteroporphyrin series with 0, 1, and 2 acetyl substituents.<sup>82</sup>

Protoheme Reduction Potential The rate of Cu(I)-induced demetalation of protoheme varies inversely with Cu(II) concentration. To explain this unusual kinetic feature, reaction (1) has been postulated:




---

<sup>†</sup>Published spectra of Macor and Spiro are ambiguous (cf. Figure 13 of reference 81).

From the Nernst equation and the kinetically-determined equilibrium constant, an overall potential for reaction (1) is calculated to be +10 mV. The constituent half-reactions of reaction (1) are the two couples Fe(III)PPIX/Fe(II)PPIX and Cu(II)/Cu(I). By adding the potential of the overall reaction to the reported reduction potential of the Cu(II)/Cu(I) aquo ion ( $E^\circ = +153$  mV), the potential of the protoheme couple can be predicted to be +163 mV. To test the validity of reaction (1), the potential of the protoheme couple was determined by spectro-electrochemical techniques to be about +92 mV. In other words, there is a discrepancy of about 70 mV between measured and calculated potentials. The significance of this discrepancy is difficult to judge, especially in consideration of the following. (1) The Cu(II)/Cu(I) potential used in the calculation applies to an SDS-free solvent system at pH 7; this potential may vary with pH or SDS concentration.<sup>63</sup> (2) The equilibrium constant for reaction 1 is determined from the intercept of a linear plot of kinetic data (Figure 15). Since reduction potential is related logarithmically to this intercept (Figure 17), small errors in determining the near-zero intercept ( $\sim 0.2$ ) will introduce large errors in the calculated protoheme potential.

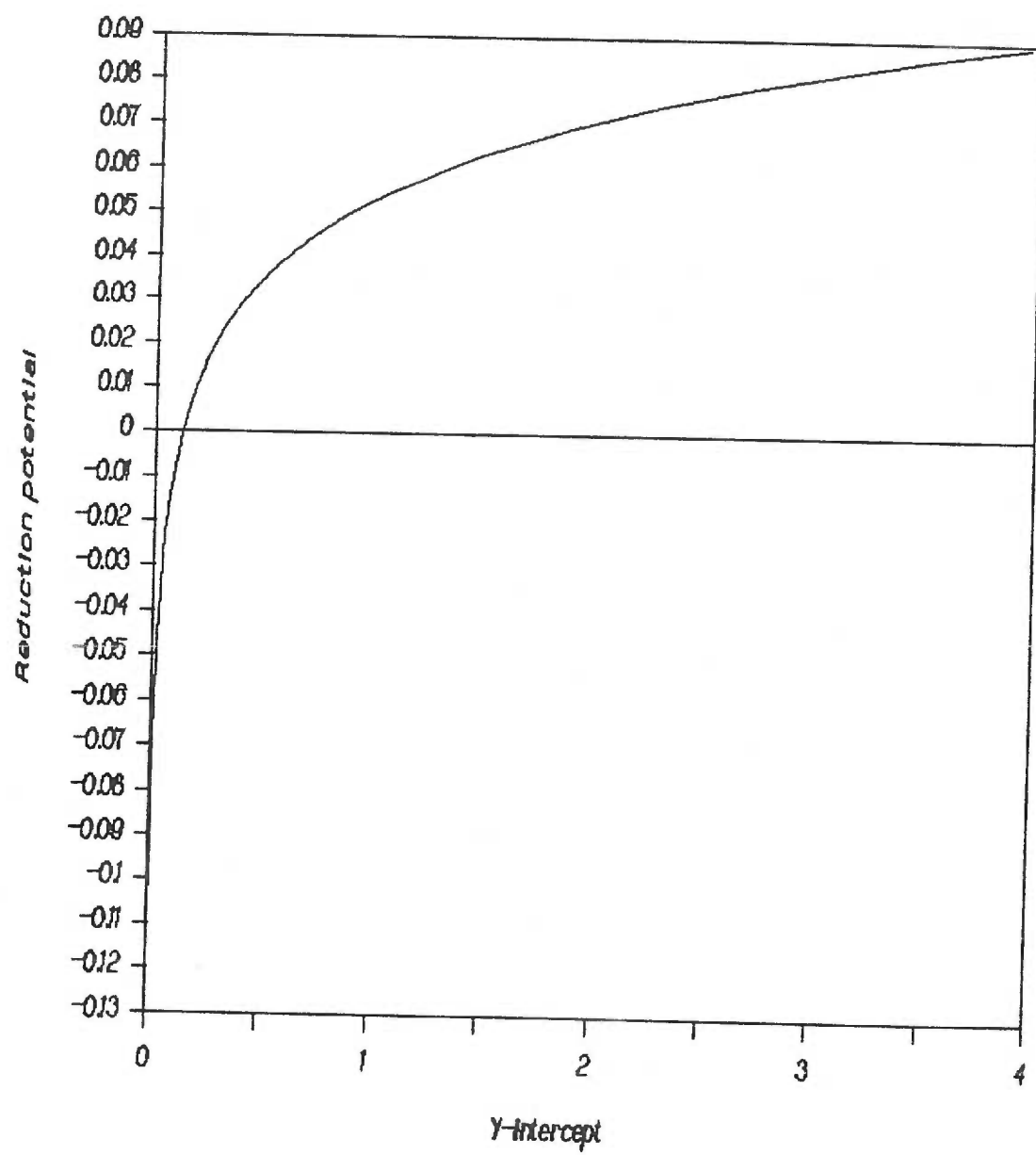
Cu(I)  $\pi$ -Bonding in Cytochrome Oxidase. The relevance of this study to cytochrome oxidase depends in large part on whether the spectroscopic properties of the enzyme demonstrate features which are characteristic of Cu(I)-vinyl  $\pi$ -bonding. Specifically, it is of interest to determine whether

---

*Figure 17*

*Dependence of calculated reduction potential on the intercept of kinetic data plotted according to Figure 15.*

---



reduction of cytochrome oxidase (1) shifts the vinyl stretching mode in vibrational spectra of the enzyme, and (2) introduces new charge transfer bands in optical spectra.

The vinyl stretching mode from the two hemes of resting oxidized cytochrome oxidase has been assigned to a single band at  $1626\text{ cm}^{-1}$ .<sup>10</sup> Since other bands overlap in this region, it is difficult to quantify the intensity change of the  $1626\text{ cm}^{-1}$  band upon reducing the enzyme. Yet in the region  $1500\text{-}1540\text{ cm}^{-1}$ , the appearance of a new, moderately intense band at  $\sim 1520\text{ cm}^{-1}$  is readily observed in reduced oxidases of both mitochondrial and microbial origin (Table 10). This new band is similar in frequency and relative intensity to the Cu(I)-protoheme band at  $1529\text{ cm}^{-1}$  which we assign to a vinyl stretching mode shifted to lower energy by Cu(I).

The literature was surveyed to determine whether cytochrome oxidase is unique among vinyl-containing heme proteins in demonstrating a new Raman band between  $1500\text{ and }1540\text{ cm}^{-1}$  upon undergoing reduction. Hemoglobin,<sup>83</sup> horseradish peroxidase,<sup>84</sup> lactoperoxidase,<sup>84</sup> intestinal peroxidase,<sup>85</sup> and chloroperoxidase<sup>86</sup> were some of the many protoheme proteins whose spectra were examined in the region  $1500\text{-}1540\text{ cm}^{-1}$  and, without exception, found to be unperturbed by reduction. On this evidence, we suggest that Cu(I)-olefin  $\pi$ -bonding may occur in the reduced oxidase.

The copurification of heme *a* and copper ion has been reported to occur beyond chromatographic fractionation.<sup>87</sup> Hence,

Table 10  
Raman Bands of Cytochrome Oxidase, 1500-1540  $\text{cm}^{-1}$  (a)

Excitation wavelength, nm	Oxidized enzyme	Reduced enzyme	Reference
406.7	1509 vw	1518 w <sup>(b)</sup>	(c)
	1506 vw	1519 m	111
	1506 vw	1519 m	112
	1506 vw	1520 m	114
413.1	Bands absent	1525 m	(c)
	~1509 vw	~1520 m	(d)
	1507 vw	1520 m	(e)
	1504 vw	1520 vw	10
	~1504 vw	~1520 m	114
441.6	Not reported	1519 w <sup>(f)</sup>	112
	Bands absent	1520 w	113
	Not reported	~1520 w	114
	Not reported	~1520 w	115
	Not reported	1519 w <sup>(g)</sup>	116
	Not reported	1519 w	116
	Bands absent	1517 w <sup>(h)</sup>	116

a) Mitochondrial enzyme, except where noted.

b) Partially-reduced form.

c) Ondrias, M.R.; Babcock, G.T. Biochem. Biophys. Res. Commun. 1980, 93, 29-35.

d) Woodruff, W.H.; Kessler, R.J.; Ferris, N.S.; Dallinger, R.F.; Carter, K.R.; Antalıs, T.M.; Palmer, G. Adv. Chem. Ser. 1982, 201, 625-659.

*Table 10, continued*

- e) Copeland, R.A.; Naqui, A.; Chance, B.; Spiro, T.G. FEBS Lett. 1985, 182, 375-379; oxidized species included the resting, 420 nm "pulsed", 420 nm "peroxy", and 428 nm "oxygenated" forms.
  - f) Enzyme from *Thermus thermophilus*.
  - g) Enzyme from yeast (*Saccaromyces cerevisiae*).
  - h) Enzyme from PS3 thermophilic bacterium.
-

heme *a*-Cu(I) binuclear ions could be generated by reducing agents when added to imperfectly purified heme *a* solutions. Because such ions cannot form when copper is completely absent, our model predicts that the heme *a* C=C stretching band will not be perturbed by reducing agents. On this point, published spectra of ostensibly pure heme *a* solutions are ambiguous. Reduced heme *a* in either of several organic or aqueous solvents shows a band in the 1500-1520  $\text{cm}^{-1}$  region. For example, resonance Raman spectra of the bis-imidazole adduct of ferrous heme *a* show a medium intensity band at 1518  $\text{cm}^{-1}$  with 406.7 nm excitation.<sup>10,88,89</sup> Although this band implies that the unusual spectral behavior of cytochrome oxidase originates with the inherent properties of the heme *a* prosthetic group, and not with a copper-heme *a* interaction, an alternate explanation appears to be more plausible. Both intensity and frequency of the heme *a* band at about 1518  $\text{cm}^{-1}$  depends strongly on excitation wavelength. As excitation wavelength is increased, the band shifts gradually in frequency and intensity, eventually becoming a weak feature at 1504  $\text{cm}^{-1}$  with 457.9 nm excitation;<sup>10</sup> no new feature appears in the region. Analogous behavior is not observed in cytochrome oxidase. Resonance Raman spectra of reduced cytochrome oxidase using 441.6-457.9 nm excitation have been reported by several investigators to contain a band of moderate intensity at 1520  $\text{cm}^{-1}$  (Table 10).<sup>10,89-93</sup> The spectral dissimilarities between heme *a* and cytochrome oxidase support our suggestion that for the reduced oxidase, Cu(I)



coordinates to the vinyl group of heme  $a_3$ .

The appearance of new UV bands upon adding Cu(I) to protoheme has been cited as evidence for binding between Cu(I) and peripheral vinyl.<sup>25</sup> Upon adding sodium dithionite to the cyanide derivative of cytochrome oxidase, a new band appears in the optical spectrum at about 305 nm,<sup>94</sup> consistent with our model for the enzyme. However, since this band is in a region of strong absorption by aromatic amino acids, the reported zero-order spectrum does not permit the new band to be assigned with certainty to Cu(I)-vinyl bonding. Moreover, the UV spectrum of bovine cytochrome c is also perturbed by adding sodium dithionite (although the character of these changes is entirely unlike those of cytochrome oxidase).<sup>94</sup> A study by higher-order absorption spectroscopy may clarify the situation.

Our model for the binding of Cu <sub>$a_3$</sub>  in reduced forms of cytochrome oxidase implies a specific distance between heme iron and vinyl-coordinated copper atom, which we calculate to be 6.0 angstroms,  $\pm 0.5$  angstrom depending on vinyl-heme coplanarity. Studies of cytochrome oxidase by EXAFS have attempted to measure iron-copper distances. EXAFS scattering from the iron atom of heme  $a_3$  of the resting enzyme indicates that the copper atom is about 3.7 angstroms from the heme iron.<sup>95</sup> Upon reduction, the enzyme undergoes a relatively large conformational change,<sup>96,97</sup> leading to the disappearance of EXAFS scattering from the outlying copper atom. This result has been interpreted to indicate either the displacement of copper to a site more than 4

angstroms from heme iron, or a large increase in static disorder of the reduced enzyme compared to the oxidized enzyme.<sup>98</sup>

A low-temperature FTIR study of carbon monoxide derivatives of cytochrome oxidase provides additional information.<sup>99</sup> When CO is bound to  $\text{Cu}_{a_3}$ , the measured half-band width of the corresponding C=O stretching mode is  $6 \text{ cm}^{-1}$ , but when CO is bound to  $\text{Fe}_{a_3}$ , the half-band width of the corresponding mode is only about  $2.4 \text{ cm}^{-1}$ . These band-widths have been suggested to provide a measure of local interactions between CO and the surrounding environment.<sup>100</sup> The large difference between iron-CO and copper-CO band-widths is the basis for a suggestion that  $\text{Fe}_{a_3}$  and  $\text{Cu}_{a_3}$  of the reduced enzyme experience quite different environments, and the two metals are probably not closer than 6 angstroms.<sup>99</sup> In summary, both FTIR and EXAFS studies report iron-copper distances at the oxygen-reducing site which are consistent with our model.

Michaelis suggested several decades ago that concerted multielectron reduction of metal-bridging dioxygen (M-O-O-M) would be thermodynamically favored over sequential electron transfer to end-bound dioxygen (M-O-O).<sup>101,102</sup> A 6 angstrom separation of iron and copper, as postulated by our model for reduced cytochrome oxidase, is probably too great for bidentate coordination of oxygen ( $\text{Fe}_{a_3}^{2+}$ -O-O- $\text{Cu}_{a_3}^{1+}$ ). For example, the distance between copper atoms of  $\mu$ -1,2-peroxo-bridged hemocyanin has been measured by EXAFS to be 3.67 angstroms.<sup>103</sup> The cobalt atoms of decammine- $\mu$ -peroxo-cobalt(III)-cobalt(IV) are known

from X-ray crystallography to be 5.09 angstroms apart,<sup>104</sup> which is about the upper limit for metal-metal distances of known  $\mu$ -dioxo and  $\mu$ -peroxo complexes. In these two instances, moreover, the O-O bond distance of bound peroxide is lengthened relative to dioxygen by a lower bond order. Our model therefore implies that the primary intermediate in the reaction between dioxygen and reduced cytochrome oxidase is a terminally-bound dioxygen-enzyme complex. Evidence for this structure has been obtained from various techniques, and involves chiefly a resemblance of the spectroscopic properties of the primary oxidase intermediate with some oxyferroheme model known to bind axial ligands end-on. From transient resonance Raman studies, for example, spectral similarities are observed between an early intermediate in the oxidase reaction and both oxyhemoglobin and oxymyoglobin.<sup>105</sup> In the case of low-temperature triple-trapping<sup>106</sup> and room temperature flow-flash studies,<sup>107</sup> the optical properties of the primary intermediate resemble those of isolated oxyferroheme  $a_3$ <sup>108</sup> and carbonmonoxy ferro-cytochrome  $a_3$ .<sup>109</sup> These observations have led others to the conclusion that dioxygen is initially bound end-on to heme  $a_3$ , as consistent with our model for reduced  $Cu_{a_3}$ .

End-on ligation of dioxygen implies that reduction proceeds, for at least the first pair of electrons, by sequential one-electron transfers. To circumvent thermodynamic barriers to this process, it has been suggested that these first electrons are transferred to oxygen in succession with sufficient speed to

exclude diffusion of partially-reduced oxygen intermediates, and prevent relaxation of nuclear configurations.<sup>109</sup> This idea agrees with measured rates of oxygen reduction, which are exceptionally fast.<sup>110,111</sup>

Once bound to heme  $a_3$ , dioxygen rapidly accepts two electrons.<sup>108,111,112</sup> In this process, heme  $a_3$  and  $\text{Cu}_{a_3}$  each furnish one reducing equivalent. The resulting oxygen intermediate is commonly assumed to be a metal-bridging peroxo species,  $\text{Cu}_{a_3}^{2+} \cdot \text{O}_2^{2-} \cdot \text{Fe}_{a_3}^{3+}$ . The existence of this intermediate is implied by the demonstration that  $\text{Cu}_{a_3}$  binds at some late stage in the catalytic cycle at least one oxygen atom derived from substrate dioxygen.<sup>113</sup> In order for  $\text{Cu}_{a_3}$  to bind one or more oxygen intermediates, the coordination shell must either expand or undergo ligand substitution.

FTIR studies of carbonmonoxy oxidase indicate that the  $\text{Cu}_{a_3}$  environment is relatively flexible, and therefore should provide little restraint to change in the geometry of ligands coordinated to copper. Whereas some copper proteins maintain a rigid copper coordination environment to optimize electron transfer, a floppy environment about copper will increase the reorganizational barrier to simple electron transfer, and enhance oxygen binding.<sup>114</sup> The function of  $\text{Cu}_{a_3}$  as a site for both binding and reduction of oxygen may make necessary the sort of coordination environment described by our model, wherein transfer of an electron from  $\text{Cu(I)}$  to oxygen is linked to the exposure of a site suitable for immediate binding of a nascent oxygen

intermediate.

The  $^{14}\text{N}$  ENDOR spectrum of  $\text{Cu}_{a_3}^{2+}$  from pulsed oxidized enzyme is identical to the spectrum of type 3 copper of laccase.<sup>115</sup> This resemblance indicates that  $\text{Cu}_{a_3}$  in the divalent oxidation state has four ligands, of which three are nitrogenous and a fourth probably water or hydroxide. Displacement of the fourth ligand may provide a site for coordination of the heme vinyl group, and subsequently, for oxygen intermediates.

The micellar Cu(I)-protoheme ions described here are potential models for the oxygen binding site of cytochrome  $a_3$ .<sup>66,96</sup> It is of interest to investigate Cu(I)-heme  $a$  ions, for which optical evidence also indicates  $\pi$ -bonding.<sup>25</sup> The physical properties and dynamic behaviour of heme  $a$  can be compared to protoheme as a basis for evaluating the physiological role of the heme  $a$  farnesyl substituent in Cu(I) binding and electron transfer. Also, it may be feasible to study the  $^{63}\text{Cu}$  NMR signal of Cu(I)-olefin in both the model complex and reduced cytochrome oxidase.<sup>116</sup>

REFERENCES

1. a) Pruckner, F. Z. Physik. Chem. Abt. A 1942, 190, 101-125. b) Drabkin, D.L. J. Biol. Chem. 1942, 146, 605-617. c) Falk, J.E.; Perrin, D.D. In: "Haematin Enzymes"; (Falk, J.E.; Lemberg, R.; Morton, R.K., Eds.); Pergamon Press: Oxford, 1961; Part 1, pp 56-71. d) Falk, J.E. "Porphyrins and Metalloporphyrins"; Elsevier: Amsterdam, 1964; pp 77-84.
2. a) Djerassai, C.; Lu, Y.; Waleh, A.; Shu, A.Y.L.; Goldbeck, R.A.; Kehres, L.A.; Crandell, C.W.; Wee, A.G.H.; Knierzinger, A.; Gaete-Holmes, R.; Loew, G.H.; Clezy, P.S.; Bunnenberg, E. J. Am. Chem. Soc. 1984, 106, 4241-4258. b) Dewar, M.J.S.; Dougherty, R.C. "The PMO Theory of Organic Chemistry"; Plenum: New York, 1975; pp 413-417.
3. Albrecht, A.C. J. Chem Phys. 1961, 34, 1476-1484.
4. Spiro, T.G.; Strekas, T.C. J. Am. Chem. Soc. 1974, 96, 338-345.
5. Adar, F. Arch. Biochem. Biophys. 1975, 170, 644-650.
6. a) Gans, P. "Vibrating Molecules. An Introduction to the Interpretation of Infrared and Raman Spectra"; Chapman & Hall: London, 1971; pp 19, 154-167. b) Wilson, E.B., Jr.; Decius, J.C.; Cross, J.C. "Molecular Vibrations. The Theory of Infrared and Raman Vibrational Spectra"; McGraw-Hill: New York, 1955; pp 197-200. c) Herzberg, G. "Molecular Spectra and Molecular Structure. II. Infrared and Raman Spectra of Polyatomic Molecules"; Van Nostrand Reinhold: New York, 1945; pp 215-219, 261-266.
7. Adar, F. Arch. Biochem. Biophys. 1977, 181, 5-7.
8. Choi, S.; Spiro, T.G.; Langry, K.C.; Smith, K.M.; Budd, D.L.; La Mar, G.N. J. Am. Chem. Soc. 1982, 104, 4345-4351.
9. Choi, S.; Spiro, T.G.; Langry, K.C.; Smith, K.M.; J. Am. Chem. Soc. 1982, 104, 4337-4344.
10. Choi, S.; Spiro, T.G. J. Am. Chem. Soc. 1983, 105, 3683-3692.

11. a) Warshel, A.; Weiss, R.M. J. Am. Chem. Soc. 1981, 103, 446-451. b) Seybert, D.W.; Moffat, K.; Gibson, Q.H.; Chang, C.K. J. Biol. Chem. 1977, 252, 4225-4231. c) Falk, J.E.; Phillips, J.N.; Magnusson, E.A. Nature 1966, 212, 1531-1533. d) Antonini, E.; Brunori, M.; Caputo, A.; Chiancone, E.; Fanelli, A.R.; Wyman, J. Biochim. Biophys. Acta 1964, 79, 284-292. e) Yamamoto, H.; Yonetani, T. J. Biol. Chem. 1974, 249, 7964-7968. f) Asakura, T.; Sono, M. J. Biol. Chem. 1974, 249, 7087-7093.
12. Asakura, T.; Lau, P.W.; Sono, M.; Adachi, K.; Smith, J.J.; McCray, J.A. In: "Hemoglobin and Oxygen Binding"; (Ho, C., Ed.); Elsevier North Holland: New York, 1982; pp 177-184.
13. Yonetani, T.; Yamamoto, H.; Woodrow, G.V. J. Biol. Chem. 1974, 249, 682-690.
14. Yamamoto, H.; Kayne, F.J.; Yonetani, T. J. Biol. Chem. 1974, 249, 691-698.
15. a) Sono, M.; Asakura, T. J. Biol. Chem. 1975, 250, 5227-5232. b) Livingston, D.J.; Davis, N.L.; La Mar, G.N.; Brown, W.D. J. Am. Chem. Soc. 1984, 106, 3025-3026. c) Rossi-Fanelli, A.; Antonini, E. Arch. Biochem. Biophys. 1957, 72, 243-246. d) Kendrew, J.C. Brookhaven Symp. Biol. 1962, 15, 216-223. e) Chang, C.K.; Ward, B.; Ebina, S. Arch. Biochem. Biophys. 1984, 231, 366-371.
16. Makino, R.; Yamazaki, I. Arch. Biochem. Biophys. 1974, 165, 485-493.
17. Desbois, A.; Mazza, G.; Stetzkowski, F.; Lutz, M. Biochim. Biophys. Acta 1984, 785, 161-176.
18. Bornheim, L.M.; Parish, D.W.; Smith, K.M.; Litman, D.A.; Correia, M.A. Arch. Biochem. Biophys. 1986, 246, 63-74.
19. La Mar, G.N.; Burns, P.D.; Jackson, J.T.; Smith, K.M.; Langry, K.C.; Strittmatter, P. J. Biol. Chem. 1981, 256, 6075-6079.
20. Satterlee, J.D.; Erman, J.E. J. Biol. Chem. 1983, 258, 1050-1056.



21. a) Ohlsson, P.-I.; Paul, K.G. Biochim. Biophys. Acta 1973, 315, 293-305. b) Yamada, H.; Makino, R.; Yamazaki, I. Arch. Biochem. Biophys. 1975, 169, 344-353. c) Ohlsson, P.-I.; Paul, K.-G.; Sjöholm, I. J. Biol. Chem. 1977, 252, 8222-8228. d) Makino, R.; Yamazaki, I. J. Biochem. (Tokyo) 1972, 72, 655-664. e) La Mar, G.N.; de Ropp, J.S.; Smith, K.M.; Langry, K.C. J. Am. Chem. Soc. 1983, 105, 4576-4580. f) Chance, B.; Paul, K.G. Acta Chem. Scand. 1960, 14, 1711-1716.
22. Caughey, W.S.; Smythe, G.A.; O'Keefe, D.H.; Maskasky, J.E.; Smith, M.L. J. Biol. Chem. 1975, 250, 7602-7622.
23. a) Herberhold, M. "Metal  $\pi$ -complexes", Vol. II, Part 2; Elsevier: Amsterdam, 1974. b) Hartley, F.R. Chem. Rev. 1973 73, 163-190.
24. a) Hurst, J.K.; J. Am. Chem. Soc. 1976, 98, 4001-4003. b) Norton, K.A., Jr.; Hurst, J.K. J. Am. Chem. Soc. 1978, 100, 7237-7242. c) Norton, K.A., Jr.; Hurst, J.K. J. Am. Chem. Soc. 1982, 104, 5960-5966.
25. Deardorff, E.A.; Carr, P.A.G.; Hurst, J.K. J. Am. Chem. Soc. 1981, 103, 6611-6616.
26. Hurst, J.K.; Lane, R.H. J. Am. Chem. Soc. 1973, 95, 1703-1709.
27. a) Hurst, J.K. Biochemistry 1979, 18, 1504-1510. b) Denning, R.G.; Hartley, F.R.; Venanzi, L.M. J. Chem. Soc. A 1967, 1322-1325. c) McIntosh, D.F.; Ozin, G.A.; Messmer, R.P. Inorg. Chem. 1980, 19, 3321-3327.
28. a) McCoy, H.N. J. Am. Chem. Soc. 1936, 58, 1577-1580. b) Espenson, J.H.; Shaw, K.; Parker, O.J. J. Am. Chem. Soc. 1967, 89, 5730-5731.
29. Dockal, E.R.; Everhart, E.T.; Gould, E.S. J. Am. Chem. Soc. 1971, 93, 5661-5667.
30. Shaw, K.; Espenson, J.H. Inorg. Chem. 1968, 7, 1619-1622.
31. Buxton, G.V.; Green, J.C.; Sellers, R.M. J. Chem. Soc. Dalton 1976, 2160-2165.
32. Inhoffen, H.H.; Brockmann, H., Jr.; Bliesener, K.-M. Justus Liebigs Ann. Chem. 1969, 730, 173-185.
33. Cox, G.S.; Krieg, M.; Whitten, D.G. J. Am. Chem. Soc. 1982, 104, 6930-6937.



34. Krieg, M.; Whitten, D. J. Am. Chem. Soc. 1984, 106, 2477-2479.
35. Beinert, H.; Orme-Johnson, W.H.; Palmer, G. Meth. Enzymology 1978, 54, 111-132.
36. Malin, M.J.; Chapoteau, E. J. Chromatography 1981, 219, 117-122.
37. Phillips, J.N. In: "Current Trends in Heterocyclic Chemistry"; (Albert, A.; Bagder, E.M.; Shoppee, C.W., Eds.); Butterworths: London, 1958; pp 30-39.
38. White, W.I. Porphyrins 1978, 5, 303-339.
39. a) Simplicio, J. Biochemistry 1972, 11, 2525-2528. b) Simplicio, J.; Schwenzer, K. Biochemistry 1973, 12, 1923-1929.
40. Narayana, P.A.; Li, A.S.W.; Kevan, L. J. Am. Chem. Soc. 1981, 103, 3603-3604.
41. Frahm, J.; Diekmann, S.; Haase, A. Ber. Bunsenges. Phys. Chem. 1980, 84, 566-571.
42. Simplicio, J. Biochemistry 1972, 11, 2529-2534.
43. Strekas, T.C.; Adams, D.H.; Packer, A.; Spiro, T.G. Appl. Spec. 1974, 28, 324-327.
44. Loehr, T.M.; Keyes, W.E.; Pincus, P.A. Anal. Biochem. 1979, 96, 456-463.
45. a) Dutton, L.P. Meth. Enzymol. 1978, 54, 411-435. b) Wilson, G.S. Meth. Enzymol. 1978, 54, 396-410.
46. a) Conant, J.B.; Alles, G.A.; Tongberg, C.O. J. Biol. Chem. 1928, 79, 89-93. b) Conant, J.B.; Tongberg, C.O. J. Biol. Chem. 1930, 86, 733-741. c) Barron, E.S.G. J. Biol. Chem. 1937, 121, 285-312.
47. a) Brdicka, R.; Wiesner, K. Coll. Czech. Chem. Commun. 1947, 12, 39-63. b) Bednarski, T.M.; Jordan, J. J. Am. Chem. Soc. 1967, 89, 1552-1558. c) Kadish, K.M.; Jordan, J. J. Electrochem. Soc. 1978, 125, 1250-1257.
48. a) Davis, D.G.; Martin, R.F. J. Am. Chem. Soc. 1966, 88, 1365-1371. b) Worthington, P.; Hambright, P. J. Inorg. Nucl. Chem. 1980, 42, 1651-1654. c) Zanello, P.; Bartocci, C.; Maldotti, A.; Traverso, O. Polyhedron 1983, 2, 791-795.

49. Shack, J.; Clark, W.M. J. Biol. Chem. 1947, 171, 143-187.
50. Kakutani, T.; Totsuka, S.; Senda, M. Bull. Chem. Soc. Jpn. 1973, 46, 3652-3657.
51. a) Behlke, J.; Scheler, W. Acta Biol. Med. Germ. 1962, 8, 88-102. b) Scheller, F.; Mohr, P.; Prumke, H.J.; Pommerening, K. Studia Biophysica 1977, 63, 199-205.
52. a) Bonnett, R.; McDonagh, A.F. Chem. Comm. 1970, 237-238. b) O'Carra, P. In: "Porphyrins and Metalloporphyrins"; (Smith, K.M., Ed.); Elsevier: Amsterdam, 1975; pp 123-153.
53. Brown, S.B.; Hatzikonstantinou, H.; Herries, D.G. Biochem. J. 1978, 174, 901-907.
54. Dutton, P.L. Biochim. Biophys. Acta 1971, 226, 63-81.
55. Covington, A.K.; Rebelo, M.J.F. Ion-Selective Electrode Rev. 1983, 5, 93-128.
56. La Mar, G.N.; Minch, M.J.; Frye, J.S. J. Am. Chem. Soc. 1981, 103, 5383-5388.
57. Silver, J.; Lukas, B. Inorg. Chim. Acta 1983, 78, 219-224.
58. Adler, A.D. In: "Hemes and Hemoproteins"; (Chance, B.; Estabrook, R.W.; Yonetani, T., Eds.); Academic Press: New York, 1966; pp 255-262.
59. Evers, E.L.; Jayson, G.G.; Swallow, A.J. J. Chem. Soc. Faraday Trans. 1977, 74, 418-426.
60. a) Eck, V.; Marcus, M.; Stange, G.; Westerhausen, J.; Holzwarth, J.F. Ber. Bunsenges. Phys. Chem. 1981, 85, 869-876. b) Bruhn, H.; Westerhausen, J.; Holzwarth, J.F.; Fuhrhop, J.H. In: "Techniques and Applications of Fast Reactions in Solution"; (Gettins, W.J.; Wyn-Jones, E., Eds.); D. Reidel Publishing Company: London, 1979; pp 523-534.
61. a) Figure 11 of reference 62b. b) Loach, P.A.; Runquist, J.A.; Kong, J.L.Y.; Dannhauser, T.J.; Spears, K.G. In: "Electrochemical and Spectroelectrochemical Studies of Biological Redox Components"; (Kadish, K.M., Ed.); American Chemical Society: Washington, D.C., 1982; pp 529-561.
62. Vanderkooi, G.; Stotz, E. J. Biol. Chem. 1966, 241, 3316-3323.

63. a) Suzuki, H.; Shinozuka, N.; Hayano, S. Bull. Chem. Soc. Jpn. 1974, 47, 1093-1096. b) Kolthoff, I.M.; Okinaka, Y. J. Am. Chem. Soc. 1959, 81, 2296-2302. c) Yeh, P.; Kuwana, T. J. Electrochem. Soc. Electrochem. Sci. Technol. 1976, 123, 1334-1339. d) Westmoreland, P.G.; Day, R.A., Jr.; Underwood, A.L. Anal. Chem. 1972, 44, 737-740.
64. a) Alcock, N.W.; Benton, D.J.; Moore, P. Trans. Far. Soc. 1970, 66, 2210-2213. b) Gorman, D.S.; Connolly, J.S. Int. J. Chem. Kinet. 1973, 5, 977-989. c) Moore, P. J. Chem. Soc. Faraday 1972, 68, 1890-1893. d) Moore, R.H.; Zeigler, R.K. Report Number LA-2367 1960, Los Alamos Scientific Laboratory, University of California, Los Alamos, New Mexico. e) Johnson, M.L.; Frasier, S.G. Meth. Enzymol. 1985, 117 301-342.
65. Spinner, E. J. Chem. Soc. 1964, 4217-4226.
66. a) Sibbett, S.S.; Hurst, J.K. In: "Biological and Inorganic Copper Chemistry", Vol. II; (Karlin, K.D.; Zubieta, J., Eds.); Adenine Press: Guilderland, New York, 1986; pp 123-141. b) Sibbett, S.S.; Loehr, T.M.; Hurst, J.K. Inorg. Chem. 1986, 25, 307-313.
67. Spiro, T.G.; Stong, J.D.; Stein, P. J. Am. Chem. Soc. 1979, 101, 2648-2655.
68. Nagai, K.; Kitagawa, T.; Morimoto, H. J. Mol. Biol. 1980, 136, 271-289.
69. Silver, J.; Lukas, B. Inorg. Chim. Acta 1983, 80, 107-113.
70. *Pertinent reviews of copper coordination chemistry:* a) Brill, A.S.; Martin, R.B.; Williams, R.J.B. In: "Electronic Aspects of Biochemistry"; (Pullman, B., Ed.); Academic Press: New York, 1964; pp 519-557. b) Jardine, F.H. Adv. Inorg. Chem. Radiochem. 1975, 17, 115-163. c) Peisach, J.; Aisen, P.; Blumberg, W.E. (Eds.) "The Biochemistry of Copper"; Academic Press: New York, 1966. d) Karlin, K.D.; Zubieta, J. (Eds.) "Copper Coordination Chemistry: Biochemical and Inorganic Perspectives"; Adenine Press: Guilderland, New York, 1983.

71. *Cu(II)-SDS*: a) Gratzel, M.; Thomas, J.K. J. Phys. Chem. 1974, 78, 2248-2254. b) Vijayan, S.; Woods, D.R.; Lowe, D. Can. J. Chem. Eng. 1979, 57, 496-514. c) Scaiano, J.C.; Leigh, W.J.; Ferraudi, G.; Can. J. Chem. 1984, 62, 2355-2358. d) Dederen, J.C.; Van der Auweraer, M.; De Schryver, F.C. J. Phys. Chem 1981, 85, 1198-1202. e) Rodgers, M.A.J.; da Silva E Wheeler, M.F. Chem. Phys. Lett. 1978, 53, 165-169. f) Baumuller, W.; Hoffmann, H.; Ulbricht, W.; Tondre, C.; Zana, R. J. Coll. Interface Sci. 1978, 64, 418-437. g) Ziemiecki, H.; Cherry, W.R. J. Am. Chem. Soc. 1981, 103, 4479-4483. h) Bonilha, J.B.S.; Foreman, T.K.; Whitten, D.G. J. Am. Chem. Soc. 1982, 104, 4215-4220. i) Atherton, S.J.; Baxendale, J.H.; Hoey, B.M. J. Chem. Soc. Far. Trans. 1 1982, 78, 2167-2181. j) Grieser, F.; Tausch-Treml, R. J. Am. Chem. Soc. 1980, 102, 7258-7264. k) Moroi, Y.; Matuura, R. J. Phys. Chem. 1985, 89, 2923-2928.
72. *Cu(I)-SDS*: a) Hodges, H.L.; de Araujo, M.A. Inorg. Chem. 1982, 21, 3236-3239. b) Ponganis, K.V.; de Araujo, M.A.; Hodges, H.L. Inorg. Chem. 1980, 19, 2704-2709.
73. *Cu(II)-olefin*: a) Zelonka, R.A.; Baird, M.C. J. Organomet. Chem. 1971, 33, 267-272. b) Bruno, J.W.; Marks, T.J.; Lewis, F.D. J. Am. Chem. Soc. 1982 104, 5580-5585.
74. a) Rousseau, D.L.; Ondrias, M.R.; La Mar, G.N.; Kong, S.B.; Smith, K.M. J. Biol. Chem. 1983, 258, 1740-1746. b) Nagai, K.; Kitagawa, T.; La Mar, G.N.; Smith, K.M., personal communication cited in reference 75.
75. Desbois, A.; Henry, Y.; Lutz, M. Biochim. Biophys. Acta 1984, 785, 148-160.
76. Turner, J.; Reed, D.E. Biochim. Biophys. Acta 1984, 789, 80-86.
77. Teraoka, J.; Kitagawa, T. J. Phys. Chem. 1980, 84, 1928-1935.
78. Adar, F.; Erecinska, M. Arch. Biochem. Biophys. 1974, 165, 570-580.
79. Curry, B.; Broek, A.; Lugtenberg, J.; Mathies, R. J. Am. Chem. Soc. 1982, 104, 5274-5286.
80. Kakitani, T. Progr. Theor. Phys. 1974, 51, 656-673.
81. Macor, K.A.; Spiro, T.G. J. Am Chem. Soc. 1983, 105, 5601-5607.

82. Willems, D.L.; Bocian, D.F. J. Am. Chem. Soc. 1984, 106, 880-890.
83. Brunner, H.; Sussner, H. Biochim. Biophys. Acta 1973, 310, 20-31.
84. Kitagawa, T.; Hashimoto, S.; Teraoka, J.; Nakamura, S.; Yajima, H.; Hosoya, T. Biochemistry 1983, 22, 2788-2792.
85. Kimura, S.; Yamazaki, I.; Kitagawa, T. Biochemistry 1981, 20, 4632-4638.
86. Remba, R.D.; Champion, P.M.; Fitchen, D.B.; Chiang, R.; Hager, L.P. Biochemistry 1979, 18, 2280-2290.
87. Bayne, R.A.; Smythe, G.A.; Caughey, W.S. In: "Probes of Structure and Function of Macromolecules and Membranes", Vol. II; (Chance, B.; Yonetani, T.; Mildvan, A.S., Eds.); Academic Press: New York, 1971; pp 613-618.
88. Callahan, P.M.; Babcock, G.T. Biochemistry 1983, 22, 452-461.
89. Babcock, G.T.; Callahan, P.M. Biochemistry 1983, 22, 2314-2319.
90. Babcock, G.T.; Salmeen, I. Biochemistry 1979, 18, 2493-2498.
91. Babcock, G.T.; Callahan, P.M.; Ondrias, M.R.; Salmeen, I. Biochemistry 1981, 20, 959-966.
92. Van-Steelandt Frentrop, J.; Salmeen, I.; Babcock, G.T. J. Am. Chem. Soc. 1981, 103, 5981-5982.
93. Ogura, T.; Sone, N.; Tagawa, K.; Kitagawa, T. Biochemistry 1984, 23, 2826-2831.
94. Horie, S.; Hasumi, H.; Takizawa, N. J. Biochem. 1985, 97, 281-293.
95. a) Powers, L.; Chance, B.; Ching, Y.; Angiolillo, P. Biophys. J. 1981, 34, 465-498. b) Scott, R.A.; Schwartz, J.R.; Cramer, S.P. Springer Proc. Phys. 1984, 2, 111-116.
96. a) Palmer, G.; Babcock, G.T.; Vickery, L.E. Proc. Natl. Acad. Sci. USA 1976, 73, 2206-2210. b) Wikstrom, M.; Krab, K.; Saraste, M. "Cytochrome Oxidase: A Synthesis"; Academic Press: London, 1981; pp 55-87. c) Freedman, J.A.; Chan, S.H.P. J. Bioenerg. Biomembr. 1984, 16, 75-100. d) Buse, G. In: "Copper Proteins and Copper Enzymes"; (Lontie, R., Ed.); CRC Press: Boca Raton, Florida, 1985; pp 119-149.



97. a) Brudvig, G.W.; Stevens, T.H.; Morse, R.H.; Chan, S.I.; Biochemistry 1981, 20, 3912-3921. b) Babcock, G.T.; Vickery, Urry, D.W.; Wainio, W.W.; Grebner, D. Biochem. Biophys. Res. Commun. 1967, 27, 625-631. c) Thomson, A.J.; Greenwood, C.; Gadsby, P.M.A.; Peterson, J.; Eglinton, D.G.; Hill, B.C.; Nicholls, P. J. Inorg. Biochem. 1985, 23, 187-197.
98. a) Scott, R.A. In: "The Biological Chemistry of Iron"; (Dunford, H.B.; Dolphin, D.H.; Raymond, K.N.; Sieker, L.C., Eds.); D. Reidel: Boston, 1982; pp 475-484. b) Scott, R.A. In: "Biological and Inorganic Copper Chemistry", Vol. I; (Karlin, K.D.; Zubieta, J., Eds.); Adenine Press: Guilderland, New York, 1986; pp 41-52.
99. a) Alben, J.O.; Altschuld, R.A.; Fiamingo, F.G.; Moh, P.P. In: "Electron Transport and Oxygen Utilization"; (Ho, C., Ed.); Elsevier North Holland, Inc.: Amsterdam, 1982, pp 205-208. b) Fiamingo, F.G.; Altschuld, R.A.; Moh, P.P.; Alben, J.O. J. Biol. Chem. 1982, 257, 1639-1650.
100. Smith, M.L.; Paul, J.; Ohlsson, P.I.; Paul, K.G. Biochemistry 1984, 23, 6776-6785.
101. Michaelis, L. Fed. Proc. 1948, 7, 509-514.
102. The idea has been reiterated elsewhere: a) Chance, B.; Saronio, C.; Leigh, J.S., Jr. Proc. Natl. Acad. Sci. U.S.A. 1975, 72, 1635-1640. b) Reed, C.A.; Landrum, J.T. FEBS Lett. 1979, 106, 265-267. c) Peisach, J.; Blumberg, W.E. In: "Cytochrome Oxidase"; (King, T.E.; Orii, Y.; Chance, B.; Okunuki, K., Eds.); Elsevier North-Holland Inc.: Amsterdam, 1979; pp 153-159. d) Malmstrom, B.G. Biochim. Biophys. Acta 1979, 549, 281-303. e) Boelens, R.; Rademaker, H.; Wever, R.; Van Gelder, B.F. Biochim. Biophys. Acta 1984, 765, 196-209.
103. Brown, J.M.; Powers, L.; Kincaid, B.; Larrabee, J.A.; Spiro, T.G. J. Am. Chem. Soc. 1980, 102, 4210-4216.
104. Bannister, W.H.; Wood, E.J. Nature 1969, 223, 53-55.
105. a) Babcock, G.T.; Jean, J.M.; Johnston, L.N.; Palmer, G.; Woodruff, W.H. J. Am. Chem. Soc. 1984, 106, 8305-8306. b) Babcock, G.T.; Jean, J.M.; Johnston, L.N.; Woodruff, W.H.; Palmer, G. J. Inorg. Biochem. 1985, 23, 243-251.
106. Chance, B.; Saronio, C.; Leigh, J.S. J. Biol. Chem. 1975, 250, 9226-9237.
107. a) Hill, B.C.; Greenwood, C. Biochem. J. 1983, 215, 659-667. b) Orii, Y. J. Biol. Chem. 1984, 259, 7187-7190.

108. Babcock, G.T.; Chang, C.K. FEBS Lett. 1979, 97, 358-362.
109. Erecinska, M.; Wilson, D.F. Arch. Biochem. Biophys. 1978, 188, 1-14.
110. Wikstrom, M.; Krab, K.; Saraste, M. "Cytochrome Oxidase: A Synthesis"; Academic Press: London, 1981; pp 119-133.
111. Hill, B.C.; Greenwood, C. Biochem. J. 1984, 218, 913-921.
112. Blair, D.F.; Witt, S.N.; Chan, S.I. J. Am. Chem. Soc. 1985, 107, 7389-7399.
113. Hansson, O.; Karlsson, B.; Aasa, R.; Vanngard, T.; Malmstrom, B.G. EMBO J. 1982, 1, 1295-1297.
114. Munakata, M.; Endicott, J.F. Inorg. Chem. 1984, 23, 3693-3698.
115. Cline, J.; Reinhammar, B.; Jensen, P.; Venters, R.; Hoffman, B.M. J. Biol. Chem. 1983, 258, 5124-5128.
116. a) Kitagawa, S.; Munakata, M. Inorg. Chem. 1984, 23, 4388-4390. b) Marker, A.; Gunter, M.J. J. Magn. Reson. 1982, 47, 118-132.
117. Gouterman, M. J. Chem. Phys. 1959, 30, 1139-1161.
118. Bonnett, R. Porphyrins 1978 1, 9-14.
119. a) Dewar, M.J.S. J. Am. Chem. Soc. 1979, 101, 783-791. b) Dewar, M.J.S. Bull. Soc. Chim. France 1951, C71-79. c) Eisenstein, O.; Hoffmann, R. J. Am. Chem. Soc. 1981, 103, 4308-4320.
120. Hill, H.A.O.; Turner, D.R.; Pellizer, G. Biochem. Biophys. Res. Commun. 1974, 56, 739-744.
121. Clark, W.M. "Oxidation Reduction Potentials of Organic Systems"; Williams & Wilkens: Baltimore, 1960.
122. *Cu(II)-carboxylic acid:* a) Doedens, R.J. Progr. Inorg. Chem. 1976, 21, 209-231. b) Lukas, B.; Miller, J.R.; Silver, J.; Wilson, M.T.; Morrison, I.E.G. J. Chem. Soc. Dalton Trans. 1982, 6, 1035-1040.
123. *Cu(I)-carboxylic acid:* a) Weber, P.; Hardt, H.-D. Inorg. Chim. Acta 1981, 64, L51-53. b) Temussi, P.A.; Vitagliano, A. J. Am. Chem. Soc. 1975, 97, 1572-1575. c) Saegusa, T.; Murase, I.; Ito, Y. J. Org. Chem. 1973, 38, 1753-1755. d) Reference 28.

## Chapter 4

### *Cytochrome Oxidase: Subunits*

Cytochrome oxidase mediates the transfer of respiratory electrons to the ultimate acceptor oxygen. No activated oxygen intermediates are released in this process,<sup>1,2</sup> which occurs rapidly<sup>3,4</sup> and with high electrochemical efficiency.<sup>5</sup> As oxygen undergoes reduction, protons are electrogenically pumped across the mitochondrial inner membrane.<sup>6-8</sup> The dual capability for oxygen reduction and proton pumping derives from a complex structure.<sup>9,10</sup> Each molecule of mammalian enzyme is composed of seven or more polypeptide subunits; the oxygen binding site incorporates a strongly interacting heme-copper pair; a second heme and a second copper are located remote from the first pair; and both heme groups are heme *a*, with formyl and farnesyl side-chains.

The presence of two hemes complicates spectro-photometric research on cytochrome oxidase. Although the properties of the individual hemes may be deduced through deconvolution,<sup>11,12</sup> this technique is hampered, in the case of cytochrome oxidase, by spectral and electrochemical interactions between hemes<sup>13-15</sup> and between heme and copper.<sup>16,17</sup> To resolve the separate spectral contributions, we have sought a physical separation of the heme chromophores. *In vivo*, these



chromophores appear to be divided between subunits I and II.<sup>18-22</sup>  
Fractions enriched in these two subunits have been obtained by  
preparative electrophoresis; resonance Raman spectra of the  
subunit heme chromophores are reported here.

### MATERIALS AND METHODS

Subunit samples were received from Professor Howard S. Mason (Oregon Health Sciences University).

Sample excitation at 406.7 and 413.1 nm was obtained from a Spectra Physics 164-01 krypton ion laser equipped with a high-field magnet. The Raman spectrometer and computer interface have been described elsewhere.<sup>23</sup> Temperature at the sample was controlled by a stream of cold dry nitrogen. No photodegradation of samples was evident in successive Raman scans. To avoid photoreduction<sup>24</sup>, holoenzyme spectra were obtained from a spinning cell using a back-scattering geometry. Subunit spectra were obtained from capillaries using a 90-degree scattering geometry.

Subunit samples demonstrated variable susceptibility to photoreduction. The spectra reported here are from samples not subject to significant photoreduction. Resistance to photoreduction may be due either to an absence of photoactive contaminants,<sup>25</sup> or to isolation of the protein in conformations which are inherently stable under laser illumination.<sup>26</sup>

The signal-to-noise ratio of subunit spectra was not improved by increasing sample concentrations, but rather diminished by enhanced fluorescence. Tween 20, an important constituent of the solvent system, appears to sensitize this fluorescence.<sup>24,27</sup> Although signal-to-noise ratios were relatively low, all but the very weak Raman features reported here were reproducible in frequency and relative intensity.

## RESULTS

Resonance Raman spectra of fractions enriched in subunits I and II demonstrate a close resemblance (Figure 18). Notably, both frequencies and relative intensities are similar for bands at 1637, ~1587, 1506, ~1472, 1371, and 1131  $\text{cm}^{-1}$ . Several very weak features also may be common to spectra of both subunits, although the low signal-to-noise ratio of the spectra makes this somewhat uncertain. All of the prominent features between 900 and 1700  $\text{cm}^{-1}$  are common to the spectra of both subunits.

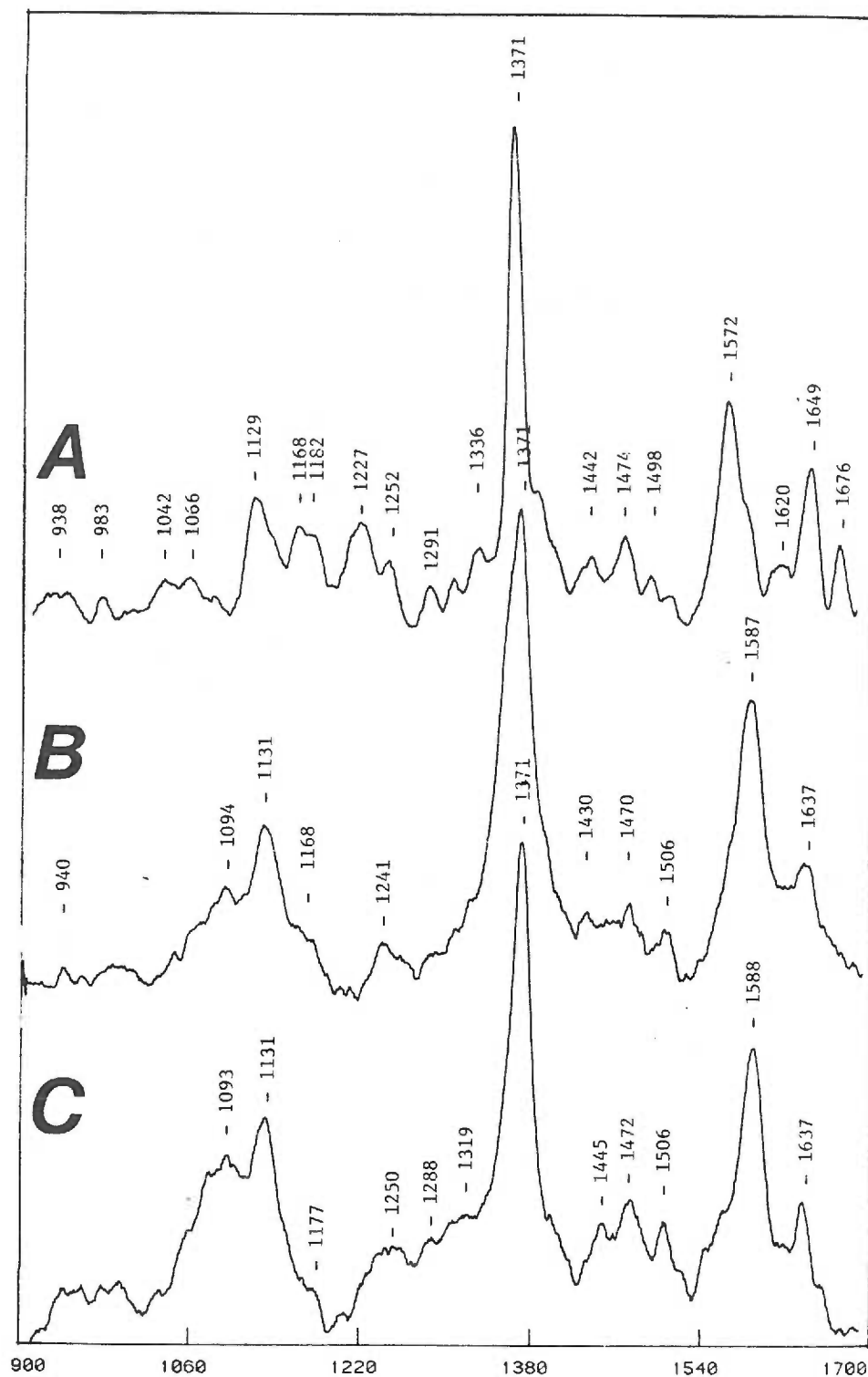
The subunit spectra differ from holoenzyme spectra primarily in the absence of certain prominent bands (Figure 18). Above 1600  $\text{cm}^{-1}$ , the subunit spectra exhibit only a single band, at 1637  $\text{cm}^{-1}$ , whereas holoenzyme shows 3 to 4 bands. The core-size marker bands of the subunits are sharp and, unlike holoenzyme, are not broadened by flanking shoulders or nearby resolved bands. A prominent holoenzyme band at 1227  $\text{cm}^{-1}$  is not observed in the subunit spectra. This band has been assigned to a ring-formyl stretch ( $\nu_{\text{C}_b=\text{CO}}$ ).

---

Figure 18

*Resonance Raman Spectra of Cytochrome Oxidase and Constituent Subunits, ~4 °C, scan rate  $1\text{ cm}^{-1}\text{ s}^{-1}$ . Upper spectrum A: holoenzyme, 406.7 nm excitation, 12 mW incident power, 17 scans. Middle spectrum B: Subunit I, 413.1 nm excitation, 25 mW, 24 scans. Lower spectrum C: Subunit II, 413.1 nm excitation, 20 mW, 60 scans. A 25-point smooth was applied to each spectrum.*

---



## DISCUSSION

Cytochrome oxidase contains two heme groups. When extracted from the enzyme, these hemes appear to be structurally identical.<sup>28,29,†</sup> Both hemes are heme *a*, characterized by formyl and farnesyl substituents. Although the two hemes of cytochrome oxidase are identical when extracted from the enzyme, they are distinct when situated in the intact holoenzyme. Spectroscopic discrimination of the intact hemes has been achieved by optical spectroscopy, EPR, CD, MCD, Mossbauer, and resonance Raman. The distinction between hemes probably originates in different environments imposed about each heme by protein and metal co-factors.

Resonance Raman spectra of cytochrome oxidase reveal different spin-states of the two intact hemes. With Soret excitation of oxidized enzyme, the presence of one high spin heme and one low spin heme is indicated by a broad feature in the core-size marker region (Figure 18A).<sup>25,30</sup> In some cases, this feature is resolved into separate bands at 1590 and 1572  $\text{cm}^{-1}$ .<sup>31</sup> In contrast, Raman spectra of both subunits I and II (Figure

---

†Extraction yields a homogeneous pool of heme. To exclude the possibility of overlooking a second distinct heme through extraction losses, Caughey's group sought and attained from beef heart nearly quantitative yields of heme (>70%).<sup>29</sup> However, in later studies on the molecular structure of extracted heme,<sup>30</sup> an additional purification step was incorporated in the original extraction procedure, resulting in yields of 50-70%. Yields of this magnitude reintroduce the possibility of overlooking a second distinct heme.

18A,B) exhibit a single narrow band at  $1587\text{--}1588\text{ cm}^{-1}$ . The frequency of this band is typical of predominately low-spin heme.

Two carbonyl stretching bands ( $\nu_{\text{C=O}}$ ) are observed in spectra of oxidized holoenzyme (Figure 18A), at  $1675$  and  $1648\text{ cm}^{-1}$ . Both of these bands have been uniquely assigned to a single formyl group and heme.<sup>33</sup> Differences in frequency have been ascribed to differences in the strength of hydrogen-bonding to carbonyl oxygen.<sup>5,30,33</sup> In polar solvents, the C=O stretch for heme *a* models is  $\sim 1640\text{ cm}^{-1}$ , about  $30\text{ cm}^{-1}$  lower than in non-polar solvents. Hence for both subunits, the C=O stretching frequency at  $1637\text{ cm}^{-1}$  describes a heme *a* moiety with a formyl group engaged in strong hydrogen-bonding, either through exposure to the aqueous exterior of the protein, or through proximity to a hydrogen-bond donor of the protein.

In addition to band pairs in the spin-state and carbonyl stretching regions, other Raman bands have been interpreted as indicators of the distinctive environments of the two hemes. Identification of these other bands has assumed selective enhancement of modes from only one of the two hemes, cytochrome *a*, upon exciting oxidized enzyme with  $441.6\text{ nm}$  laser light.<sup>25,31</sup> Under other excitation and sample conditions, there also occurs enhancement of modes from the other heme, cytochrome *a*<sub>3</sub>. Consequently, some bands have been uniquely assigned to a single heme. In spectra of oxidized holoenzyme, for example, a band at  $1506\text{ cm}^{-1}$  has been assigned exclusively to the heme of cytochrome *a*, whereas a band at  $1478\text{ cm}^{-1}$  has

been assigned exclusively to the heme of cytochrome  $a_3$ .<sup>25,26</sup> These two bands also are observed in subunit spectra; indeed, they are observed in the spectra of *both* subunits I and II. Physical separation of the hemes therefore does not disentangle those bands uniquely assigned by previous workers to one heme or the other. This observation poses a dilemma: either the unique assignments are in error, or the vibrational properties of the isolated subunit hemes bear no direct relationship to the intact hemes of the holoenzyme.

Resonance Raman discriminates between the two hemes in the holoenzyme, but not in the isolated subunits I and II. It seems likely therefore that the procedure for obtaining heme-bearing subunits affects the vibrational structure of one or both hemes. Isolating subunits may permit heme dissociation, followed by spontaneous but dysfunctional reassociation of heme. Alternatively, the holoenzyme may be formed by asymmetric binding of subunits I and II such that two vibrationally similar hemes become differentiated through subunit-subunit interactions; disaggregation of holoenzyme into constituent subunits leads to loss of these interactions and the vibrations which distinguish the two hemes. Since structural changes appear to attend subunit dissociation, it may prove difficult to relate in a meaningful way the structure of heme in an isolated subunit to the structure of heme in the holoenzyme.



REFERENCES

1. Chance, B.; Saronio, C.; Leigh, J.S. Proc. Natl. Acad. Sci. USA 1975, 72, 1635-1640.
2. Brunori, M.; Rotilio, G. Meth. Enzymology 1984, 105, 22-35.
3. Gibson, Q.H.; Greenwood, C. Biochem. J. 1963, 86, 541-554.
4. Chance, B.; Erecinska, M. Arch. Biochem. Biophys. 1971, 143, 675-687.
5. Van Steelandt-Frentrup, J.; Salmeen, I.; Babcock, G.T. J. Am. Chem. Soc. 1981, 103, 5981-5982.
6. Wikstrom, M. Nature, 1984, 308, 558-560.
7. Thelen, M.; O'Shea, P.S.; Petrone, G.; Azzi, A. J. Biol. Chem. 1985, 260, 3626-3631.
8. Nicholls, P.; Shaughnessy, S. Biochem. J. 1985, 228, 201-210.
9. Wikstrom, M.; Krab, K.; Saraste, M. "Cytochrome Oxidase: A Synthesis", Academic Press: New York, 1981.
10. Freedman, J.A.; Chan, S.H.P. J. Bioenerg. Biomembr. 1984, 16, 75-100.
11. Vanneste, W.H. Biochemistry 1966, 5, 838-848.
12. Carter, K.; Palmer, G. J. Biol. Chem. 1982, 257, 13507-13514.
13. Greenwood, C.; Wilson, M.T.; Brunori, M. Biochemistry 1974, 137, 205-215.
14. Erecinska, M.; Wilson, D.F. Arch. Biochem. Biophys. 1974, 188, 1-14.
15. For rebuttal, see: a) Wikstrom, M. In: "Electron Transport and Oxygen Utilization"; (Ho, C., Ed.); Elsevier North Holland: New York, 1982; pp 271-277. b) Boelens, R.; Wever, R.; Van Gelder, B.F. Biochim. Biophys. Acta 1982, 682, 264-272.
16. Greenaway, F.T.; Chan, S.H.P.; Vincow, G. Biochim. Biophys. Acta 1977, 490, 62-78.

17. Blair, D.F.; Bocian, D.F.; Babcock, G.T.; Chan, S.I. Biochemistry 1982, 21, 6928-6935.
18. Winter, D.B.; Bruyninckx, W.J.; Foulke, F.G.; Grinich, N.P.; Mason, H.S. J. Biol. Chem. 1980, 255, 11408-11414.
19. Mason, H.S. In: "The Biological Chemistry of Iron"; (Dunford, H.B.; Dolphin, D.; Raymond, K.N.; Sieker, L., Eds.); D. Reidel Publishing Company: Dordrecht, Holland, 1981; pp 459-473.
20. Welinder, K.G.; Mikkelsen, L. FEBS Lett. 1983, 157, 233-239.
21. Corbley, M.J.; Azzi, A. Eur. J. Biochem. 1984, 139, 535-540.
22. Wielburski, A.; Nelson, B.D. FEBS Lett. 1984, 177, 291-294.
23. Loehr, T.M.; Keyes, W.E.; Pincus, P.A. Anal. Biochem. 1979, 96, 456-463.
24. Adar, F.; Yonetani, T. Biochim. Biophys. Acta 1978, 502, 80-86.
25. Babcock, G.T.; Callahan, P.M.; Ondrias, M.R.; Salmeen, I. Biochemistry 1981, 20, 959-966.
26. Copeland, R.A.; Naqui, A.; Chance, B.; Spiro, T.G. FEBS Lett. 1985, 182, 375-379.
27. Kessler, R.J., *Ph.D. Dissertation*, University of Texas, Austin, 1982, p 95.
28. York, J.L.; McCoy, S.; Taylor, D.N.; Caughey, W.S. J. Biol. Chem. 1967, 242, 908-911.
29. Caughey, W.S.; Smythe, G.A.; O'Keefe, D.H.; Maskasky, J.E.; Smith, M.L. J. Biol. Chem. 1975, 250, 7602-7622.
30. Choi, S.; Lee, J.J.; Wei, Y.H.; Spiro, T.G. J. Am. Chem. Soc. 1983, 105, 3692-3707.
31. Woodruff, W.H.; Dallinger, R.F.; Anatalis, T.M.; Palmer, G. Biochemistry 1981, 20, 1332-1338.
32. Callahan, P.M.; Babcock, G.T. Biochemistry 1983, 22, 452-461.
33. Salmeen, I.; Rimai, L.; Babcock, G. Biochemistry 1978, 17, 800-806.

### Appendix

Most experiments in the physical sciences are designed and interpreted according to some theoretical model. To demonstrate conformity between a given model and a body of relevant experimental data, one common approach is to cast the model in mathematical terms so that dependent and independent variables, when operated on by appropriate functions and then plotted graphically, yield a straight line. For some models, however, it is intrinsically impossible to obtain descriptive mathematical expressions that relate the variables in a linear manner. Nor is it always possible to obtain exact values for the the physical constants of a given experiment which must be included in the mathematical expression of an experimental model. In such cases, the procedure of non-linear least squares permits a rigorous analysis of conformity between data and model, and an evaluation of unknown constants.

Numerous introductions to the non-linear least squares method have been published.<sup>†</sup> The following program was written in IBM PC-BASIC. The menu structure follows Lotus 1-2-3: commands may be selected either by typing the first letter of

---

<sup>†</sup> a) Sagnella, G.A. Trends Biochem. Sci. 1985, 10, 100-103. b) Duggleby, R.G. Anal. Biochemistry 1981, 110, 9-18. c) Copeland, T.G. J. Chem. Ed. 1984, 61, 778-779. d) Long, J.R.; Drago, R.S. J. Chem. Ed. 1982, 59, 1037-1039. e) Johnson, M.L. Anal. Biochemistry 1985, 148, 471-478. f) Blascow, S.M., Jr.; Donnelly, J.A. Hewlett-Packard J. 1984, July, pp 22-24. g) Cornish-Bowden, A.; Endrenyi, L. Biochem. J. 1981, 193, 1005-1008.

a command keyword, or by moving the cursor over a command keyword and then hitting the carriage return. In all other aspects, the program provides self-guided instruction.

```

10  DEFINT A-Z:N=0:A=0:B=0:T=0:KEY OFF:KEY 6,
    "list .-"+CHR$(13):CLEAR: DIM T(180),P(180),U(180,3),
    V(3,180),W(180),Z(180),B(3,3),C(3),D(3,3), E(3),F(3),
    A(180,6):ON ERROR GOTO 640

20  REM ...MASTER MENU...

30  CLS:PRINT
    "ENTER          CRUNCH          REVISE          FETCH          STOP",:
    Y=1:X=0

40  COLOR 0,7:FOR L=1 TO 6:LOCATE Y,X+L:C$=CHR$(SCREEN(Y,X+L)):
    PRINT C$:NEXT: COLOR 7,0

50  REM ...Turn off CapsLock and NumLock...

60  DEF SEG=64:POKE 23, &HBF AND PEEK (23):POKE 23, &HDF AND PEEK
    (23)

70  REM ...Crunch=99 Enter=101 Revise=114 Fetch=102 Stop=115...

80  K$=INKEY$:IF LEN(K$)=0 THEN 80 ELSE IF LEN(K$)=2 THEN 100
    ELSE Q=ASC(K$):IF Q=99 THEN 120 ELSE IF Q=101 THEN 530 ELSE
    IF Q=114 THEN 140 ELSE IF Q=102 THEN GOSUB 590:GOTO 30 ELSE
    IF Q=115 THEN STOP ELSE IF Q=13 THEN 110 ELSE 60

90  REM ...Cursor right=77 Cursor left=75...

100 A=ASC(RIGHT$(K$,1)):IF A=77 AND X<46 THEN GOSUB
    570:X=X+13:GOTO 40 ELSE IF A=77 THEN GOSUB 570:X=0:GOTO 40
    ELSE IF A=75 AND X>12 THEN GOSUB 570:X=X-13:GOTO 40 ELSE IF
    A=75 THEN GOSUB 570:X=52:GOTO 40 ELSE GOTO 80

110 IF X=0 THEN 530 ELSE IF X=13 THEN 120 ELSE IF X=26 THEN 140
    ELSE IF X=39 THEN GOSUB 590:GOTO 30 ELSE IF X=52 THEN STOP
    ELSE 80

120 GOTO 200

130 REM ...REVISE DATA...

140 CLS:FOR J=1 TO 23:GET 1,J:A(J,1)=CVS(A$):A(J,2)=CVS(B$):
    GET 1, J+23:A(J+23,1)=CVS(A$):A(J+23,2)=CVS(B$):
    GET 1,J+46:A(J+46,1)=CVS(A$):A(J+46,2)=CVS(B$)

150 IF NOT (A(J,1)=1000 OR A(J+23,1)=1000 OR A(J+46,1)=1000) THEN
    160 ELSE 180

160 PRINT USING "   ##";J;:PRINT USING "   #.###";A(J,1);:
    PRINT USING "   #.####";A(J,2);

```

```

170 PRINT USING "  ##";J+23;:PRINT USING "  #.###";A(J+23,1);:
    PRINT USING "  #.#####";A(J+23,2);:PRINT USING "  ##";J+46;:
    PRINT USING "  #.###";A(J+46,1);:
    PRINT USING "  #.#####";A(J+46,2):NEXT:PRINT

180 INPUT "Number of data pair?",I:PRINT I;:
    INPUT "      ",A(I,1),A(I,2):LSET A$=MKS$(A(I,1)):
    LSET B$=MKS$(A(I,2)):PUT 1,I:GOTO 30

190 REM ...DATA RETRIEVAL, INTIAL GUESSES...

200 CLS:FOR J=1 TO 180:GET 1,J:T(J)=CVS(A$):P(J)=CVS(B$):IF NOT
    (T(J)=1000) THEN NEXT ELSE N=J-1:AI=P(1):AF=P(N):
    EV=T(INT(N/2))

210 INPUT "Number of electrons";M

220 CLS:I=0:PRINT:COLOR 0,7:
    PRINT N "data pairs in " Z$ ", fitted to N =" M:
    COLOR 7,0:PRINT

230 PRINT USING "&";" N";:PRINT USING "&";"      Abs(t=0)      ";;
    PRINT USING "&";"      E      ";;
    PRINT USING "&";" Abs(f)      ";;PRINT USING "&";"      S.D.";
    GOSUB 630:GOSUB 510

240 REM ...ITERATE...

250 FOR I=1 TO 5:G=0:H=0

260 REM ...INITIALIZE MATRICES...

270 FOR A=1 TO N:FOR B=1 TO 3:U(A,B)=0:W(A)=0:V(B,A)=0:Z(A)=0:
    NEXT:NEXT

280 FOR A=1 TO 3:FOR B=1 TO 3:B(A,B)=0:C(A)=0:D(A,B)=0:E(A)=0:
    F(B)=0:NEXT:NEXT

290 D(1,1)=1:D(2,2)=1:D(3,3)=1

300 REM ...COMPUTE PARTIALS AND ASSEMBLE NORMAL EQUATIONS IN
    MATRIX FORM...

310 FOR J=1 TO N:F=1+EXP(M*38.9484*(T(J)-EV)):E8=1/F:
    E7=((F-2)/(F^2))+1: E9=(AF-AI)*(F-1)*E8^2*M*38.9484:
    W(J)=P(J)+(E8*(AI-AF))-AI:U(J,1)=E7:U(J,2)=E8:
    U(J,3)=E9:NEXT

320 REM ...COMPUTE MATRICES...

```

```

330 FOR A=1 TO N:FOR B=1 TO 3:V(B,A)=U(A,B):
    Z(A)=W(A):NEXT: NEXT

340 FOR C=1 TO 3:FOR B=1 TO 3:FOR A=1 TO N:
    B(B,C)=B(B,C)+(V(B,A)*U(A,C)):NEXT:NEXT:NEXT

350 FOR B=1 TO 3:FOR A=1 TO N:C(B)=C(B)+(V(B,A)*W(A)):
    NEXT:NEXT

360 T=B(1,1):FOR B=1 TO 3:B(1,B)=B(1,B)/T:D(1,B)=D(1,B)/T:
    NEXT

370 FOR A=2 TO 3:T=B(A,1):FOR B=1 TO 3:
    B(A,B)=B(A,B)-(T*B(1,B)):
    D(A,B)=D(A,B)-(T*D(1,B)):NEXT:NEXT

380 T=B(2,2):FOR B=1 TO 3:B(2,B)=B(2,B)/T:
    D(2,B)=D(2,B)/T:NEXT

390 T=B(1,2):FOR B=1 TO 3:B(1,B)=B(1,B)-(T*B(2,B)):
    D(1,B)=D(1,B)-(T*D(2,B)):NEXT

400 T=B(3,2):FOR B=1 TO 3:B(3,B)=B(3,B)-(T*B(2,B)):
    D(3,B)=D(3,B)-(T*D(2,B)):NEXT

410 T=B(3,3):FOR B=1 TO 3:B(3,B)=B(3,B)/T:D(3,B)=D(3,B)/T:
    NEXT

420 FOR A=1 TO 2:T=B(A,3):FOR B=1 TO 3:
    B(A,B)=B(A,B)-(T*B(3,B)):D(A,B)=D(A,B)-(T*D(3,B)):
    NEXT:NEXT

430 FOR B=1 TO 3:FOR A=1 TO 3:E(B)=E(B)+(D(B,A)*C(A)):
    NEXT:NEXT

440 FOR A=1 TO 3:H=H+(C(A)*E(A)):NEXT:FOR A=1 TO N:
    G=G+(Z(A)*W(A)):NEXT

450 REM ...COMPUTE IMPROVED ESTIMATES AND START AGAIN...

460 IF G<H THEN E0=SQR(G/(N-3)) ELSE E0=SQR((G-H)/(N-3))

470 AI=AI+E(1):AF=AF+E(2):EV=EV+E(3):GOSUB 510:NEXT

480 REM ...COMPUTE AND DISPLAY STANDARD ERRORS...

490 E1=E0*SQR(D(1,1)):E2=E0*SQR(D(2,2)):E3=E0*SQR(D(3,3)):
    GOSUB 630:PRINT:PRINT "Standard errors":PRINT "E1:":E1:
    PRINT "E2:":E2:PRINT "E3:":E3:GOSUB 610:GOTO 30

500 REM ...SUBROUTINE FOR DISPLAY OF CURRENT ESTIMATES...

```

```

510 PRINT USING "##";I;:PRINT USING "      #.####";AI;:
    PRINT USING "      #.####";EV;:
    PRINT USING "      #.####";AF;:
    PRINT USING "      ##.###^^^";EO:RETURN

520 REM ...DATA ENTRY...

530 ERROR 54

540 CLS:COLOR 0,7:PRINT "      RULES FOR ENTERING DATA      ":
    COLOR 7,0:PRINT "1. Enter E first, in units of volts.":
    PRINT "2. Enter a comma.":PRINT "3. Enter absorbance.":
    PRINT "4. Press carriage return.":
    PRINT "5. Terminate by entering '1000,1'"

550 GOSUB 610:FOR I=1 TO 180:PRINT I;:
    INPUT "      ",A(I,1),A(I,2):
    LSET A$=MKS$(A(I,1)):LSET B$=MKS$(A(I,2)):PUT 1,I:
    IF NOT (A(I,1)=1000) THEN NEXT ELSE 30

560 REM ...SUBROUTINE FOR MENU SELECTION...

570 FOR L=1 TO 12:LOCATE Y,X+L:
    PRINT CHR$(SCREEN(Y,X+L)):NEXT:F$=LEFT$(F$,0):RETURN

580 REM ...FETCH DATA...

590 CLS:COLOR 0,7:PRINT " Data files on disk in B: ";:
    COLOR 7,0:PRINT:FILES "b:*.stt":COLOR 0,7:
    PRINT " Enter device:filename : ";:COLOR 7,0:INPUT " ",Z$:
    CLOSE 1:OPEN "R",1,Z$,8:FIELD 1,4 AS A$,4 AS B$:RETURN

600 REM ...SUBROUTINE FOR PAUSES...

610 PRINT:PRINT "Press RETURN to continue."

620 K$=INKEY$:IF LEN(K$)=0 THEN 620 ELSE IF 13=ASC(K$) THEN
    RETURN ELSE 620

630 PRINT "-----"
    RETURN

640 IF ERR=54 AND ERL=530 THEN GOSUB 590:RESUME 540 ELSE IF
    ERR=54 THEN GOSUB 590:RESUME ELSE PRINT "Error ";ERR:ON ERROR
    GOTO 0:ERROR ERR:STOP

```



*Biographical Note*

Scott S. Sibbett obtained his B.S. in 1979 from the University of California, Berkeley. His degree program was Soils and Plant Nutrition. Following graduation, he joined the staff at the University of Nevada, Reno, to work on a project developing scientific methods for research in the humanities. In the fall of 1980, he began his doctoral program in inorganic chemistry at the Oregon Graduate Center. His work was conducted under the guidance of Professors James K. Hurst and Thomas M. Loehr. Sibbett completed his studies for the Ph.D. in the fall of 1985. He then took a postdoctoral position at Stanford University under Professor Henry Taube.

Sibbett is married. Apart from chemistry, he says he enjoys Twain, Shakespeare, Milne, Keillor, Monet, Mozart, skiing, river rafting, sailing and hiking. He was born in 1955 in Berkeley, California.